

**DEVELOPMENT OF HEMATOPOIETIC, ENDOTHELIAL, AND PERIVASCULAR
CELLS FROM HUMAN EMBRYONIC AND FETAL STEM CELLS**

by

Tea Soon Park

B.S, Ajou University, 1999

M.S, Ajou University, 2001

Submitted to the Graduate Faculty of
Swanson School of Engineering in partial fulfillment
of the requirements for the degree of
Doctor of Philosophy

University of Pittsburgh

2008

UNIVERSITY OF PITTSBURGH
SWANSON SCHOOL OF ENGINEERING

This dissertation was presented

by

Tea Soon Park

It was defended on

July 18th, 2008

and approved by

Albert D. Donnenberg, Ph.D., Professor, Department of Surgery

Johnny Huard, Ph.D., Professor, Orthopaedic Surgery, Department of Bioengineering

Bradley B. Keller, M.D., Professor, Department of Pediatrics and Bioengineering

Charles Sfeir, Ph.D., D.M.D., Professor, Department of Bioengineering

Dissertation Director: Bruno Péault, Ph.D., Professor, Department of Pediatrics and Cell

Biology, McGowan Institute for Regenerative Medicine

Copyright © by Tea Soon Park

2008

DEVELOPMENT OF HEMATOPOIETIC, ENDOTHELIAL, AND PERIVASCULAR CELLS FROM HUMAN EMBRYONIC AND FETAL STEM CELLS

Tea Soon Park, PhD

University of Pittsburgh, 2008

Studies of hemangioblasts (a common progenitor of hematopoietic and endothelial cells) during human development are difficult due to limited access to early human embryos. To overcome this obstacle, the *in vitro* approach of using human embryonic stem cells (hESC) and the embryoid body (hEB) system has been invaluable to investigate the earliest events of hematopoietic and endothelial cell formation. Herein, firstly, optimal culture conditions of hEB were determined for differentiation of hESC toward hematopoietic and endothelial cell lineages and then different developmental stages of hEB were characterized for angio-hematopoietic cell markers expression. Day-8 to day-10 hEB included the highest numbers of hematopoietic and endothelial progenitor cells, and CD34⁺ CD45⁻ day-10 hEB cells were sorted to evaluate their hemangioblastic cell potential. Next, we established an *in vivo* chick embryo system that allowed sorted candidate hemangioblast populations to proliferate, migrate, and differentiate. Different stages of hEB cells, day-10 hEB cells purified for expression of CD34, and human peripheral blood hematopoietic stem/progenitor cells were examined for their engraftment capacity in chick embryos. Meanwhile, we examined the multi-lineage differentiation potentiality of CD146⁺ CD34⁻ differentiating hESC. Recently, our group characterized pericytes/perivascular cells, that displayed positive expression of CD146 (and a lack of mature endothelial cell markers) in a variety of human organisms. Differentiating hESC include a CD146⁺ population that concomitantly expresses endothelial progenitor cell markers (CD31, CD34, CD133, and BB9).

CD146+ pericyte-like hESC were tested for their hematopoietic, myogenic, and neurogenic potential. Finally, perivascular cells were obtained from human fetal placenta villi in order to evaluate their myogenic differentiation, migration ability, and mesenchymal stem cell phenotype. Placental villi are exceptionally rich in fetal microvessels; these might prove to be a beneficial source for stem cells that reside within blood vessel walls. Both CD146+ pericytes isolated from freshly dissociated placenta and purified blood vessel vasculature of placenta were observed for their myogenic potential. In summary, this project provided approaches to understand the early events of hematopoiesis using hESC and a chick embryo model, and allowed for observation of the mesenchymal lineage potential of perivascular cells derived from hESC and human fetal placenta.

TABLE OF CONTENTS

PREFACE	xvi
1.0 INTRODUCTION	1
1.1 HUMAN EMBRYONIC STEM CELLS	1
1.1.1 Characteristics of human embryonic stem cells	1
1.1.2 Differentiation of hESC	2
1.1.2.1 Embryoid body formation	2
1.1.2.2 hESC co-culture with stromal cells	3
1.2 HEMANGIOBLASTS	4
1.2.1 The ontogeny of human hemangioblast	4
1.2.2 Hemangioblasts derived from hESC	5
1.3 PROJECT OBJECTIVES	5
1.3.1 Objective 1: Determine the conditions to promote the hemangioblastic cell population from differentiating hESC.	6
1.3.2 Objective 2: Establish a chick embryo model for development of hematopoietic and endothelial progenitors.	7
1.3.3 Objective 3: Characterize pericyte-like CD146+ hESC, and investigate the multi-lineage differentiation potential.	9
1.3.4 Objective 4: Examination of placenta vascular-derived cells for mesenchymal stem cell marker expression, migration ability, and myogenic regeneration capacity.	9
2.0 HUMAN EMBRYONIC STEM CELL DIFFERENTIATION	11
2.1 INTRODUCTION	11

2.1.1	Hemangioblasts development from hESC and hEB.....	11
2.1.2	Renin-angiotensin system in hematopoiesis.....	12
2.2	METHODS	13
2.2.1	Human embryonic stem cell culture	13
2.2.2	Embryoid body formation: 3-dimensional culture	14
2.2.3	Medium differentiation: 2-dimensional culture.....	15
2.2.4	hEB dissociation for FACS analysis and cell sorting.....	15
2.2.5	Quantitative RT-PCR.....	16
2.3	RESULTS	17
2.3.1	Undifferentiated hESC	17
2.3.2	Differentiating hESC: hEB	19
2.3.3	Differentiating hESC: Medium differentiation.....	20
2.3.4	Hematopoietic and endothelial cells marker expression of hEB	21
2.3.5	Renin angiotensin system (RAS) component expression in differentiating hESC.....	24
2.3.6	Angiotensin converting enzyme (ACE) activity in BB9 expressing cells	26
2.4	DISCUSSION	27
2.5	CONCLUSION	29
2.6	ACKNOWLEDGMENT	29
3.0	DEVELOPMENT OF HEMATOPOIETIC AND ENDOTHELIAL CELLS DERIVED FROM HUMAN EMBRYONIC STEM CELLS IN CHICK EMBRYOS	30
3.1	INTRODUCTION	30
3.1.1	The chick embryo system to understand hematopoiesis	31
3.1.2	The chick embryo system as a model to study different types of human stem cells	32
3.1.3	The limitation of existing engraftment models for human hematopoietic stem cells derived from embryonic stem cells	33

3.2	METHODS	34
3.2.1	Microinjection of human cells into the chicken yolk sac.....	34
3.2.2	Flow cytometry analysis	36
3.2.3	Immunofluorescent staining	37
3.2.4	Hematopoietic methylcellulose assay	38
3.2.5	Statistical analysis	38
3.3	RESULTS	39
3.3.1	Human hematopoietic cells engrafted into chicken embryos	39
3.3.2	Potential of adult or ES cell-derived human blood progenitor cells to engraft into the blood system of chicken embryos.....	40
3.3.3	hESC-derived blood progenitors produce human erythro-myeloid and lymphoid cells in the chick embryos.....	45
3.3.4	Angiogenic potential of hEB cells in the chicken yolk sac.....	48
3.4	DISCUSSION	51
3.5	CONCLUSION	53
3.6	ACKNOWLEDGMENT	54
4.0	PERICYTE-LIKE CELLS DERIVED FROM HUMAN EMBRYONIC STEM CELLS	55
4.1	INTRODUCTION	55
4.1.1	Pericyte/ Perivascular cells.....	55
4.1.2	CD146-expressing cells, from endothelial to hematopoietic lineage	56
4.1.3	Perivascular cells derived from hESC	57
4.2	METHODS	58
4.2.1	FACS sorting pericyte-like hESC.....	58
4.2.2	Myogenesis.....	59
4.2.3	Hematopoiesis.....	59

4.2.4	Neurogenesis.....	60
4.3	RESULTS.....	61
4.3.1	Characteristics of CD146+ hESC	61
4.3.2	Myogenic potential.....	64
4.3.3	Hematopoiesis.....	67
4.3.4	Neurogenesis.....	68
4.4	DISCUSSION.....	71
4.5	CONCLUSION	73
5.0	HUMAN FETAL PLACENTA BLOOD VESSEL CELLS: MIGRATION AND MYOGENIC REGENERATION POTENTIAL.....	74
5.1	INTRODUCTION	74
5.1.1	Human placental structure	74
5.1.2	Stem cells derived from human placenta.....	76
5.1.3	CD146 in placenta.....	76
5.2	METHODS.....	77
5.2.1	Isolation of vasculature from human fetal placenta	77
5.2.2	Immunofluorescent staining	78
5.2.3	Flow cytometry analysis and cell sorting.....	80
5.2.4	<i>In vitro</i> myogenic differentiation	80
5.2.5	<i>In vivo</i> myogenic differentiation	81
5.2.6	Adhesion assay	81
5.2.7	<i>In Vitro</i> Migration/ Wound Healing Assay.....	82
5.3	RESULTS	83
5.3.1	Isolation and characterization of placenta villi.....	83
5.3.2	Characterization of vessel outgrown cells and enzymatically digested cells	86

5.3.3	<i>In vivo</i> migration and myofiber formation from total vessel transplants..	89
5.3.4	<i>In vitro</i> myogenesis of sorted populations from placenta villi.....	91
5.3.5	Angiogenic effect of human cells on host environment	95
5.3.6	Adhesion and migration assays on CD146+ and CD146- cells	97
5.3.7	Mesenchymal stem cell marker expression of cells outgrown from placenta villi.....	100
5.4	DISCUSSION.....	101
5.5	CONCLUSION	103
5.6	ACKNOWLEDGMENT	104
6.0	DISCUSSION	105
	APPENDIX A.....	108
	APPENDIX B	112
	APPENDIX C	113
	BIBLIOGRAPHY.....	115

LIST OF TABLES

Table 2-1. Primers designed for quantitative RT-PCR.....	17
Table 2-2. Hematopoietic and endothelial cell marker expression on hESC, day-5, day-10, and day-17 hEB. (mean values of percentages \pm standard deviation, N=5 \pm 2).....	22
Table 5-1. Mesenchymal stem cell marker expression of CD146+ and CD146- sorted cells from placenta villi vasculature out-grown cells.....	100

LIST OF FIGURES

Figure 2-1. Renin angiotensin system (RAS) pathway [52].....	13
Figure 2-2. Undifferentiated hESC colonies, x100.....	18
Figure 2-3. Immunohistostaining of undifferentiated hESC colonies on alkaline phosphatase, Tra-1-60 and Tra-1-81 (from left).....	18
Figure 2-4. FACS analysis of GFP positive hESC on the expression of Oct-4.....	18
Figure 2-5. Phase contrast images of different stages of hEB	19
Figure 2-6. Quantitative RT-PCR results of different stages of hEB	20
Figure 2-7. Medium differentiating hESC.....	21
Figure 2-8. CD34 expression in different stages of hEB development (mean values of percentages \pm standard deviation).....	23
Figure 2-9. Flow cytometry analysis of day-10 hEB.....	23
Figure 2-10. Immunofluorescent staining on day-10 hEB sections for endothelial cell markers expression.	24
Figure 2-11. Actin (1), AGTR-1 (2), AGTR-2 (3), and angiotensinogen (4) expression in differentiating hESC.	25
Figure 2-12. Quantitative RT-PCR of BB9+ hEB cells and blast colonies.....	26
Figure 2-13. BB9 expression of HUVEC and blast colonies.....	27
Figure 2-14. ACE enzymatic activity in the medium control (EGM2 Ctrl), HUVEC, and blast colonies.	27
Figure 3-1. Hamburger and Hamilton (HH) stage 12 chick embryo and injection sites of human cells (arrow heads). HP: head process, NT: neural tube, S: somite, SR: sinus rhomboidalis, and scale bar is 500 μ m.	35
Figure 3-2. Scheme of experiment to develop chick embryo model	35

Figure 3-3. Engraftment rate.....	40
Figure 3-4. FACS analysis of chimeric bursa of Fabricius following injection of different numbers of human peripheral blood stem/progenitor cells.....	41
Figure 3-5. FACS analysis of bursa of Fabricius and spleen from two embryos (#1-5 and #3-2, E15) that received 2×10^6 or 5×10^5 hPBSC at E2.	41
Figure 3-6. Immunohistostaining of thymus after injection of peripheral blood stem/progenitor cells	42
Figure 3-7. FACS analysis of blood forming organs of chick embryos that were injected with different types of human hematopoietic cells	43
Figure 3-8. Anti-human CD45 expression in the organs of chick embryos injected with CD34+ day-10 hEB cells (a, b, c, and d) or PBS (e, f, g, and h) as a control.....	44
Figure 3-9. Immunofluorescent staining of spleen and bursa of Fabricius that was injected with CD34+ hEB cells (a and b) or PBS (c and d) at E2 and analyzed at E16.....	45
Figure 3-10. Erythro-myeloid and lymphoid cell detection in spleen or bursa of Fabricius of embryos that were injected with CD34+ day-10 hEB cells (a, b, and c) or PBS (d, e, and f).	46
Figure 3-11. Methylcellulose colony assay of spleen cells from chicken embryos that were injected CD34+ day-10 hEB cells (a and b) or PBS (c and d) at E2 and harvested at E16.	47
Figure 3-12. Average number of CFU-GM produced from chimeric spleen cells that were injected with CD34+ day-10 hEB cells.	47
Figure 3-13. Immunofluorescent staining on sections of yolk sacs that received CD34+ day-10 hEB cells (a, b, and c), day-10 unsorted hEB cells (d), and PBS (e and f) at E2 and were analyzed at E15 to E16 of development.....	48
Figure 3-14. Flow cytometry analysis of enzymatically analyzed chimeric or control yolk sacs that stained positively for antibodies CD31 and Ulex europaeus agglutinin-1 (UEA-1) ligand.	49
Figure 3-15. Sorting gates of enzymatically digested chimeric yolk sac (E14) that were injected with CD34+ day-10 hEB cells at E2.....	50
Figure 3-16. Methylcellulose colony assay of enzymatically digested yolk sacs (E14) which received CD34+ day-10 hEB cells at E2.	50
Figure 4-1. Immunofluorescent staining of CD146 (red) on day-8 hEB (left) and a medium differentiated day-2 hESC colony (right)	61

Figure 4-2. FACS analysis of different stages of hEB on expression of CD34, CD146, and NG2.	62
Figure 4-3. FACS analysis of different days of medium-differentiated hESC on expression of CD146, CD34, CD133, CD144, and CD56.	62
Figure 4-4. CD34, CD146, and NG2 staining of frozen sections of day-6 hEB.	63
Figure 4-5. FACS analysis on expression of CD146 and CD34; isotype controls (left), day-8 hEB (middle), and day-2 medium differentiated hESC (right).	63
Figure 4-6. <i>In vitro</i> myogenic differentiation of CD146+ hEB (left) and CD146- hEB (right). ..	64
Figure 4-7. Dystrophin-positive muscle fibers derived from CD146 pericyte-like hESC.	65
Figure 4-8. Desmin staining of SCID/NOD mice muscle that was injected with day-8 CD146+ hEB cells and green fluorescent beads (3 weeks post-transplantation).	66
Figure 4-9. Human nuclear antigen (HNA)-positive human cells in the muscle of SCID/NOD mice that were injected with day-8 CD146+ hEB cells.	66
Figure 4-10. Hematopoietic differentiation of CD146+ hESC on MS5 stromal cells.	67
Figure 4-11. FACS analysis after hematopoietic differentiation of CD146+ hESC.	68
Figure 4-12. Nestin and neurofilament (NF) expression of CD146+ hESC before (Day 0) and after (Day 6 and Day 10) neural differentiation.	69
Figure 4-13. Neuronal marker expression of CD146+ hESC after 10 days of <i>in vitro</i> differentiation.	70
Figure 4-14. Neuronal marker expression of CD146- hESC after 10 days of <i>in vitro</i> differentiation.	70
Figure 5-1. Structure of human placenta [128].	75
Figure 5-2. Scheme of human placenta chorionic plate and villi [130].	75
Figure 5-3. Isolation of placenta villi vasculature	83
Figure 5-4. Immunofluorescent staining of villi vasculature.	84
Figure 5-5. Immunofluorescent staining of cross sections of placenta villi	85
Figure 5-6. Immunofluorescent staining of villi micro-vasculature with CD144 and CD146	85
Figure 5-7. FACS analysis and sorting gates of enzymatically digested villi vasculature.	86
Figure 5-8. Phase contrast pictures of out-grown cells in EGM2 or PM.	87

Figure 5-9. Proliferation rates of out-grown cells in different culture conditions	87
Figure 5-10. FACS analysis of out-grown cells from villi vasculature	88
Figure 5-11. Immunocyto staining of out-grown cells	89
Figure 5-12. In vivo transplant of villi vasculature and human cell migration.....	90
Figure 5-13. <i>In vivo</i> myofiber formation of human placenta villi vasculature.	91
Figure 5-14. Phase contrast images of sorted vascular and non-vascular populations from human placenta villi.....	92
Figure 5-15. <i>In vitro</i> myogenic differentiation for 15 days stained with Desmin (red, left) and quantification of the four populations (right).....	93
Figure 5-16. Quantitative RT-PCR for mRNA expression of CD56 on pre- and post-differentiated cells.....	94
Figure 5-17. <i>In vitro</i> myogenic differentiation of out-grown cells from different culture conditions.....	95
Figure 5-18. Angiogenic effect on SCID/mdx mouse muscle after injection of human cells.....	96
Figure 5-19. Migration assay of CD146+ or CD146- cells sorted from out grown cells.	97
Figure 5-20. Quantification of migration assay.....	98
Figure 5-21. Adhesion assay of CD146+ or CD146- sorted out-grown cells on different extracellular substrates.....	99
Figure 5-22. FACS analysis of MSC markers on CD146+ and CD146- sorted out grown cells.	101
Figure 5-23. mRNA expression (RT-PCR) of Brachyury on CD146+ and CD146- out-grown cells from placenta villi vasculature (M: size marker).....	101
Figure 6-1. Scheme of the developmental interactions from hESC to lineage differentiated cells.	107

PREFACE

The journey had begun, as it always does in life.

There are so many people to whom I cannot adequately express my sincere thanks. Firstly, my advisor, Dr. Bruno Péault has my deepest gratitude for his guidance, mentorship, and patience. He provided me with wonderful opportunities to explore stem cell research, to be an independent scientist, and to develop my career. I also wish to thank my committee members, Drs. Johnny Huard, Charles Sfeir, Albert Donnenberg, and Bradley B. Keller, all of whom generously offered expertise and supported toward the completion of my doctorate.

Dr. Elias T. Zambidis deserves my heartfelt appreciation for his invaluable collaboration. I truly enjoyed working with Dr. Jennifer Lucitti and am grateful for her teamwork. I must also thank Dr. Rebecca Landes McNamee for giving me a chance to start a new journey, and Drs. Vera Donnenberg, Tosiho Miki, Kimimasa Tobita, Gwan Jin Jung, Yong Li, and James Wang for their encouragement and kindhearted attention. I offer my genuine appreciation to Dr. Harvey Borovetz, Dr. David A. Vorp, and Lynette Spataro.

Dr. Bin Sun, Dr. Solomon Yap, Mihaela Crisan, Dr. Manuela Gavina, Dr. William Chen, Mirko Corselli, Alison Logar, Mitra Lavasani, and Dr. Burhan Gharaibeh deserve my special thanks for their assistance, advice, and for being great lab friends, and I thank Rosanne Perry for her warm care. I am thankful to all the members of the Stem Cell Research Center, and I truly

appreciate to the support of Drs. Jean-Paul Giacobino, Louis Casteilla, Laure Croisille, Bridget Deasy, and Baohong Cao for the opportunity to work with and learn from each of them.

I was fortunate to have many great friends around during my dissertation work. I express my sincere thanks to each of the following for their support and friendship: Bonnie Teng, Karanee Leelavanichkul, Nan Boonyachut, Sean Jefferson, Angela Criscimanna, Min Jung Kim, Jong Sik Kim, Eul Soon Park, Hye Young Kim, Se Young Kim, and Sung Hong Park. I wish to also express thank to good friends, David Humiston and Brian Hood for their proofreading, editing, and advice regarding my dissertation, and I must give special thanks to Ludovic Zimmerlin for his great and constant support, and understanding. Finally, I am deeply thankful to my parents for their love, encouragement, and support. My family in Korea always believed in me; they knew I would be strong enough to overcome any hard times by relying on their ever present love and support. I am about to start another journey in my life, and hope to have the good fortune of being able to take it with people as nice as those I have had pleasure of living and working with here in Pittsburgh.

1.0 INTRODUCTION

1.1 HUMAN EMBRYONIC STEM CELLS

Human embryonic stem cells (hESC) have shown invaluable potential for curing numerous diseases or restoring damaged tissues as a result of their capacity to generate all types of functional tissue-specific cells. Detailed studies continue to explore the intricacies of lineage differentiation and patient-specific embryonic stem cell generation as a means of producing clinically relevant cells. As hematopoiesis is one of the well-studied facets of stem cell research, generating hematopoietic cells from hESC has been largely defined by the considerable groundwork already completed by numerous groups [1-8]. Despite this fact, many facets of this process remain undefined. Among them, are the elements that finely control hESC differentiation toward hematopoietic/endothelial lineages, the identification of a common progenitor for hematopoietic and endothelial cells, and the development of an *in vivo* model to observe hESC-derived hematopoietic stem cell expansion and differentiation.

1.1.1 Characteristics of human embryonic stem cells

Human embryonic stem cells (hESC) were isolated from blastocysts and cultured for the first time in 1998 by Thomson J.A. et al. [9] after more than 15 years studying of mouse embryonic stem cells (mESC) [10]. Initially, Thomson defined the properties of undifferentiated hESC to

include the following: (1) derivation from the pre-/peri-implantation embryo; (2) prolonged undifferentiated proliferation; and, (3) consistent developmental potential to form derivatives of all three embryonic germ layers (teratoma formation) [11]. Several cell surface markers (stage-specific embryonic antigens (SSEA)-3, SSEA-4, TRA-1-60 and TRA-1-81), transcription factors (Oct-4 and Nanog) and alkaline phosphatase are commonly used indicators to confirm the undifferentiated state of hESC [12].

1.1.2 Differentiation of hESC

Three methods have been developed to differentiate hESC *in vitro*: (1) Human embryoid body (hEB) formation (three-dimensional aggregates of hESC); (2) co-culturing hESC with lineage differentiation supporting stromal cells; and, (3) monolayer culture of hESC on extracellular matrix substances with serum or defined cytokine mixtures [13, 14]. Several groups have defined specific inducers in serum-free medium that are capable of controlling lineage differentiation of hESC [5, 7, 8]. A combined method that borrows among the 3 methods (i.e., co-cultures stromal cells with defined cytokine mixtures) is also used for hematopoietic lineage differentiation [15, 16]. Herein, the first two methods (hEB and co-culture systems) that are more frequently used in hematopoiesis of hESC are described in detail.

1.1.2.1 Embryoid body formation

Mouse embryoid body (mEB) formation was first documented in 1975 by Martin G.R. and Evans M.J., who used pluripotent embryonic carcinoma stem cells and discovered that there were similarities between the process of embryoid body formation and the early events of mouse embryo differentiation [17]. Differentiation of mESC into the hematopoietic lineages is well

summarized in review articles of Keller G.M. [18, 19], which describe two different methods to produce mEB: (1) the use of methylcellulose or liquid medium in petri-dishes; and, (2) the use of hanging drops. The first method is commonly used to produce hematopoietic precursors, and the second method is more often used to generate muscle cells [20]. Within mEB, the establishment of the hematopoietic system is most extensively documented from the initial description of yolk sac-like blood islands in cystic mEB [21] to the development of various erythroid, myeloid and, to a lesser extent, lymphoid lineages within mEB [18, 21-30]. Based on the significant amount of research on mEB, the framework to generate human embryoid body (hEB) for hematopoietic lineage progenitors is well established, and can be implemented with modifications of the culture protocols [4, 31-34]. The hEB system allowed for documentation of the yolk sac-like primitive hematopoiesis and adult type definitive hematopoiesis which were occurred between day-5 to day-20 of hEB [4]. Day-8 to -10 hEB cells included the highest amount of primitive angio-hematopoietic stem cells, which gave rise to both endothelial and embryonic nucleated erythrocytes in a same culture plates [4]. While the hEB system as a robust system to recapitulate the earliest events of hematopoiesis, there is a lack of *in vivo* model to study the behavior and functionality of primitive hematopoietic progenitor cells derived from hESC.

1.1.2.2 hESC co-culture with stromal cells

Researchers in the field of hematopoiesis first began to use mouse bone marrow stromal cells in the 1940s and 1950s as a means of supporting the growth of human hematopoietic progenitor cells. The co-culture of primitive hematopoietic stem progenitor cells with supporting stromal cells is powerful since it has proved that single bone marrow derived-cells could give rise to colonies of differentiated blood cells that include long term proliferating (LTP) stem progenitor cells [35]. Further, it has been shown that cell lines derived from mouse bone marrow (S17) or

yolk sac (C166) hematopoietic tissues support hESC differentiation into hematopoietic lineages [1]. This co-culture system is an efficient approach for the high yield production of CD34+ hESC cells [30, 36]. However, the advantages of co-culturing burdens us with two shortcomings: the precise manner by which stromal cells provide growth support to hematopoietic progenitor cells is not defined, and, hence somewhat poorly controlled, and the long period of co-culture carries the risk of possible contamination of mouse genome to human cells, which remains a controversial issue.

1.2 HEMANGIOBLASTS

1.2.1 The ontogeny of human hemangioblast

Emergence of blood islands in the yolk sac is associated with the concomitant production of endothelial and hematopoietic cells, leading to hypothesize the existence of a common progenitor, the hemangioblast [37-39]. While it is true that primitive hematopoiesis occurs in the yolk sac, independent development of definitive hematopoiesis has also been characterized in the aorta-gonad-mesonephros (AGM), an intra-embryonic region where blood forming endothelial cells generate definitive hematopoietic cells [40, 41]. The authors described clusters of cells in the ventral endothelium of the aorta and vitelline artery which were visible from day 27 to day 40 of development. These clusters of hemogenic endothelial cells express CD45, CD34, CD31, CD43, CD44, KDR, GATA2, GATA3, SCL/Tal and c-kit [37-39, 42, 43], and migrate into the liver before eventually colonizing the thymus and bone marrow [18].

1.2.2 Hemangioblasts derived from hESC

The hypothesis, that hemangioblasts exist in the yolk sac and AGM has been difficult to confirm. This is mainly due to the lack of reliable markers for this population and constrained accessibility to early human embryos. However, recent hESC research allowed producing derivation of hEB progenitors with hemangioblastic potential that are documented to develop into primitive hematopoietic and endothelial cells [1-5, 7, 8]. The methodology and exogenous inducers to generate hemangioblasts from hESC are well described by Zambidis, et al. [44]. Mature hemangioblast (blast) colonies express cell surface markers including CD164, CD43 and CD41, and weaker expression of CD34, KDR and CD45. Most importantly, blast colonies express abundant amounts of BB9 (also known as ACE, angiotensin converting enzyme or CD143), which is also described as being expressed in human embryonic dorsal aorta [32, 45, 46]. These findings, including the observation that hemangioblast derived hESC were functional for the repair of ischemia injury of mice retina [7], underscore the need for an *in vivo* model to document the bi-potentiality of these cells in an individual study model.

1.3 PROJECT OBJECTIVES

The overall goal of this thesis is to provide general methods to develop hematopoietic, endothelial, and perivascular cells from human embryonic stem cells (hESC) or fetal stem cells. First, we have determined the differentiation conditions for hESC using the hEB system and characterized gene expression at different hEB developmental stages (Objective #1). Next, we established an *in vivo* chick embryo system to allow sorted candidate hemangioblast populations

to grow and differentiate (Objective #2). Sorted CD34+ hEB cells were used for further characterization of hematopoietic and endothelial cells as a hemangioblast candidate population. Also we examined the multi-lineage differentiation potential of CD146+ pericyte-like hESC (Objective #3). Finally, human fetal placenta blood vessel cells were tested for their myogenic differentiation potential (Objective #4). This project provided a functional method to study primitive hematopoietic stem cell derivation from hESC *in vivo* and brought greater clarity to the science and suitability of perivascular cells as a source of mesenchymal progenitor cells.

1.3.1 Objective 1: Determine the conditions to promote the hemangioblastic cell population from differentiating hESC.

The hEB system is a well-known approach for differentiating hESC into the 3 germ layers. By controlling medium conditions and culture time, we were able to determine optimal conditions to obtain hematopoietic and endothelial cell markers expressing cells in the hEB. Identification of these conditions, i.e., those that produced the greatest number of cells co-expressing hemogenic endothelial cell markers, was essential to our ability to harvest our candidate population for further experiments.

As differentiation began, we observed a loss of pluripotent cell markers and an increase in lineage specific markers during hEB development. The hEB culture system generated heterogeneous populations of cells. Depending on the length of time in culture, different types of cells developed, and a decreasing number of cells expressing pluripotent cell markers such as Oct-4 and Nanog was observed. To determine the existence of any differentiation towards the mesodermal, ectodermal, and endodermal lineages, we examined, respectively, Brachyury,

NeuroD, and α -fetoprotein (α -FP). Different growth stages of hEB were harvested and used for analysis by quantitative reverse transcriptase-polymerase chain reaction (RT-PCR). Doing this, we were able to determine the stage at which hEB develop into the mesodermal lineage, from which all hemogenic and endothelial cells originate.

Expression timing of hemangioblast marker candidates including CD34, KDR, BB9, CD133, and CD146 (and lack of CD45 expression) was observed and recorded. Protein expression levels during hEB differentiation were evaluated by fluorescence activated cell sorter (FACS) analysis. The first aim of this work focused on observation of proposed hemangioblast marker expression, as well as the expression of mature endothelial [CD31, CD144, vWF, and Ulex europaeus agglutinin-1 (UEA-1)] and hematopoietic (CD45) cell markers. By examining the expression kinetics of hematopoietic and endothelial cell markers, we could determine the hEB stage that was best for obtaining primitive angio-hematopoietic stem progenitor cells.

1.3.2 Objective 2: Establish a chick embryo model for development of hematopoietic and endothelial progenitors.

In the second specific aim, we developed and optimized *in vivo* model to provide a favorable environment for the differentiation of hemangioblasts into their committed lineages. Stem cells are often quiescent and requiring signals to migrate and differentiate. These signals could be cytokines, growth hormones, cell-cell interactions and others. Using our *in vivo* model, we transplanted the candidate hemangioblastic population in the yolk sac near blood islands that trigger the initial emergence of blood and blood vessels. Our chick embryo model provided many advantages including easy access to early stage embryos, the possibility to operate a large

number of embryos in ovo, fast analysis, the absence of maternal blood circulation, and low material cost.

Early stage chick embryos were used to inject human angio-hematopoietic stem progenitor cells, which then developed into mature hematopoietic and endothelial cells *in vivo*. Our hemangioblast candidate population (CD34+ CD45- hEB cells) was injected at embryonic day 2 (E2) of chick embryo. At this stage [Hamburger and Hamilton (HH) stage 10-12, around 42 hours of incubation], blood islands start to form while the heart has just begun beating. Injecting at this early stage ensures human cell growth without the risk of immune response since development of blood cells has just begun [47]. Less than 12 hours after human cells were injected into the yolk sac, chick blood circulation initiated as vitelline arteries formed and the heart started to beat. This is an optimal environment for providing signals to hemangioblasts in terms of leading them to migrate and differentiate into mature lineages.

Human-specific monoclonal antibodies were used to detect the presence of developed human cells in the chick embryos. Blood forming organs from human cells injected chick embryos were harvested and analyzed by FACS analysis and immunofluorescent staining. Anti-human CD34 and CD45 antibodies were used to identify hematopoietic cells in blood, spleen, thymus, and bursa of Fabricius (BF, an organ which exists only in birds and produces B cells). Erythroid (CD71 and glycophorin A), myeloid (CD13, CD14), and lymphoid (CD19, IgM) cell markers were also used to detect mature human blood cells in the chick organs. Additionally, the yolk sacs that received human cells were analyzed to detect human endothelial cells.

1.3.3 Objective 3: Characterize pericyte-like CD146+ hESC, and investigate the multi-lineage differentiation potential.

Recently, pericytes have been characterized in muscle, pancreas, and adipose tissues in regard to their marker expression profile, anatomic location, and multi potent ability to differentiate into mesenchymal cell lineages [48]. This study showed that pericytes express the cell adhesion molecule CD146 while none of the other tested mature endothelial cell markers (CD31, CD34, CD144, UEA-1 and von Willebrand factor (vWF)) were detected. Since CD146 is proposed as a pericyte marker and the CD146+ cell population emerges from early hEB cells, we isolated pericyte-like hESC expressing CD146+ CD34- CD45- CD56- from the hEB. These pericyte-like hESC appear at the specific stage (day 6-10) when hEB cells develop other hemogenic endothelial cell markers. We examined whether this population could give rise to hematopoietic, myogenic, and neurogenic lineages.

1.3.4 Objective 4: Examination of placenta vascular-derived cells for mesenchymal stem cell marker expression, migration ability, and myogenic regeneration capacity.

In this aim, we hypothesized that the vasculature within the human fetal placenta might serve as a source of stem/progenitor cells that could be useful in efforts to regenerate skeletal muscle fibers. CD34 and CD146 antibodies were used to detect endothelial cells and pericytes. Four populations [endothelial cells (CD34+ CD146- CD45- CD56-), pericytes (CD34- CD146+ CD45- CD56-), non vascular cells (CD34- CD146- CD45- CD56-), and unsorted cells] were separated by enzymatic digestion and cell sorting. These cell populations were quantitatively compared for their *in vitro* myogenic differentiation and their effect on angiogenesis *in vivo*

using an established model of degenerative muscle disease, Severe combined immunodeficiency/X-linked muscular dystrophy (SCID/mdx) mice. In the other hand, purified blood vessel segments from placental villi area were transplanted into the gastrocnemius muscle of SCID/mdx mice. Myofibers produced by human cells were detected 2 weeks post surgery. The abovementioned purified blood vessel segments were also cultured in different conditions, producing selective migration of different cell types as detected by endothelial and perivascular cell markers. We could optimize culture conditions to obtain perivascular cells that expressed CD146, PDGF receptor beta (PDGFR- β), NG2 and mesenchymal stem cell markers (and a notable lack of other mature endothelial cells markers). CD146+ and CD146- populations from purified blood vessel culture out-growth cells were compared in regard to migration capacity *in vitro*, their interaction with extracellular matrix, and their gene expression related to migration and remodeling.

2.0 HUMAN EMBRYONIC STEM CELL DIFFERENTIATION

2.1 INTRODUCTION

Endothelial cells may share a common precursor with hematopoietic cells, termed the hemangioblast. Candidate markers of the hemangioblast population have been proposed including SCL, KDR (also known as Flk-1 or VEGFR-2), CD34, CD133, and BB9 [4, 49, 50]. Studies of hemangioblasts during human development are difficult due to the limited availability of early human embryos. Recently, proposed hemangioblastic cell markers have been found in early differentiating hESC. To overcome the obstacle of limited access to human embryos, the hESC and hEB systems will be helpful for further studies on hemangioblasts.

2.1.1 Hemangioblasts development from hESC and hEB

In the hEB culture system, hemangioblastic cell marker expression is maximal between day-8 and day-12. This expression peaks earlier when undifferentiated hESC are cocultured with murine stromal cells (from day-6 to day-9), but both expression curves indicate that hemangioblastic cell populations arise at particular and slightly controllable stages of differentiation. The proposed hemangioblastic populations all showed a strong ability, *in vitro*, for hematopoiesis, but the *in vivo* potential was rarely shown. Indeed, one publication [36] described *in vivo* hematopoiesis from hESC committed to the hematopoietic cell lineage. In that

study, hESC were cocultured with mouse stromal cells and then discriminated according to CD34 and CD38 expression to transplant CD34⁺ CD38⁻ sorted cells into sheep fetuses. Human cells were engrafted into the bone marrow of a primary recipient and, after recovery and a new cell sorting, to a secondary recipient. Even though human hematopoietic cells were detected at low levels (<0.1%), this report supported the long term hematopoietic potential of CD34⁺ hESC. As reports are inconclusive however, it remains to be seen whether these cells are involved with endothelial lineage differentiation in an *in vivo* model.

2.1.2 Renin-angiotensin system in hematopoiesis

The renin-angiotensin system (RAS) is known to regulate blood pressure, inflammation and angiogenesis in adult (Figure 2-1) [51, 52]. Recently Jokubaitis, et al. demonstrated that the BB9 monoclonal antibody identifies angiotensin converting enzyme (ACE, also known as CD143), a key regulator of RAS known for its role as vasoconstrictor and catalyst of angiotensin I to angiotensin II [46]. Interestingly, BB9/ACE expression identified emerging hematopoietic cells in the areas of human yolk sac, intra-embryonic splanchnopleura, hemogenic endothelium of AGM region, and fetal liver [45, 46, 53, 54]. The recognition of the ACE role on these primitive hematopoietic progenitors raises the possibility that RAS has an previously undetermined function in regulation of the earliest stages of human hemato-endothelial differentiation [55], [Zambidis, Blood 2008].

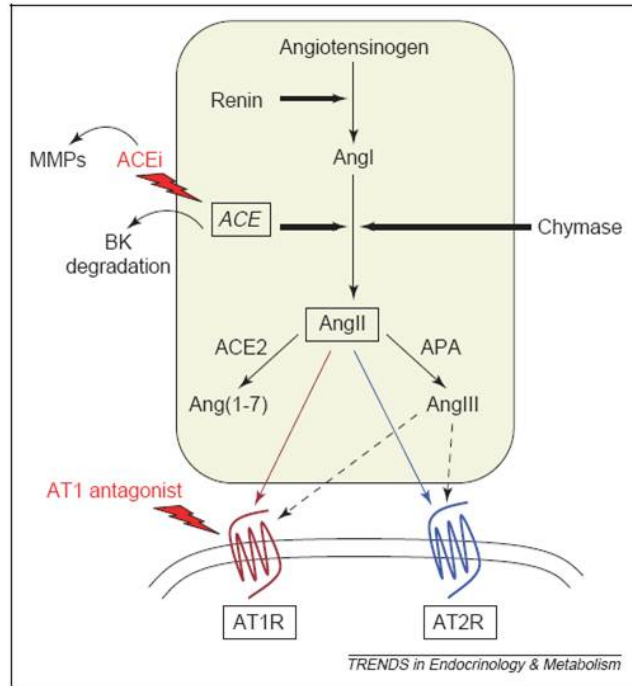


Figure 2-1. Renin angiotensin system (RAS) pathway [52]

2.2 METHODS

2.2.1 Human embryonic stem cell culture

The hESC used in these experiments, hESC line H1 (NIH code: WA01) were obtained from WiCell Research Institute (Madison, WI). To maintain hESC in an undifferentiated state, they were cultured over irradiated primary mouse embryonic fibroblasts (PMEF) layers derived from CF1 strain mice embryos (PMEF-CF, Millipore, Billerica, MA), as previously described [4, 9] (Figure 2.1). Cells were cultured in Dulbecco's modified Eagle's medium/F12 (DMEM/F12; Invitrogen, Carlsbad, CA), containing 20% knockout serum replacement (KOSR, Invitrogen),

1mM L-glutamine (Invitrogen), 0.1mM MEM non-essential amino acids (MEM-NEAA, Invitrogen), 0.1 mM 2-mercaptoethanol (2-ME, Invitrogen), and 4 ng/mL basic fibroblast growth factor (bFGF, Invitrogen). Medium was renewed daily, and cells were incubated at 37°C in 5% CO₂. hESC colonies were passaged every 6 to 7 days into new feeder layers.

2.2.2 Embryoid body formation: 3-dimensional culture

Human embryoid bodies (hEB) were generated in semi-solid methylcellulose and liquid medium in order to induce hematopoietic cell differentiation [4]. Briefly, hESC were routinely grown until they reached 80 to 90% confluency, on irradiated PMEF. Cells were then washed once with phosphate buffered saline (PBS, Sigma, St. Louis, MO). Prior to hEB formation, hESC were fed for 24 hours with Iscove's modified Dulbecco's medium (IMDM, Lonza, Basel, Switzerland) containing 20% ES-certified heat-inactivated fetal calf serum (FCS, HyClone, South Logan, UT), 1 mM L-glutamine, 0.1mM MEM-NEAA, 0.1 mM 2-ME, and 4 ng/mL bFGF. hESC were subsequently harvested with a cell scraper after 5 min of incubation in 1mg/mL collagenase type IV (Invitrogen) at 37°C. Then, cells were washed twice in IMDM and cultured in ultra-low adherence culture dishes (StemCell Technologies Inc, Vancouver, Canada) for hEB formation in 1% methylcellulose medium (METHOCULT SF H4236, StemCell Technologies), 15% FCS (StemCell Technologies), 4% IMDM, 50 µg/mL ascorbic acid (Sigma), and 0.5% cholesterol/lipoprotein supplements (Ex-Cyte, Millipore). After 2 to 3 days of culture, formed hEB were collected and washed twice in PBS. The second wash was set for 5 min followed by aspiration of two thirds of the supernatant to allow most PMEF to be removed. After one additional wash in PBS, hEB were moved into StemSpan serum free expansion medium (SFEM, StemCell Technologies) supplemented with 10% FCS (StemCell Technologies), 50µg/mL

ascorbic acid and 0.5% cholesterol/lipoprotein supplements. Medium was replaced every 3 to 4 days.

2.2.3 Medium differentiation: 2-dimensional culture

hESC were differentiated spontaneously due to the presence of fetal bovine serum (FBS) in the culture medium. Four to six days following the last passage, hESC colonies reached about 70% confluency. Cells were then washed with PBS, and hESC medium was replaced with differentiation medium containing DMEM/F12 medium, 10% FBS (Invitrogen), 1 mM L-glutamine (Invitrogen), 0.1 mM MEM-NEAA (Invitrogen), and 0.1 mM 2-ME (Invitrogen). Medium was exchanged every 2 days, and cells were harvested at multiple time points (day 1 to day 10 of differentiation) using trypsin/EDTA (0.25%, Invitrogen) whereupon they were analyzed via FACS analysis.

2.2.4 hEB dissociation for FACS analysis and cell sorting

hEB were harvested at sequential time points and dissociated into single cell suspensions for fluorescence activated cell sorting (FACS) analysis and purification. Day 3 to 12 hEB were dissociated with 0.05% trypsin/EDTA (Invitrogen) in PBS, whereas day 12 to 17 hEB were treated with 1 mg/mL collagenase type IV followed by 0.05% trypsin/EDTA (Invitrogen). Enzyme treated hEB were gently passed through a 21-gauge needle three times, and filtered through a 100- μ m cell strainer (BD Biosciences, San Jose, CA). Monoclonal antibodies used in cell analysis and sorting included mouse anti-human CD31-APC (R&D Systems, Minneapolis, MN), CD34-FITC, CD133-PE (both from Miltenyi Biotec, Auburn, CA), CD34-PE, CD45-APC,

CD144-PE, CD146-PE, BB9-APC (all from BD Pharmingen, San Jose, CA), and von Willebrand factor-FITC (vWF, US Biological, Swampscott, MA). Non-viable cells were excluded after taking up 7-amino-actinomycin D (7AAD, BD Pharmingen). Isotypic controls included mouse IgG-FITC, IgG-PE (both from Chemicon, Temecula, CA, USA), and IgG-APC (BD Pharmingen). FACS analysis was conducted on a FACSAria flow cytometer (Becton Dickinson, Franklin Lakes, NJ, USA) using the FACSDiva software (Becton Dickinson).

2.2.5 Quantitative RT-PCR

Different stages of hEB or blast colonies were collected for mRNA expression using quantitative RT-PCR. The following sequences were used to detect mRNA expression of angiotensin converting enzyme (ACE), angiotensinogen, angiotensin II type-1 receptor (AGTR-1), and angiotensin II type-2 receptor (ACTR-2). Triplicate samples of cells were collected at each target gene expression. Comparative quantification (fold change expression) of each target gene was performed based on cycle threshold (C_T) normalized to actin using the $2^{-\Delta\Delta C_T}$ method (see Appendix B) [4, 44, 56, 57].

Table 2-1. Primers designed for quantitative RT-PCR

Name	Sequences
ACE-forward	5' GCG CAC CGC GTC ATG GGG GCC GCC TCG GGC 3'
ACE-reverse	5' GAG CTG AGA CAC TCC TGA GGT GAC CCG G 3'
Angiotensin-forward	5' ACA CCG AAG ACA AGT TGAG G 3'
Angiotensin-reverse	5' GGT GCA GTT CTT GTC CTT CC 3'
AGTR-1-forward	5' GCA CAA TGC TTG TAG CCA AA 3'
AGTR-1-reverse	5' CCC TAT CGG AAG GGT TGA AT 3'
AGTR-2-forward	5' GGC AAC AAT GAG TCT ACC T 3'
AGTR-2-reverse	5' TAA ATC AGC CAC AGC GAG G 3'

2.3 RESULTS

2.3.1 Undifferentiated hESC

hESC were maintained in an undifferentiated state, for over thirty passages, using a mouse feeder layer and medium that included knockout serum replacement and bFGF. hESC colonies were enzymatically disaggregated to smaller size and placed in a new feeder layer every week. The morphology of undifferentiated hESC colonies was easily distinguishable compared to the spontaneously differentiating colonies by their clean edges and even layered cell structure.

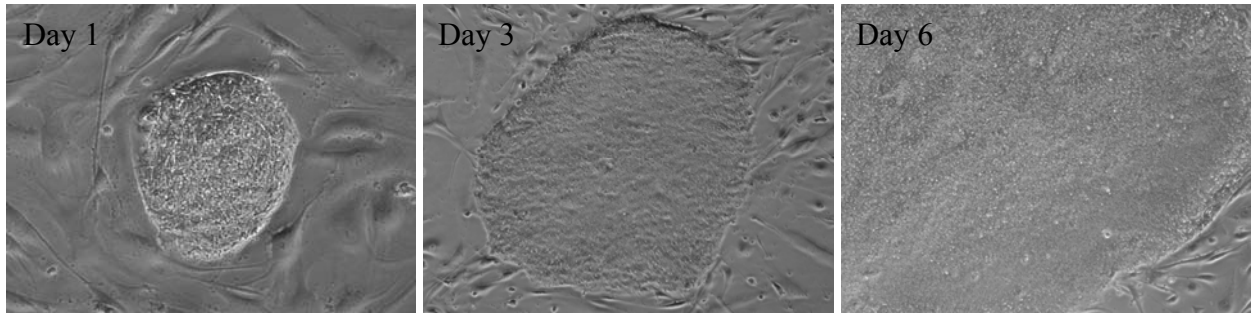


Figure 2-2. Undifferentiated hESC colonies, x100.

Undifferentiated hESC expressed alkaline phosphatase, Tra-1-60, and Tra-1-81 (Figure 2.3). Also, expression of Oct-4 (figure 2-4), Nanog, SSEA-3 and SSEA-4 was confirmed for cells in the undifferentiated state (not shown).

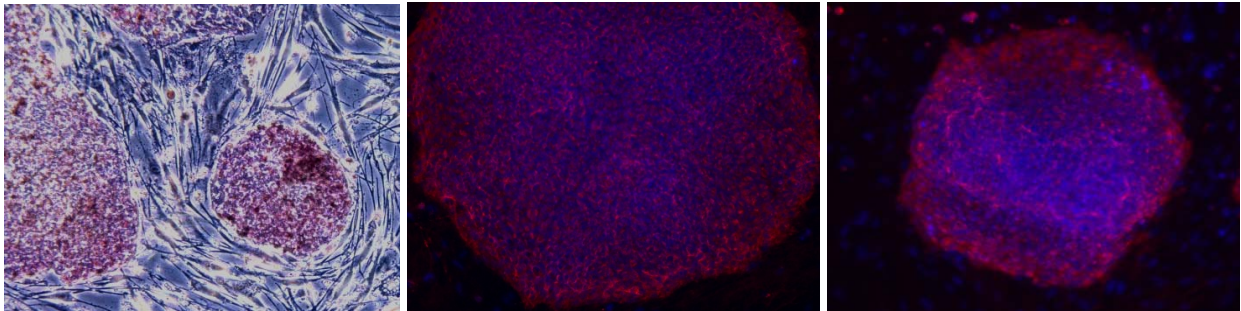


Figure 2-3. Immunohistostaining of undifferentiated hESC colonies on alkaline phosphatase, Tra-1-60 and Tra-1-81 (from left).

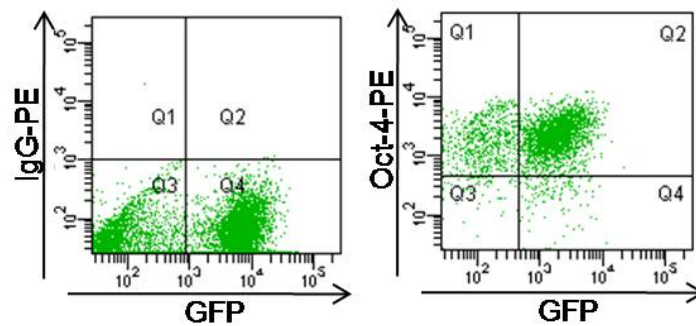


Figure 2-4. FACS analysis of GFP positive hESC on the expression of Oct-4

2.3.2 Differentiating hESC: hEB

hESC were differentiated into hematopoietic and endothelial cell lineages via hEB formation as previously described [1, 32, 33]. Figure 2-5 shows an undifferentiated hESC colony (hESC), day-5 hEB [hEB (D5)], day-10 hEB [hEB (D10)], scale bars represent 100 μm], and day-25 hEB [hEB (D25), scale bar is 500 μm]. Culture in semi-solid methylcellulose medium and StemSpan liquid medium produced uniformly sized hEB, with a diameter of $183 \pm 29 \mu\text{m}$ ($n=10$) at day 10, containing 300 to 500 cells. The size of hEB increased with time in culture and cystic hEB were seen from day-6 to day-8.

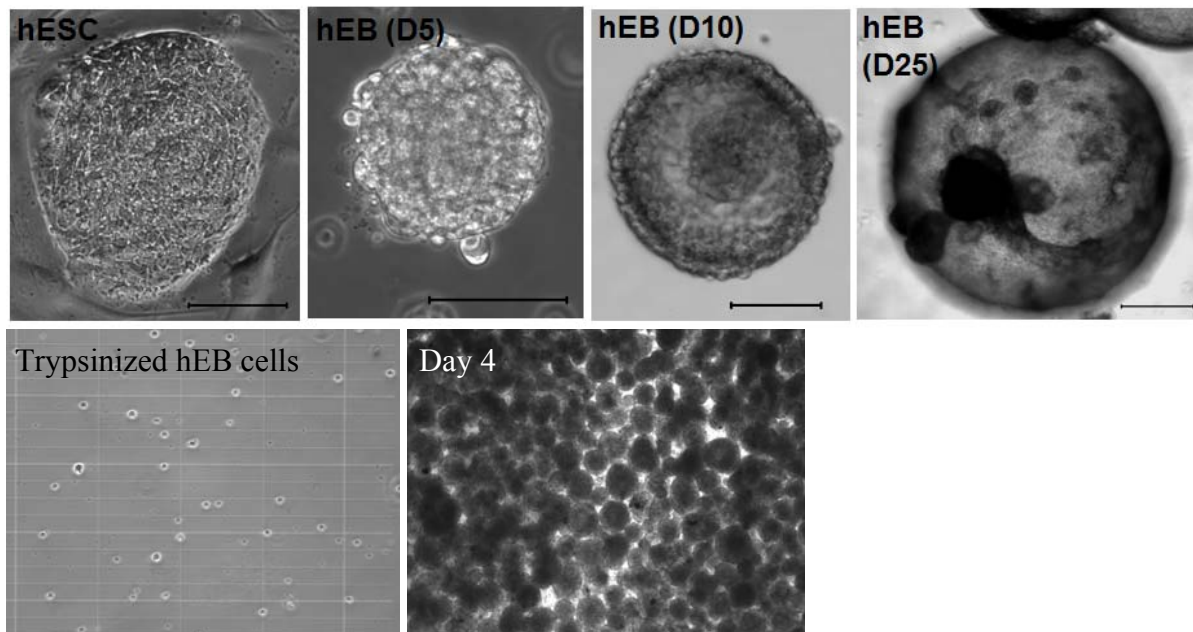


Figure 2-5. Phase contrast images of different stages of hEB

Different stages of hEB were collected and processed for quantitative RT-PCR analysis to observe mRNA expression of Oct-4 (pluripotency), Neuro-D (ectoderm), Brachyury (mesoderm), and alpha fetoprotein (α -FP, endoderm) (Figure 2-6). Oct-4 expression was decreased as differentiation began, and Brachyury was expressed in the early stages of hEB development (day-3 to day-5), while endoderm and ectoderm markers were up-regulated in the later stages of hEB development (day-10 to day-15). This data indicates that mesodermal lineage differentiation occurred in the early stage of hEB development, thereafter emergence of hematopoietic and endothelial cells will follow.

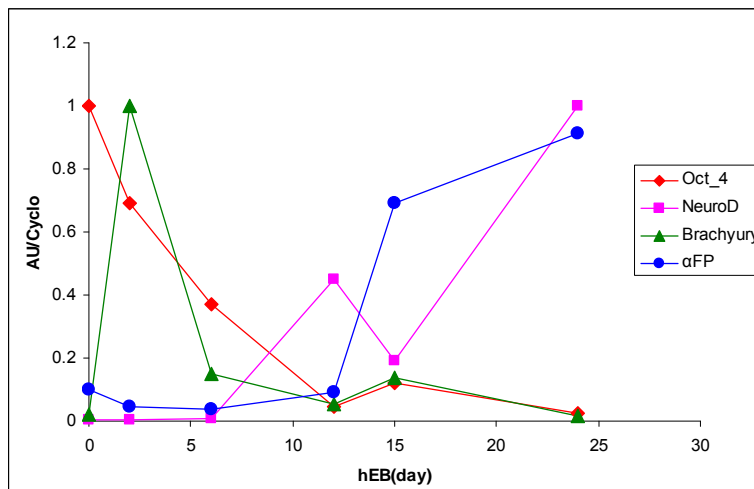


Figure 2-6. Quantitative RT-PCR results of different stages of hEB

2.3.3 Differentiating hESC: Medium differentiation

Undifferentiated hESC spontaneously differentiated into unspecified lineages in the presence of serum (e.g., fetal bovine serum) and absence of bFGF. The morphology of hESC colonies changed in one to two days showing undefined colony edges, clear nuclear visibility in each

cells, and monolayer formation from multilayered cells (Figure 2.7, upper row). As the culture period extended, more heterogeneous cell types were shown, and polygonal, round, slightly attached endothelial cell morphology, and cobblestone hematopoietic cell morphology were seen around day-6 to day-10 (Figure 2.7, lower row). Between day-10 to day-20 of culture, elongated tubular structures were seen (Figure 2.7, lower right).

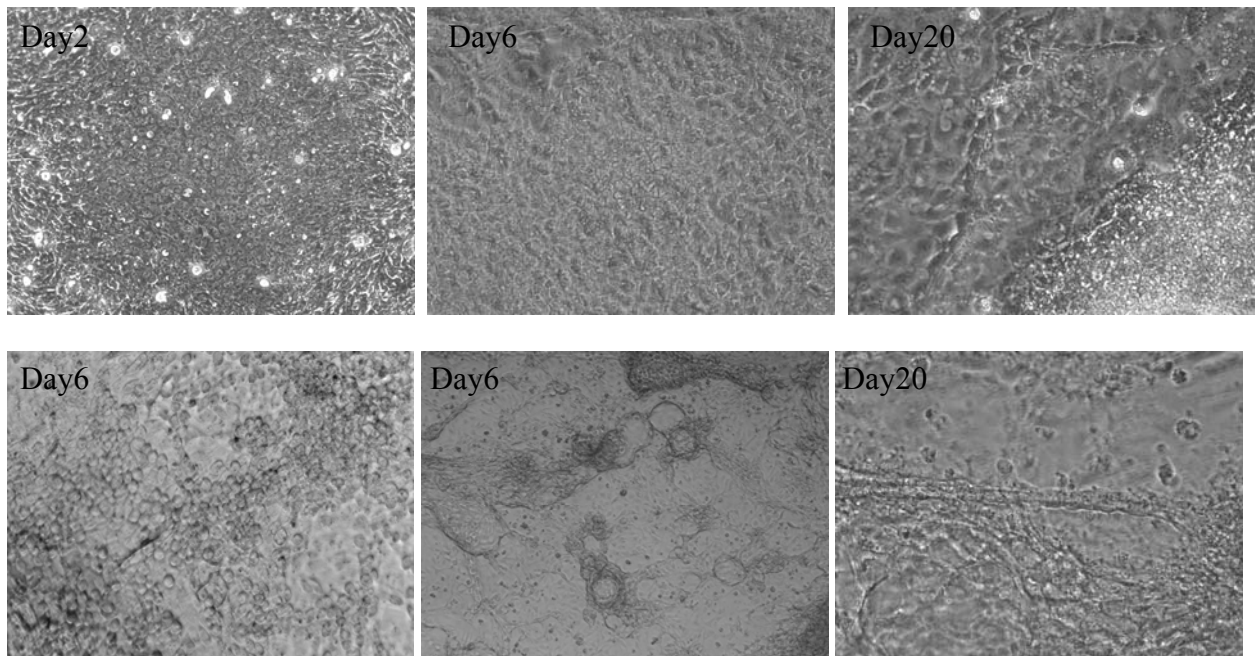


Figure 2-7. Medium differentiating hESC.

2.3.4 Hematopoietic and endothelial cells marker expression of hEB

Different stages of hEB were harvested, enzymatically digested, and analyzed by FACS. CD34 antigen expression was detected from 3 to 4 days of differentiation. The population of CD34+ cells within hEB increased until day-10 up to $2.46 \pm 0.34\%$ (Figure 2-8), whereas CD45

expression was not detected until after 12 to 14 days (Table 2-2). The expression of angio-hematopoietic cell markers in day-5, -10, and -17 in hEB is shown in Table 2-2.

Table 2-2. Hematopoietic and endothelial cell marker expression on hESC, day-5, day-10, and day-17 hEB. (mean values of percentages \pm standard deviation, N=5 \pm 2)

Antigen	hESC	hEB-Day5	hEB-Day10	hEB-Day 17
CD34	0.28\pm0.05	0.8\pm0.3	2.46\pm0.34	2\pm0.4
CD45	0.05\pm0.05	0.04\pm0.5	0.08\pm0.15	2\pm0.8
CD31	0.1\pm0.07	1.5\pm0.8	5.6\pm0.3	3.34\pm0.5
CD144	0.05\pm0.07	0.2\pm0.06	2.05\pm0.9	0.4\pm0.3
CD146	3.7\pm0.4	12.05\pm1.9	27.8\pm3.7	5.3\pm0.3
CD133	25.7\pm16.8	21.7\pm3.8	34.1\pm7.1	7\pm1.8
BB9	0.3\pm0.2	0.9\pm0.6	4.6\pm2.6	1.1\pm0.3

Day-10 hEB were chosen for CD34+ cell purification, since this is the stage at which they contain the most primitive hematopoietic progenitors [4]. Indeed, no CD45+ cells were present in day-10 hEB, whereas other hematopoietic/endothelial cell markers were detected including BB9, KDR (VEGF-receptor 2 or flk-1), CD31, CD133, and CD146 (Figure 2-9). Other endothelial cell markers were also detected by immunofluorescent staining (Figure 2-10).

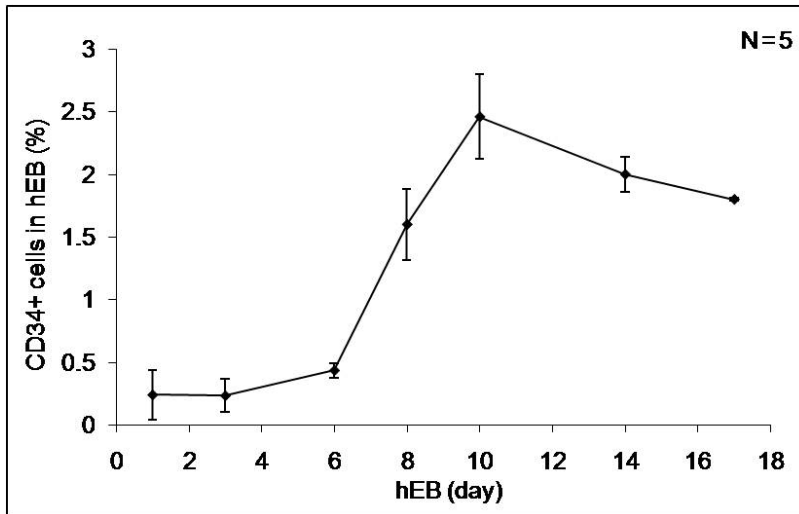


Figure 2-8. CD34 expression in different stages of hEB development (mean values of percentages \pm standard deviation).

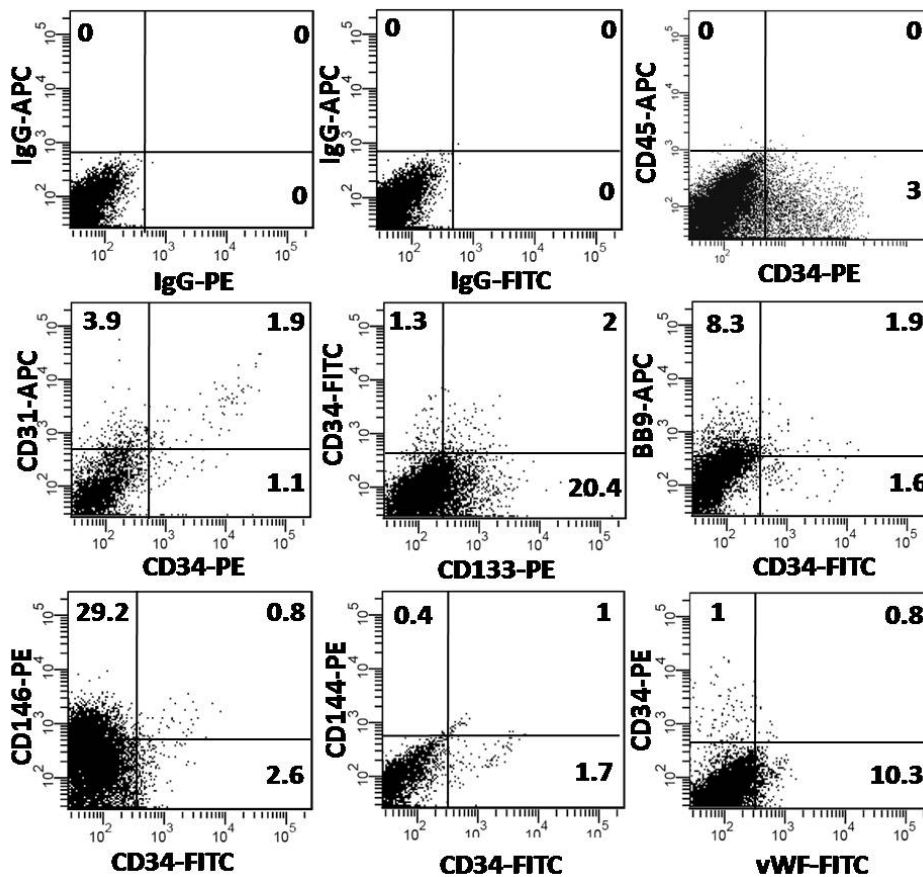


Figure 2-9. Flow cytometry analysis of day-10 hEB.

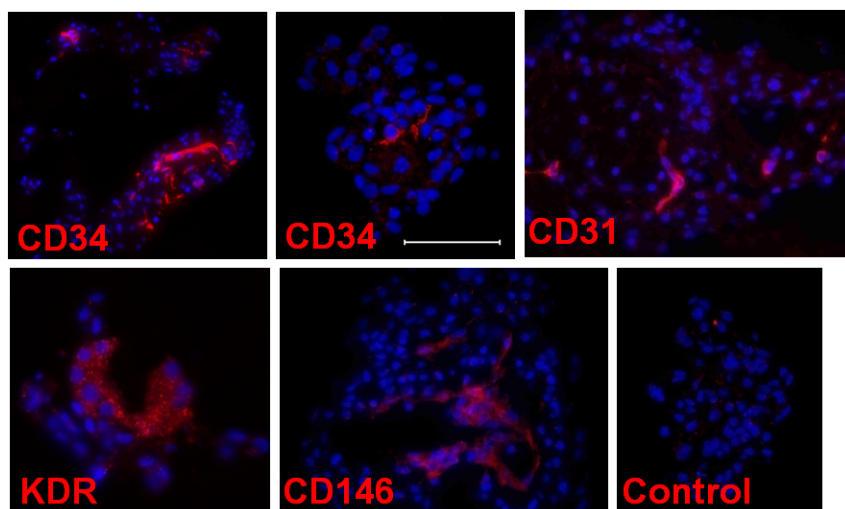


Figure 2-10. Immunofluorescent staining on day-10 hEB sections for endothelial cell markers expression.

2.3.5 Renin angiotensin system (RAS) component expression in differentiating hESC

Sorted day-9 hEB cells based on BB9 expression (BB9- and BB9+), and blast colonies derived from day-9 hEB cells were tested for expression of RAS components. Also, human umbilical vein endothelial cells (HUVEC*) were used as a source of endothelial cells expressing BB9 (Figure 2-13), and CD34+ human peripheral blood stem/progenitor cells (CD34+ PBSC**) were used as an adult-type blood stem cell for comparison. RT-PCR results revealed that there were differential expressions of angiotensin II type-1 receptor (AGTR-1, line 2, 164bp), Angiotensin II type-2 receptor (AGTR-2, line 3, 195bp), and angiotensinogen (line 4, 240bp). Actin (line 1, 213bp) was used as a housekeeping gene (Figure 2-11). Interestingly, BB9+ hEB cells express AGTR-2 but not in BB9- hEB cells. Also, blast colonies include expression of both receptors of angiotensin II.

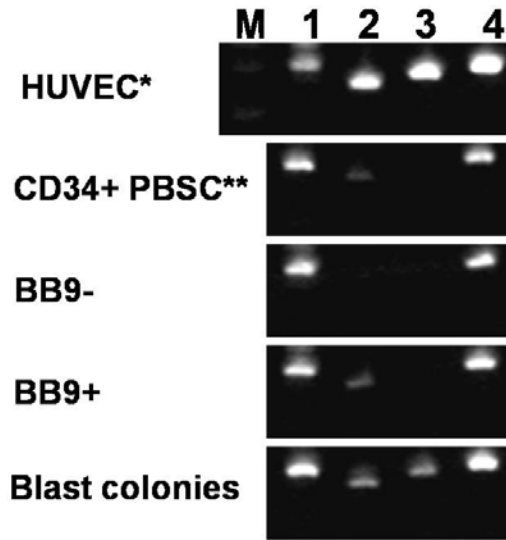


Figure 2-11. Actin (1), AGTR-1 (2), AGTR-2 (3), and angiotensinogen (4) expression in differentiating hESC.

Quantitative comparison between day-9 BB9+ hEB and blast colonies derived from day-9 hEB were shown in Figure 2-12. The fold change expression differences indicate levels of transcripts (calculated using the $2^{-\Delta\Delta CT}$ method, see Appendix B) of pooled day-9 blast colonies, in comparison to expression levels from sorted day-9 BB9+ hEB cells. AGTR-1, AGTR-2, and angiotensinogen (Angio) are all over-expressed in blast colonies compared to day-9 BB9+ hEB cells. Interestingly, AGTR-2, which is usually abundant in fetal cells but rarely expressed in adult tissue [54, 58, 59], was noticeably observed in blast colonies.

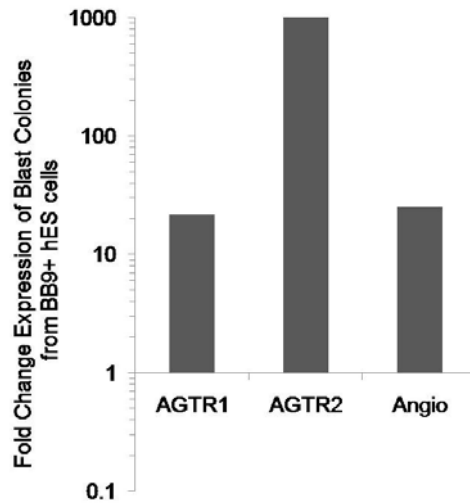


Figure 2-12. Quantitative RT-PCR of BB9+ hEB cells and blast colonies.

2.3.6 Angiotensin converting enzyme (ACE) activity in BB9 expressing cells

Angiotensin converting enzyme (ACE) activity was examined in BB9+ day-9 blast colonies derived from day-9 hEB cells. HUVEC were used as endothelial cells expressing BB9 (Figure 2-13). Blast colonies with BB9/ACE expression had robust enzymatic ACE activity, which means angiotensin I was catalyzed efficiently into bioactive peptide angiotensin II by ACE. Interestingly, the percentages of ACE-expressing cells were lower in blast colonies (23%) than HUVEC (42%), but the ACE activity was > 2 fold higher in blast colonies than HUVEC (Figure 2-14).

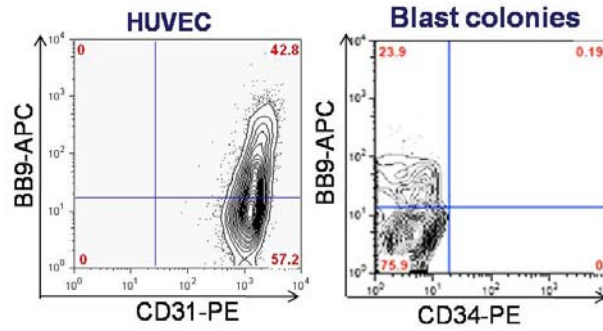


Figure 2-13. BB9 expression of HUVEC and blast colonies.

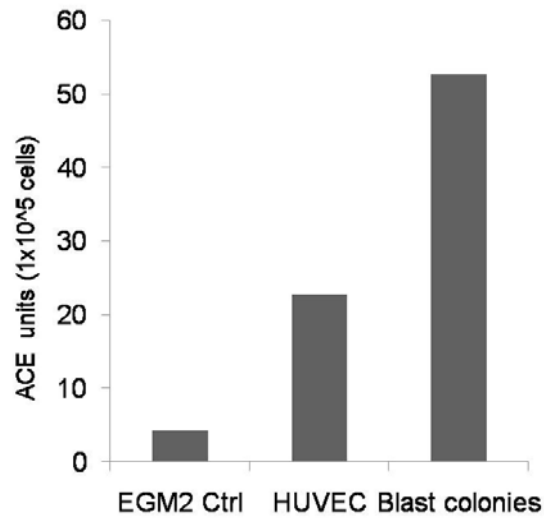


Figure 2-14. ACE enzymatic activity in the medium control (EGM2 Ctrl), HUVEC, and blast colonies.

2.4 DISCUSSION

What may have appeared to be impossible to investigate in developmental biology of human blood cell emergence is gradually revealed by research using hESC. The methodology behind

using hEB for hematopoietic and endothelial lineage differentiation is reproducible and consistent. In this dissertation, hEB generation was performed using medium containing fetal bovine serum (FBS) which provides characteristically undefined growth factors. Recently however, a few groups have developed modified culture conditions that finely control the differentiation of hESC via a precise combination of cytokine mixtures and little or no exposure to serum [7, 8, 44]. The focus of their strategy was to first produce high quantity and homogeneous mesodermal lineage progenitors from hESC in the early stages of hEB differentiation, and then to generate more specified hemangioblastic cells or hematopoietic progenitor cells in later stages of differentiation. It is important to recognize, however, that the conventional method, i.e., using serum containing medium, is also valuable as a reproducible three-dimensional culture method to produce both primitive and definitive hematopoietic cells that does not require supplemental growth factors or xenogenic stromal co-culture.

This work characterized that hESC-derived hemangioblasts expressed surface angiotensin converting enzyme (ACE) and other rennin angiotensin system (RAS) elements. We further demonstrated that BB9/ACE⁺ day-9 hEB cells expressed angiotensin II type-1 receptor (AGTR-1), but BB9/ACE⁻ hEB cells did not. Neither population expressed angiotensin II type-2 receptor (AGTR-2) but it was found to be up-regulated in blast colonies derived from day-9 hEB cells. Zambidis, et al. also documented that BB9/ACE⁺ hemangioblasts are found within not only CD34⁺ cells, but also, and even more robustly, among CD34⁻ hEB cells. This result is also equivalent with immunohistochemical analysis of the human AGM, which demonstrates the migration of ACE⁺ CD34⁻ CD45⁻ mesoderm cells from the splanchnopleura toward the dorsal aorta prior to the onset of intra-embryonic hematopoiesis [32, 46]. Therefore, BB9/ACE appears

as the earliest known marker of human angio-hematopoietic stem cells (a.k.a. hemangioblast or hemogenic endothelial cells).

2.5 CONCLUSION

In summary, we showed that the hEB approach provided a valid *in vitro* model to develop angio-hematopoietic progenitors. We have documented a number of hematopoietic and endothelial cells markers and confirmed that day-8 to day-10 hEB include the highest amount of hemangioblastic cell populations. BB9/ACE expressing cells and blast colonies derived from hEB cells were characterized for RAS components expression. BB9+ blast colonies also demonstrated high enzymatic angiotensin converting enzyme activity.

2.6 ACKNOWLEDGMENT

Large portion of this project was performed by collaboration with Dr. Elias T. Zambidis.

3.0 DEVELOPMENT OF HEMATOPOIETIC AND ENDOTHELIAL CELLS DERIVED FROM HUMAN EMBRYONIC STEM CELLS IN CHICK EMBRYOS

3.1 INTRODUCTION

Although a number of studies have demonstrated the robustness of the hESC/ hEB system for the generation of human hematopoietic progenitors, a convenient and, if possible, inexpensive *in vivo* model is missing for the investigation of blood and blood vessel development from hESC [60]. Xeno-transplantation models that utilize mouse embryos [7, 29] and sheep fetuses [36, 61-63] are powerful but have practical limitations that preclude accurate transplantation of human cells into desired anatomic locations at very early developmental stages and can be prohibitively expensive. In contrast, avian embryos are accessible to experimentation from the earliest stages of development and are available in large numbers at a low cost. Indeed, the avian embryo has been the primary model used by embryologists to study blood and blood vessel formation since the 1920's [47, 64-69]. Therefore, we hypothesized that hESC-derived human angio-hematopoietic progenitors can differentiate into blood and vascular elements following transplantation into avian embryos. To test this hypothesis, and to develop a model system for studying the earliest steps of human hemato-endotheliogenesis, we injected adult human hematopoietic stem-progenitor cells or hEB cells into the embryonic day-2 chicken yolk sac. We

then measured the engraftment of differentiated human blood and vascular cells in the blood-forming tissues and yolk sac of the developing host.

3.1.1 The chick embryo system to understand hematopoiesis

Availability to large number of embryos, easy accessibility to early stage development, and data reproduction are some of the main advantages for using avian embryos which led to pioneering research on the ontogeny of hematopoiesis. Historically, the chicken embryo was the primary material for embryologists and hematologists including Moore, Owen, Dieterlen-Lievre, and Le Douarin who pioneered the study of blood formation in chick embryos starting in the 1920's [64-66]. In the chicken, hematopoietic colonization occurs in the rudiments of the thymus (from embryonic day (E) 6.5), bursa of Fabricius (BF, from E8), and bone marrow (from E10) [67, 70, 71]. The initial site in which hematopoiesis occurs, the yolk sac, is an extra-embryonic structure that is shared by amniote embryos from birds to mammals. Therefore, in birds as in humans, primitive hematopoiesis develops extra-embryonically via formation of blood islands in the yolk sac, and, as this initial phase of hematopoiesis disappears, definitive hematopoiesis seems to independently spread out from the ventral floor of the dorsal aorta where clusters of endothelial and hematopoietic cells are visible. These clusters became a source of great interest, leading many to hypothesize the existence of a hemogenic endothelium from which hematopoietic cells would be generated [37, 43, 49]. The hematopoietic clusters lining the aorta in the AGM territory are positive for CD45, CD117 (c-kit), CD146, KDR, GATA-2, and SCL-1 in both chickens and humans. Some of these markers are shared by both hematopoietic and endothelial cells, originating from hemangioblasts or hemogenic endothelium; however, the exact origin and

identification using specific markers for sub-populations involved in these processes, as well as accurate understanding of chronology and mechanisms, remains unclear [38, 49].

3.1.2 The chick embryo system as a model to study different types of human stem cells

To investigate the role, potential, and fate of human stem cells, a number of groups have used the chick embryo as a model for engraftment. In 2002, Goldstein, et al. engrafted colonies of hESC into epithelial-stage somites of chick embryos at 1.5 to 2 days of development. The engrafted cells survived and differentiated into the neuronal lineage in structures such as dorsal root ganglion and neurons [72, 73]. This group showed the capacity of hESC to survive in an *in ovo* system, to divide, to differentiate, and, finally, to integrate host tissues. These results suggested a modulation of hESC differentiation by the host embryonic environment. Coles, et al. demonstrated in 2004 that the injection of human retinal stem cells from different regions of human eyes into chick embryo eyes allowed the human cells to differentiate into all different retinal cell types. This experiment was performed at a later stage (3.5 to 4 days) than that selected for the work by Goldstein's group, and, notably, immunological rejection of the injected human cells was observed [74]. More recently, Sigurjonsson, et al. (2005) managed to produce neurons by injecting bone-marrow-derived adult human CD34+ hematopoietic stem cells (HSC) into regenerating chick embryo spinal cord [75]. These studies demonstrate that human stem cells can survive, proliferate, and differentiate after injection into a chick embryo system. This microenvironment provides signals that are recognized by the injected human stem cells, depending on the location or the presence of injuries for instance, and might lead the stem cells to differentiate towards a specific lineage. A number of recent studies using the chick embryo as a model to differentiate hESC exist principally in the field of neuronal regeneration, but few

significant articles report this system as an environment for human hematopoietic and endothelial cells derived from hESC development as of yet.

3.1.3 The limitation of existing engraftment models for human hematopoietic stem cells derived from embryonic stem cells

The development of an *in vivo* hematopoietic system for hESC-derived progenitors has been limited based on several reports. The murine model, the most frequently used *in vivo* hematopoietic reconstitution model, has also proved to be a difficult one for the engraftment of embryonic hematopoietic stem progenitor cells. Repopulation occurs for greater than 6.5 months at levels ranging from 0.1% to 6% of lymphoid cells in peripheral blood, and no donor-derived myeloid, macrophage, and mast cells were found in long term repopulated recipients. One of the reasons suggested is that these embryonic hematopoietic progenitor cells possess a different developmental potential compared to the fetal or adult stages of blood stem cells that can engraft in adult mouse recipients [29]. Ideally, the primitive hematopoietic stem progenitor cell-derived ESC should be injected into the mouse embryo before the hematopoietic colonization of thymus and liver, but this is technically infeasible. Wang, et al. (2005) showed that hESC-derived hematopoietic progenitors develop into mature lineages by injection into the femur of a severe combined immunodeficiency/nonobese diabetic (SCID/NOD) mouse. However, this HSC did not migrate into other organs/blood circulation from the femur, thus failing to demonstrate one of the general HSC properties [76]. Similar studies were performed using sheep embryo. However, the low efficiency of HSC engraftment (less than 0.1%) in the blood and bone marrow of sheep models following injection of CD34 positive ESC-derived cells is also suggested as an example of the difficulties with producing a valid *in vivo* model [36].

3.2 METHODS

3.2.1 Microinjection of human cells into the chicken yolk sac

Human cells were prepared in PBS lacking calcium and magnesium to avoid clumping. Injection volumes were set to 10 to 15 μL per embryo. Injected cell numbers differed depending on cell populations; 5×10^3 CD34+ hEB cells, 5×10^4 CD34- hEB cells, or 5×10^4 unfractionated hEB cells were injected into each embryo. Human G-CSF-mobilized CD34+CD45+ peripheral blood hematopoietic stem-progenitor cells (hPBSC) were used as a positive control for adult-type hematopoietic cells, and 0.5 and 2×10^6 hPBSC were injected per embryo.

Fertilized chick eggs were provided by Utah State University (Logan, UT). Eggs were placed at 37.5°C in an incubator saturated with humidity to resume development. HH stage 10 to 12 embryos were collected after 42 to 44 hours of incubation (10 to 15 pairs of somites).

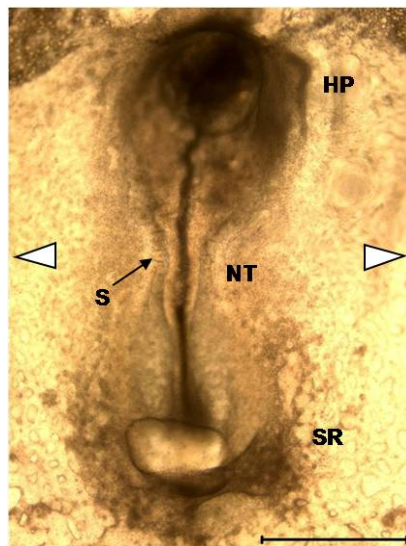


Figure 3-1. Hamburger and Hamilton (HH) stage 12 chick embryo and injection sites of human cells (arrow heads). HP: head process, NT: neural tube, S: somite, SR: sinus rhomboidalis, and scale bar is 500 μm .

A lateral round opening (2 to 2.5cm) was created in the egg shell with a 21-gauge needle and forceps. The vitelline membrane was also removed carefully using fine forceps under a dissecting microscope (SZH10, Olympus, Center Valley, PA). Human cells, or PBS as a control, were injected using glass capillary micropipettes (1mm diameter, World Precision Instruments, Sarasota, FL) pulled on a micropipette pulling machine (PUL-1, World Precision Instruments). Cells were injected into the mesodermal layer of the yolk sac (Figure 3-1, arrow heads). Sterile PBS was then added over the injected region and embryo to prevent dryness. The shell was sealed with Parafilm (Pechiney Plastic Packaging, Chicago, IL) and eggs were placed in the incubator at 37.5°C. Viability of the embryos was checked daily.

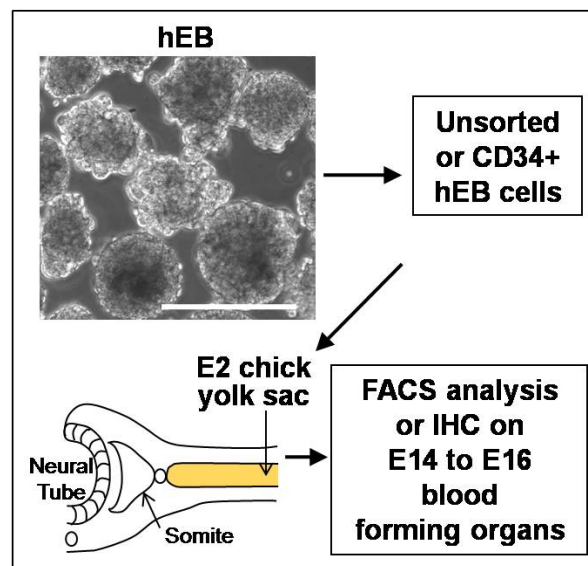


Figure 3-2. Scheme of experiment to develop chick embryo model

Injected embryos were sacrificed between embryonic day-14 (E14) and E16. Heparinized (0.1mg/μL, Sigma) blood, spleen, BF, and thymus were harvested for analysis by flow cytometry and immunohisto staining. The experimental scheme is shown in Figure 3-2. This experiment has been approved by the ESCRO (embryonic stem cell research oversight) committee at the University of Pittsburgh.

3.2.2 Flow cytometry analysis

Human cell-injected chick embryos were sacrificed between E14 and E16, and harvested hematopoietic organs were dissociated mechanically between two glass slides for flow cytometry analysis. Disaggregated cells were filtered through 70-μm cell strainers and stained with mouse anti-human CD45-PE (Beckman Coulter, Fullerton, CA), CD34-PE (BD Pharmingen), CD71-PE (BD Pharmingen), glycophorin A-FITC (CD235a, Immunotech, Marseille, France) CD13-PE (BD Pharmingen), CD19-APC-Cy7 (BD Pharmingen) or goat anti-human F(ab')₂ immunoglobulin μ heavy-chain (IgM)-FITC (TAGO Inc, Burlingame, CA).

Yolk sacs were harvested and enzymatically digested for flow cytometry analysis. Thoroughly washed yolk sacs were minced and suspended in 10 mL of collagenase type I, II, and IV (each 1 mg/mL, Sigma). After 30 min of incubation in a shaker at 150 rpm, 37°C, trypsin (final concentration 0.25%, Invitrogen) was added for another 10 min. Cells were filtered through 100-μm cell strainers and washed. Cells were then re-suspended in red cell lysis buffer and incubated for 15 min at room temperature. Following another wash and filtration through 70-μm cell strainers, cells were stained with mouse anti-human CD31-PE (SantaCruz Biotechnology) or biotinylated UEA-I (Vector Laboratories, Burlingame, CA), followed by the addition of streptavidin-PE-Texas Red (BD Pharmingen) and flow cytometry analysis.

3.2.3 Immunofluorescent staining

Four percent (4%) paraformaldehyde (PFA, Electron Microscopy Sciences, Hatfield, PA) fixed organs were incubated sequentially in phosphate buffer and phosphate buffered 30% sucrose solution for 1 hour. Organs were embedded in a phosphate buffered 7.5% gelatin/15% sucrose mixture and frozen in methylbutane (Fisher Scientific, Pittsburgh, PA) cooled between -50 and -60°C by liquid nitrogen. Frozen blocks were sectioned on a cryostat and sections (6-8 μ m) were stained with mouse anti-human CD45-FITC (Dako, Glostrup, Denmark), or unconjugated mouse anti-human CD14 (Miltenyi Biotec), or -CD19 (BD Pharmingen). Biotinylated goat anti-mouse IgG (Dako) and streptavidin-Cy3 (Sigma) were then successively added to the sections to reveal the anti-CD14 and -CD19 antibodies.

In another process, 4% PFA-fixed yolk sacs were frozen using tissue freezing medium (Triangle Biomedical Sciences, Durham, NC) in liquid nitrogen vapor. Frozen yolk sac sections were stained with unconjugated mouse anti-human CD144 (VE-cadherin, SantaCruz Biotechnology) or FITC conjugated sheep anti-human vWF (US Biological, Swampscott, MA) to detect human endothelial cells. Next, biotinylated goat anti-mouse IgG antibody and streptavidin-Cy3 were sequentially added to the sections, and 4',6-diamidino-2-phenylindole (DAPI, Molecular Probes, Eugene, OR) was added to stain nuclei. Photographs were captured using a Nikon Eclipse TE2000-U microscope and Snap Advanced software (Nikon, Melville, NY).

3.2.4 Hematopoietic methylcellulose assay

Either CD34⁺ day-10 hEB cells or PBS was injected into E2 embryos, and spleens were obtained at E16. A total of 1×10^6 single cells were suspended in 100 μ L of IMDM/ 5% FBS and then mixed thoroughly in 1 mL of methylcellulose hematopoietic colony assay medium (MethoCult H4434, StemCell Technologies). Cell mixtures were moved into 35mm diameter pre-tested culture dishes (StemCell Technologies) and cultured for up to 20 days. Hematopoietic colonies were taken picture under phase contrast microscope and pooled in PBS for flow cytometry analysis. Cells gathered in pellet were stained with unconjugated mouse anti-human CD15 (AbD Serotec, Raleigh, NC) and followed by goat anti-mouse biotin (Dako, Glostrup, Denmark) and streptavidin-pacific blue (Molecular Probes, Eugene, OR).

3.2.5 Statistical analysis

Data are summarized as mean \pm standard deviation of the mean. Statistical comparison between groups was performed using analysis of variance (ANOVA) and two-tailed Student's t-test (95% confidence interval) using SPSS software version 14.0.0 (SPSS Inc, Chicago, IL). *P* values are reported in the text of figures.

3.3 RESULTS

3.3.1 Human hematopoietic cells engrafted into chicken embryos

Human adult PBSC as well as hEB cells at different stages of development were injected into 42- to 44-hour (HH stage 11) chick yolk sacs (Figure 3-1, arrow heads) and host embryos were analyzed at E14 to E16 (experiment scheme shown in Figure 3-2). We used a total of 450 embryos for this study. The percentage of surviving embryos among all human cell-injected embryos was $38 \pm 14.4\%$. The negative control group (injection of sterile PBS instead of human cells) showed a viability of $37.9 \pm 9.3\%$ ($n=22$ embryos), which demonstrated that the human cells were not toxic to the embryos. No teratoma was ever seen on gross anatomic observation of all sacrificed host embryos. Human cells were detected with human specific anti-CD34 and -CD45 antibodies in the host blood forming organs. Each analysis included a negative control performed with an isotype-matched antibody. Engraftment rate (%), defined as the ratio of chimeric embryos relative to the total number of embryos analyzed, was $68.4 \pm 12.4\%$ for 65 embryos analyzed. Engraftment rates were compared between embryos injected with different types of human hematopoietic progenitor cells, which all participated in blood cell development following transplantation: hPBSC, day-10 hEB, day-17 hEB, day-10 hEB CD34+ cells and day-10 hEB CD34- cells ($n=12 \pm 5$ embryos per group). Day-10 hEB CD34+ cells showed the highest efficiency for engraftment (85%), as compared with hPBSC (54.6%) and day-17 hEB cells (57.9%) (Figure 3-3).

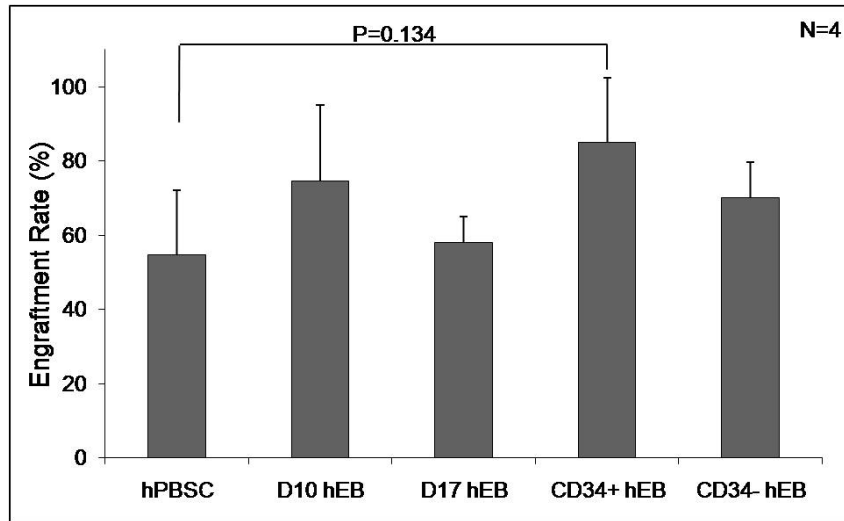


Figure 3-3. Engraftment rate

3.3.2 Potential of adult or ES cell-derived human blood progenitor cells to engraft into the blood system of chicken embryos

CD34+CD45+ hPBSC were injected into HH stage-11 chick yolk sacs (0.5 and 2×10^6 cells per embryo), and blood-forming organs were analyzed from E14 to E16. Chick embryos that had received 2×10^6 hPBSC contained 4- to 5-fold greater concentrations of human CD45+ cells in the BF than embryos that received only 5×10^5 cells (Figure 3-4, $n=4$ embryos in each group). The BF and spleen from an individual host embryo contained higher numbers of human CD45+ cells following injection of larger numbers of human cells (Figure 3-5).

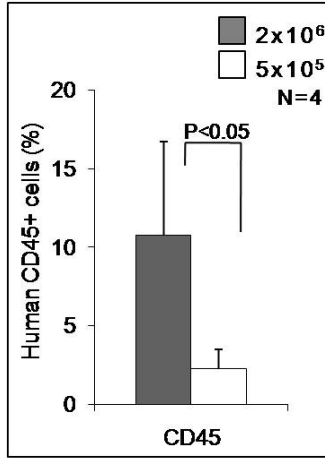


Figure 3-4. FACS analysis of chimeric bursa of Fabricius following injection of different numbers of human peripheral blood stem/progenitor cells

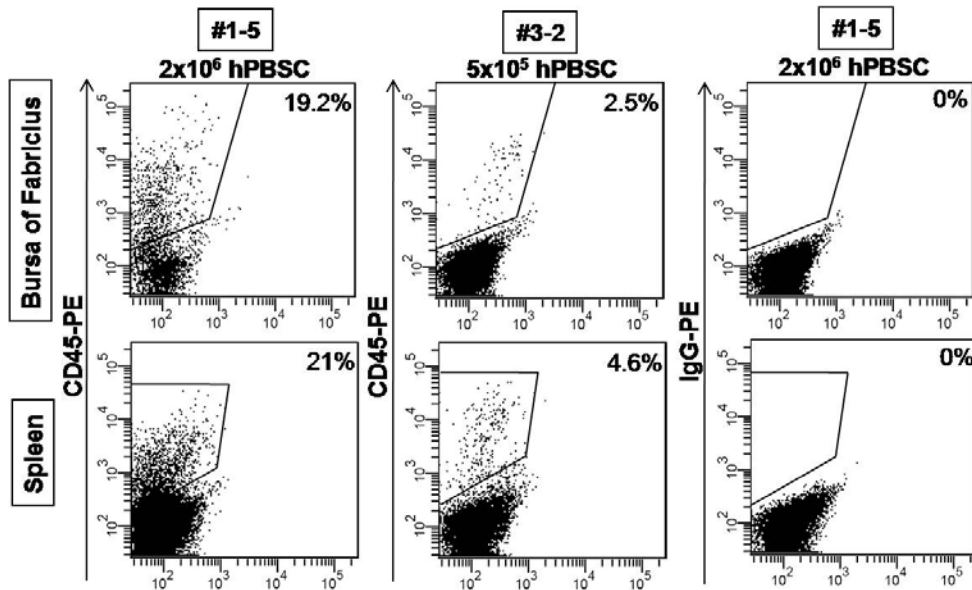


Figure 3-5. FACS analysis of bursa of Fabricius and spleen from two embryos (#1-5 and #3-2, E15) that received 2x10⁶ or 5x10⁵ hPBSC at E2.

A cluster of human myeloid cells were also detected by immunofluorescent staining in the frozen sections of chimeric thymus (E14) after injection of hPBSC at E2 (Figure 3-6).

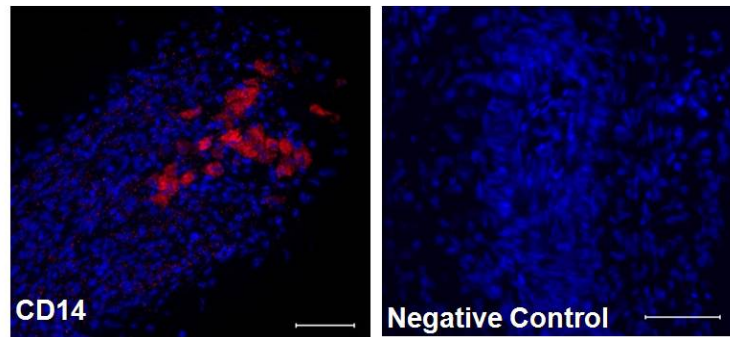


Figure 3-6. Immunohistostaining of thymus after injection of peripheral blood stem/progenitor cells

A total of 5×10^4 unfractionated hEB cells (day-10 and day-17), 5×10^3 CD34+ cells, or 5×10^4 CD34- cells purified from day-10 hEB were injected per yolk sac at E2. These different donor cells produced various numbers of human CD45+ cells in the blood forming organs of the E14 to E16 host embryos. The BF contained the highest number of human CD45+ cells, of all analyzed organs, regardless of the origin of the donor cells. Day-10 hEB cells produced a higher number of CD45+ cells than day-17 hEB cells. Overall, CD34+ hEB cells exhibited the highest efficiency for generating human hematopoietic cells in the spleen and BF. Intriguingly, unfractionated day-10 hEB cells produced the highest number of human CD45+ cells in the thymus ($2.7 \pm 1.1\%$), as compared to the other injected human cell populations (Figure 3-7).

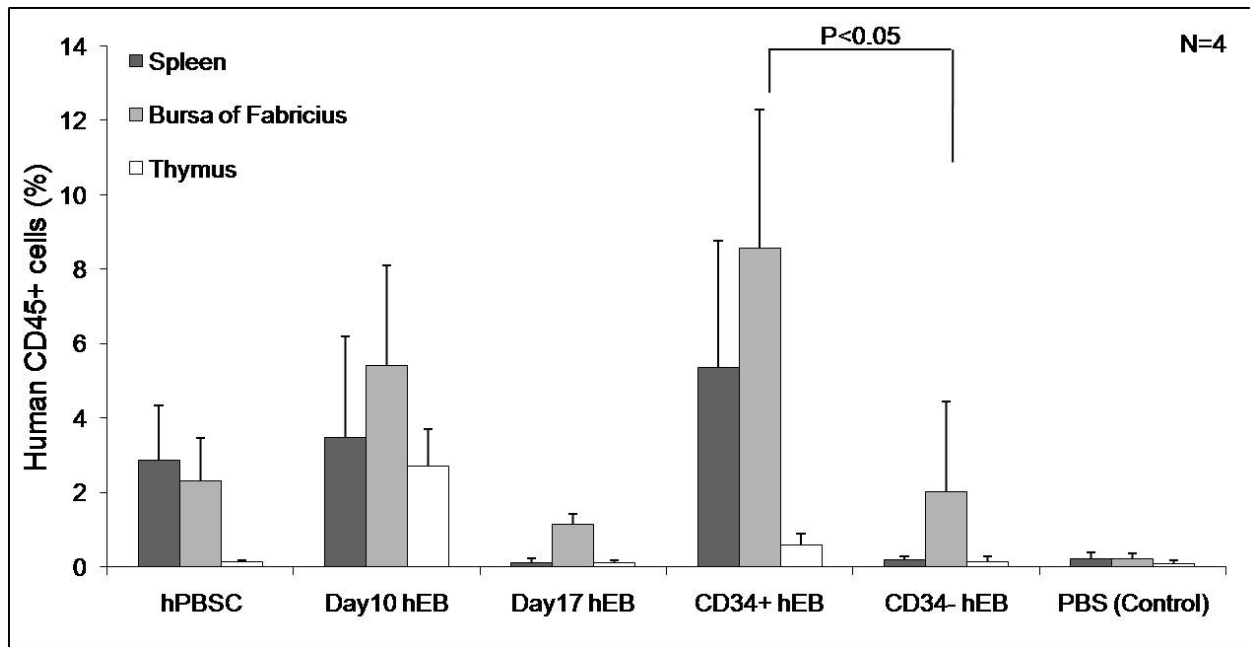


Figure 3-7. FACS analysis of blood forming organs of chick embryos that were injected with different types of human hematopoietic cells

The analysis of E16 embryos that were injected with 5×10^3 day-10 CD34+ hEB cells is illustrated in Figure 3-8. All analyzed tissues contained human CD45+ cells, with the highest proportion found in the BF (13.8%). There was no non-specific binding of IgG-negative controls in the corresponding organs of human cells injected host embryos. Also, we could not detect anti-human CD45+ cells in the PBS-injected control embryos.

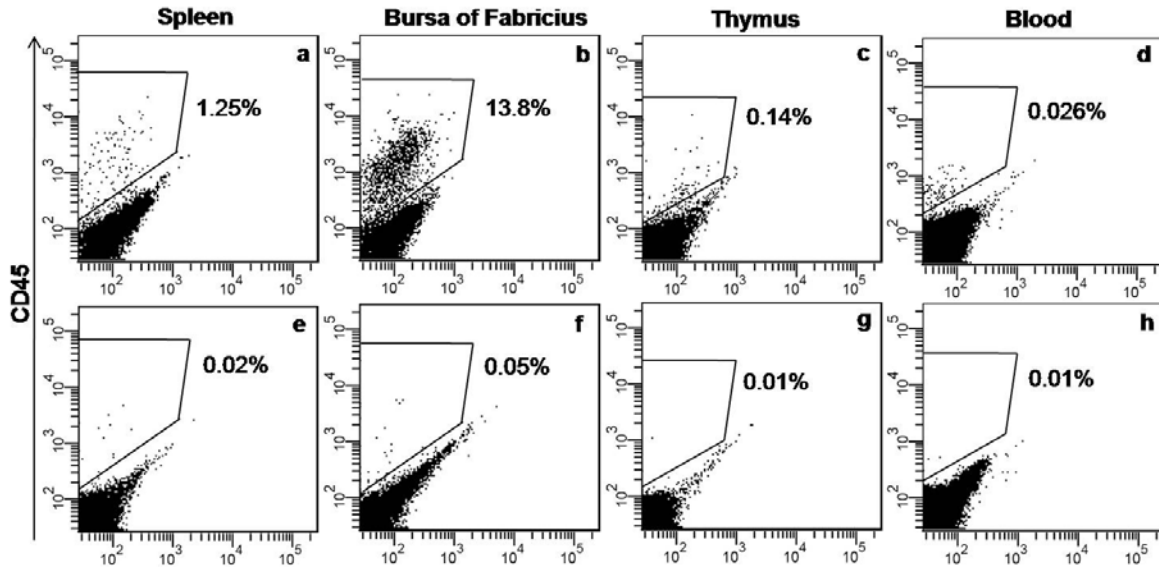


Figure 3-8. Anti-human CD45 expression in the organs of chick embryos injected with CD34+ day-10 hEB cells (a, b, c, and d) or PBS (e, f, g, and h) as a control

Human CD45+ cells were confirmed by immunofluorescent staining to be present on sections of the spleen and BF of the CD34+ day-10 hEB cell-injected host (Figure 3-9). Human cells were usually identified as clusters on sections; occasionally, individual CD45+ cells were detected in the micro-vessels of blood forming organs.

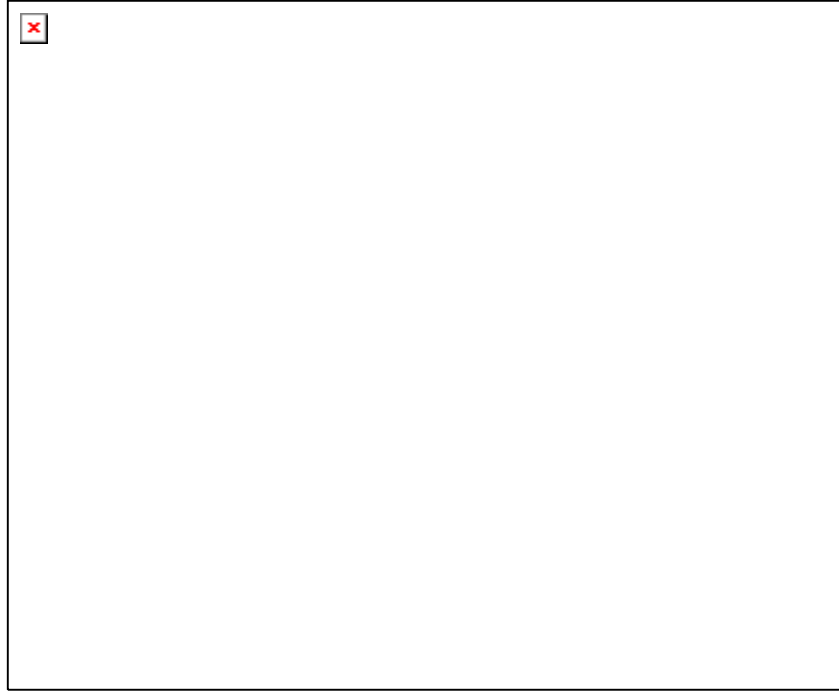


Figure 3-9. Immunofluorescent staining of spleen and bursa of Fabricius that was injected with CD34+ hEB cells (a and b) or PBS (c and d) at E2 and analyzed at E16

3.3.3 hESC-derived blood progenitors produce human erythro-myeloid and lymphoid cells in the chick embryos

FACS-purified CD34+ day-10 hEB cells were injected into the E2 chick yolk sac and the E14 to E17 spleen and bursa of Fabricius were analyzed for the presence of human erythroid, myeloid, and lymphoid cells. Human specific glycophorin A and CD71 were used in the blood and spleen as markers of human erythroid cells. These markers were not convincingly detected in the embryonic blood, but we observed the presence of about 30% glycophorin A+ human red blood cells in the embryonic spleen (Figure 3-10, left column). The chimeric spleen also contained about 5% CD13+ human myeloid cells (Figure 3-10, middle column). Several BF revealed

human CD19+ B cells in varying ranging between 2.8 to 64.3%. One of the BFs that was found to include human B cells expressing CD19 and IgM [34] is shown in Figure 3-10 (right column).

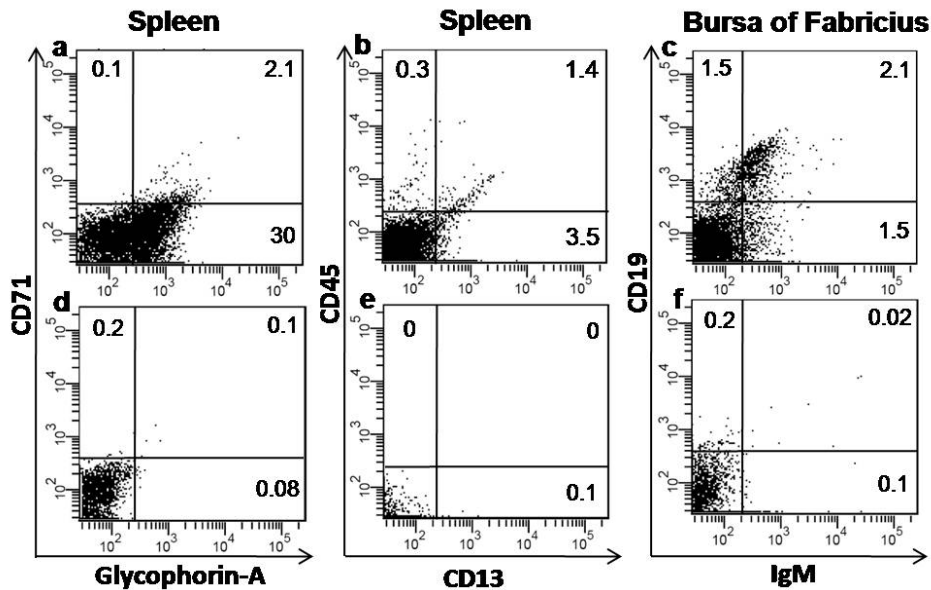


Figure 3-10. Erythro-myeloid and lymphoid cell detection in spleen or bursa of Fabricius of embryos that were injected with CD34+ day-10 hEB cells (a, b, and c) or PBS (d, e, and f).

Additionally, spleens of CD34+ day-10 hEB cells-injected and PBS-injected embryos were obtained at E16, and single cells of dissociated spleen were cultured in human cytokine mixtures of hematopoietic colony assay methylcellulose medium. A total of 1×10^6 cells were cultured up to 20 days, and colony forming units-granulocyte macrophage/monocyte (CFU-GM) were observed (Figure 3-11, a). Colony size was relatively smaller (10 to 200 cells) compared to the colonies observed from human bone marrow cells under the same assay conditions. The average numbers of colonies obtained from 1×10^6 cells were 111 ± 41.5 ($n=5$, Figure 3-12). When the colonies/cells were gathered from methylcellulose medium and analyzed with human CD15 antibody, about 5 to 10% of human myeloid cells were detected (Figure 3-11, b).

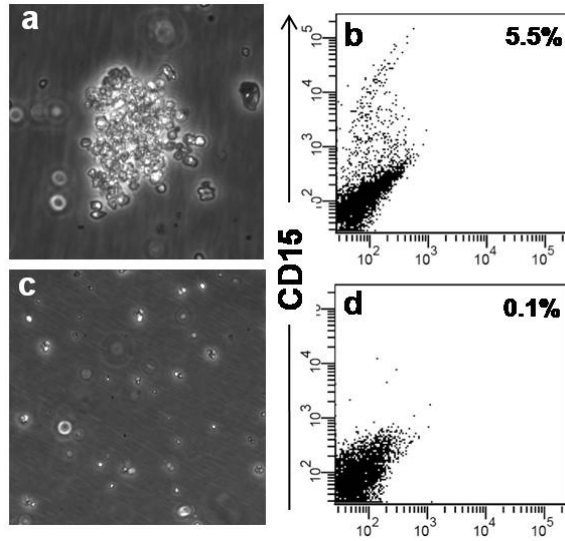


Figure 3-11. Methycellulose colony assay of spleen cells from chicken embryos that were injected CD34+ day-10 hEB cells (a and b) or PBS (c and d) at E2 and harvested at E16.

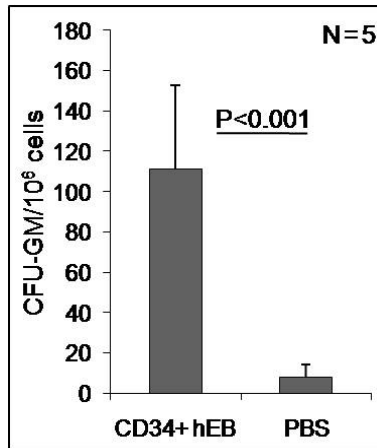


Figure 3-12. Average number of CFU-GM produced from chimeric spleen cells that were injected with CD34+ day-10 hEB cells.

3.3.4 Angiogenic potential of hEB cells in the chicken yolk sac

Yolk sacs which had been injected with unsorted day-10 hEB cells (Figure 3-13, d), CD34+ day-10 hEB cells (a, b, and c), or PBS (e and f) were analyzed by immunofluorescent staining at E14. VE-cadherin+ or vWF+ human endothelial cells were detected in the walls of chick blood vessels (Figure 3-13).

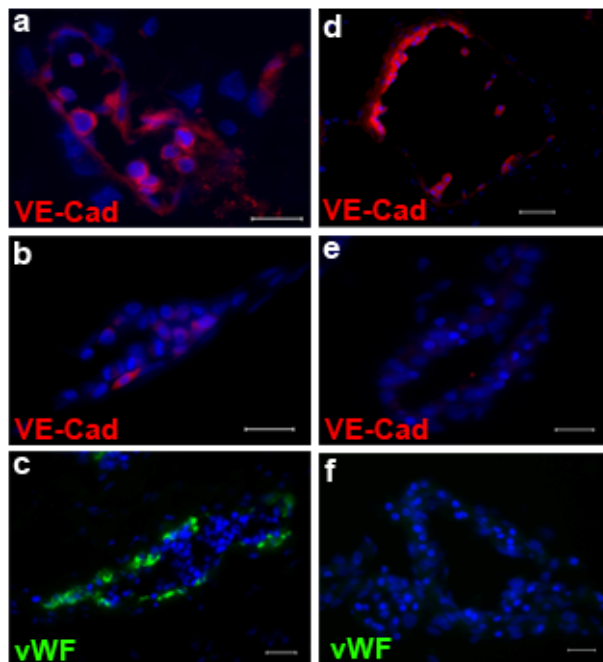


Figure 3-13. Immunofluorescent staining on sections of yolk sacs that received CD34+ day-10 hEB cells (a, b, and c), day-10 unsorted hEB cells (d), and PBS (e and f) at E2 and were analyzed at E15 to E16 of development.

Enzymatically digested chimeric or control yolk sacs were also analyzed by flow cytometry. CD34+ day-10 hEB cells derived CD31+ (9.8%) and Ulex europaeus ligand+ (10.5%) endothelial cells are shown in Figure 3-14 (upper row).

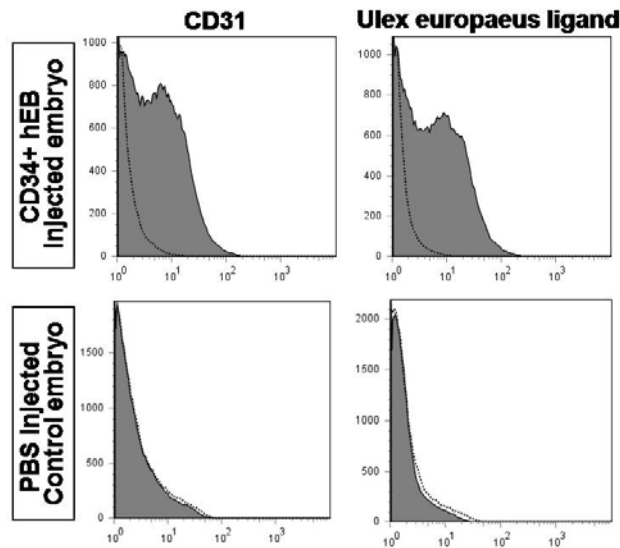


Figure 3-14. Flow cytometry analysis of enzymatically analyzed chimeric or control yolk sacs that stained positively for antibodies CD31 and Ulex europaeus agglutinin-1 (UEA-1) ligand.

In order to discern the presence of any human hemogenic endothelial cells in the chick yolk sacs, enzymatically digested chimeric yolk sacs, which were injected with CD34+ day-10 hEB cells, were sorted on expression of endothelial cell markers. Both CD31- and CD34-positive human endothelial cells were sorted (Figure 3-15) and cultured in the methylcellulose colony assay condition using human cytokine mixtures. Two weeks later, some colonies were observed, but the colony size (less than 20 cells/colony) and the numbers of colonies (less than 10 colonies/ 1×10^6 cells) were small (Figure 3-16). We posit that this matter might be more accurately investigated by modifying the culture conditions to preferentially expand the rare

population of hemogenic endothelium *in vitro* so that one might further analyze their hematopoietic differentiation ability.

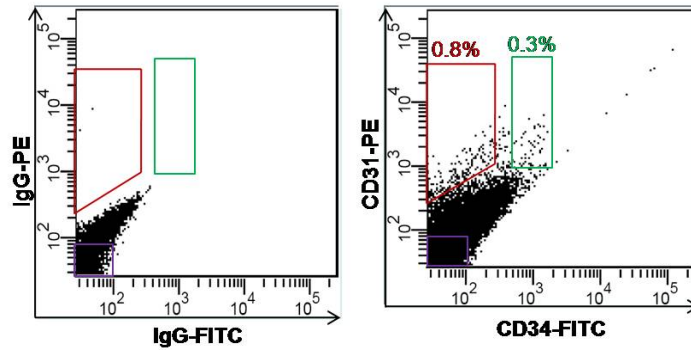


Figure 3-15. Sorting gates of enzymatically digested chimeric yolk sac (E14) that were injected with CD34+ day-10 hEB cells at E2.

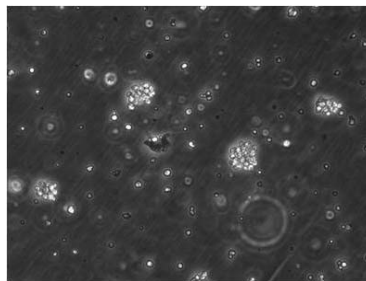


Figure 3-16. Methylcellulose colony assay of enzymatically digested yolk sacs (E14) which received CD34+ day-10 hEB cells at E2.

3.4 DISCUSSION

Although human embryonic stem cells can produce blood cells in culture, engraftment of hESC-derived hematopoietic cells *in vivo* has not been convincingly demonstrated yet. This is partially due to the lack of an appropriate, relevant xenochimeric model. However, even mouse ESC-derived hematopoietic stem cells do not engraft adult mice [29], probably because these ancestral stem cells cannot colonize the developed bone marrow on intravenous infusion. Indeed, ESC-derived HSC are related to the earliest blood-forming cells that emerge in the yolk sac and/or AGM region during ontogeny, and therefore are more likely to colonize embryonic blood-forming tissue rudiments than the bone marrow, which is the latest acquisition of the incipient hematopoietic system [77]. Ideally, ESC-derived HSC should be injected into the mouse embryo prior to the colonization of the liver and thymus rudiments (i.e. before E10), but this is technically infeasible. In contrast, the avian embryo is readily accessible to experimentation from the earliest stages of development. We took advantage of this availability to follow the development *in vivo* of the hESC-derived hemato-endothelial progenitors we have previously identified [4, 44]. We first committed hESC into hematopoietic/endothelial cell lineages, via hEB formation, then different stages (day 10 and day 17) and types (CD34+ or CD34-) of hEB cells were injected into the yolk sacs of E2 chicken embryos. CD34+CD45+ G-CSF mobilized hPBSC were used, in the same setting, as well characterized adult hematopoietic progenitor cells. Human cell engraftment was evaluated by FACS and immunohistochemical detection of human CD45+ cells in the blood-forming organs of the E14 to E17 host embryos.

All human cell populations injected engrafted the chicken embryos and yielded a progeny of blood cells, albeit with quantitative variations. Day-10 hEB cells produced higher numbers of human hematopoietic cells in host embryos compared with day-17 hEB cells. hEB derived

CD34⁺ cells yielded a larger progeny of human blood cells in the chicken than did the counterpart CD34⁻ cells. Conceptually, these observations confirm the ability of hESC derived progenitors to sustain hematopoiesis in an animal embryo, as previously suggested following *in utero* transplantation in the sheep [36, 61]. Furthermore, both unseparated and sorted CD34⁺ day-10 hEB cells produced human endothelial cells that participated in vitelline vascular development, as assessed by detection of human VE-cadherin and vWF on yolk sac sections. This confirms the ability of CD34⁺ day-10 hEB cells to develop into endothelial cells, that was previously demonstrated in culture [4, 44, 78, 79].

In addition to CFU-GM committed progenitors and CD13⁺ and CD14⁺ myeloid cells, substantial amounts (around 30%) of human erythroid cells were detected, by glycophorin A expression, in the spleens of chicken recipients of CD34⁺ day-10 hEB cells. In contrast, circulating human red cells were seldom found in the blood of host embryos, suggesting either that human red blood cells were considerably diluted in the chicken blood circulation, or that human erythroid progenitors maturing in the spleen were not released in the blood circulation in this experimental setting. Importantly, CD19⁺ IgM⁺ human lymphoid cells were also present in the bursa of Fabricius of host embryos, confirming, on the one hand, that multipotent, lympho-myeloid HSC were programmed in the hEB system used, mimicking AGM-type, rather than yolk sac hematopoiesis [37]. On the other hand, the presence of human B cells in host embryos demonstrated that chicken hematopoietic organs can also support the lymphoid development of human HSC, and therefore uncover the full repertoire of human blood cell lineages

Our results establish as a proof of principle that primitive human stem cells can sustain angio-hematopoiesis in the avian embryo. It is presumed that hESC derived hemangioblasts injected into the yolk sac mesoderm participated in the formation of vitelline vessels and blood

islands prior to contributing to embryonic hematopoiesis. The observed wave of human hematopoiesis is therefore likely primitive, transient, and should be eventually relayed, at later stages of development, to an intra-embryonic location. Alternatively, since hEB include progenitors of both primitive and definitive hematopoieses [4], we may have recapitulated both primitive and (adult) definitive waves of human blood cell ontogeny in these human/chicken chimeras. The latter hypothesis is supported by the detection of both human erythro-myeloid and lymphoid cell lineages in the host embryos. The assumption that the early avian embryo is permissive to the development of definitive, adult-type blood cell progenitors is also supported by the observation that adult hPBSC could also engraft on injection into yolk sac mesoderm. Evaluation of human blood cell compartments in such chimeric embryos at the latest stages of incubation and during post-hatching life should clarify these issues.

3.5 CONCLUSION

In conclusion, we propose a novel surrogate live model of human angio-hematopoiesis relying on the targeted transplantation of primitive stem cells into avian blastoderms. The following practical and theoretical advantages of this system can be highlighted; (1) chick embryos are accessible from the earliest stages of development and cells to be tested can be precisely injected in the anatomic site where incipient angio-hematopoiesis occurs, i.e., the yolk sac mesoderm. In contrast, mammalian hosts are restricted in these respects, and the route of injection (intra-peritoneal or intra-hepatic) is not as precise. (2) the transplanted cells seed an immunologically non-developed host [47] that is readily amenable to xeno-transplantation in the absence of

conditioning; and, (3) many embryos can be manipulated in the same experiment and embryo survival is satisfactory (up to 50%). The cost of fertilized chicken eggs is particularly low, as compared to that of laboratory mammals, and housing costs during development are negligible.

3.6 ACKNOWLEDGMENT

This project could be done with great help of Dr. Elias T. Zambidis, Dr. Jennifer Lucitti, Dr. Kimimasa Tobita, Joseph Tinney and Dr. Bradley B. Keller. We also thank to Dr. Solomon Yap, Bonnie Teng, and Kara T. Kleber for their help.

4.0 PERICYTE-LIKE CELLS DERIVED FROM HUMAN EMBRYONIC STEM CELLS

4.1 INTRODUCTION

4.1.1 Pericyte/ Perivascular cells

Pericytes are known as mesenchymal lineage cells that closely surround endothelial cells in the walls of small blood vessels (microvessels and capillaries) [80]. Perivascular cells include pericytes and smooth muscle cells that are recognized as mural cells residing in larger size blood vessel walls including arterioles and venules over 100 μm diameter. It has been reported that pericytes are relatively undifferentiated cells that can differentiate into fibroblasts, smooth muscle cells, or macrophages, as required [81-84]. They are important in blood brain barrier stability [85] as well as angiogenesis, regulation of blood vessel wall flexibility, migration of lymphocytes and monocytes, thus, and metastasis of tumorigenic cells [86-89]. In addition, pericytes are believed to be progenitors of a variety of other cell types including chondrocytes, adipocytes [90], and osteocytes [91, 92], which led to our speculation that this cell population could represent mesenchymal stem progenitor cells. Detailed studies were carried out to examine the myogenic potential of pericytes isolated from muscles [93], which were directed to the hypothesis that mesoangioblasts and muscle derived stem cells might be closely related to

perivascular cells [94-96]. Our group recently documented the anatomic location/source for pericytes, their cell surface marker expression, techniques for isolation and *in vitro* expansion, mesenchymal stem cell markers expression (in naïve pericytes and culture expanded pericytes), and mesenchymal lineage differentiation potential [48]. This groundwork concluded that CD146 is a crucial surface marker for the isolation pericyte/ perivascular cells from a broad range of human organisms including muscle, fat, pancreas, placenta, brain, heart, and skin.

4.1.2 CD146-expressing cells, from endothelial to hematopoietic lineage

CD146 is a membrane glycoprotein whose different homologs have already been identified and studied in the zebra fish, chick, mouse, and human [97-100]. This member of the immunoglobulin gene superfamily has been designated in the human species by various names. CD146 was first defined as a human melanoma-associated antigen [101-104] named MUC-18, Mel-CAM, M-CAM, or A32 melanoma-associated antigen; the chick homolog has also been reported as gicerin, HEMCAM (Hemopoietic, MUC18 related, Cell Adhesion Molecule), or c264 [99]. This variety of appellations and the conservation of this molecule through species suggest critical roles even if its cellular function is not yet completely understood.

Designated as S-endo-1, CD146 was later localized *in vitro* at the level of intercellular junctions of confluent endothelial cells [44, 45] before being identified as the antigen targeted by the endothelium-specific monoclonal antibody P1H12 [105]. Subsequently, this cell adhesion molecule [102, 106] was considered to be a new endothelial marker with identified roles in tumor, development and stem cell biology [106, 107]. Recently, human CD146 knockdown was performed using siRNA, indicating that CD146 had an implied role in vascular endothelial cell activity and angiogenesis by promoting migration and proliferation [108].

In 2005, CD146 was characterized in circulating endothelial cells (CEC) in peripheral blood [57]. CEC, which identified as CD146+ CD34+ CD105+ CD11b- cells, showed their ability to form capillaries in matrigel. Interestingly, expression of two stem cell markers, KDR and CD133, were elevated in this population *in vitro*. The author proposed that CD146-expressing CEC were angioblast-like endothelial progenitor cells (EPC) [57]. The hematopoietic/lymphoid potential of CD146-expressing cells was already suggested in 1996 by Vainio, et al. who demonstrated the lymphoid potential (in chicken) of double positive c264+ (later known as CD146) and c-kit+ cells. Structural similarities to, and a high sequence homology with, human MUC18 [99] was then established. Furthermore, CD146 has been proposed as an activation antigen of human T-lymphocytes. In 2005, Elshal, et al. identified a CD146+ lymphocyte subset in normal human peripheral blood. Peripheral blood monocytes include less than 1% CD146+ CD45+ cells, and subpopulations include CD3+, CD4+, and CD8+ T-cells (2 to 2.5%) as well as CD19+ B-cells (about 0.7%). The author of this article suggested that CD146+ T-cells exhibit an increased ability to adhere to endothelial cells as determined by an *in vitro* binding assay. The author concluded that CD146 is an intrinsic and inducible antigen of multiple lymphocyte subsets, and is possibly involved in adherence to the endothelium [98]. Based on previously mentioned publications it would be logical to investigate CD146 roles in the human hematopoietic system.

4.1.3 Perivascular cells derived from hESC

A few studies have documented the ability to generate endothelial cells and mural cells (perivascular cells and smooth muscle cells) from embryonic stem cells. However, the detailed marker expression profile for pericytes was not previously well defined, so most studies relied on

the expression of alpha smooth muscle actin (α -SMA) [109-111], which includes both smooth muscle cells and perivascular cells. Pericytes in microvessels and capillaries have been characterized to express CD146, NG2, and PDGFR- β , but not CD31, CD144, vWF, or α -SMA. In addition, α -SMA, an intracellular marker, is not viable for cell sorting. Based on our detailed characterization of pericytes in various human fetal and adult organisms, we conclude that using CD146 expression with a concomitant lack of mature endothelial cell markers (CD34, CD31, and/ or CD144) is essential as a means of identifying pericytes. We have observed the significant up- and down-regulation of CD146 in differentiating hESC with kinetics that followed the expression of the mesodermal lineage marker, Brachyury. Therefore, we aimed to determine whether CD146⁺ CD34⁻ CD45⁻ pericyte like-hESC as a potential subpopulation of mesenchymal stem cells.

4.2 METHODS

4.2.1 FACS sorting pericyte-like hESC

Different stages of hEB or medium differentiated hESC were harvested for FACS analysis or cell sorting. The hEB dissociation method is outlined in Chapter 2.2.4. Medium differentiated hESC were harvested by using 0.25% trypsin/EDTA (Invitrogen) for 5 min, followed by filtration through 70 μ m cell strainers. Cells were incubated with mouse anti-human monoclonal antibodies, including CD34-PE, CD146-FITC, and CD45-APC. Pericytes were sorted for

negative expression of CD34 and CD45 and positive expression of CD146. Also, a population negative for CD34, CD45 and CD146 was sorted for comparison of experiments.

4.2.2 Myogenesis

In vitro myogenesis was performed on the CD146⁺ or CD146⁻ sorted cells from medium differentiated hESC. Sorted cells were cultured for 2 passages to expand total the cell numbers, and then replated (2×10^4 cell/cm²) in proliferation medium composed of DMEM, 10% FBS (Invitrogen), 10% horse serum, and 1% PS. When cells reached about 90% confluency, proliferation medium was replace with fusion medium, i.e., DMEM, 1% FBS, 1% horse serum, 1% PS, and 1% chick embryo extract (Accurate Chemicals). Medium was refilled every 2 to 3 days for 2 weeks.

A total of 1×10^5 CD146⁺ or CD146⁻ day-6 hEB cells were injected into cardiotoxin (2 μ g)-injured gastrocnemius muscles of SCID/NOD mice to examine *in vivo* myogenesis. Muscles were harvested 3 weeks post-surgery, and frozen in methylbutane cooled in liquid nitrogen. Mouse anti-human dystrophin (Novo Castra), desmin (Sigma), and human nuclear antigen (Chemicon) antibodies were used to detect human myofibers in mouse muscle.

4.2.3 Hematopoiesis

An MS5 murine stromal cell co-culture system was used for *in vitro* hematopoiesis. Day-2 differentiating hESC were sorted for expression of CD146, and 500 sorted cells were plated to the monolayer of MS5 that was prepared 1 day before co-culture. For hematopoietic medium we used Myeolcult 5100 (StemCell Technologies) with or without human erythropoietin (EPO) and

granulocyte-colony stimulating factor (G-CSF). Half of the medium was replenished every week. After 3 weeks of co-culture (without EPO and G-CSF), the cells were collected by trypsinization and re-cultured in hematopoietic methylcellulose semi-solid medium (H4434, StemCell Technologies), which included human hematopoietic cytokine mixtures. After 2 weeks in culture, cells were pooled in PBS, observed for morphology, and analyzed for their expression of CD34, CD45, CD56, and CD146.

4.2.4 Neurogenesis

Sorted CD146⁺ or CD146⁻ day-6 hEB cells were plated in 24-well plates (2×10^4 cells/cm²) in DMEM with 10% FBS. The next day, this medium was replaced by a pre-induction medium composed of DMEM, 20% FBS, and 1mM 2-ME. Neuronal differentiation was initiated 24 hours later by replacing with differentiation medium, composed of DMEM, 2% dimethylsulfoxide, and 200 μ m butylated hydroxyanisole (BHA) [62]. Medium was replaced every 2 to 3 days for 10 days, and fixed with 1% paraformaldehyde prior to immunofluorescent staining with nestin (Santa Cruz), neurofilament (NF, Chemicon), tyrosine hydroxylase (TH, Chemicon), and CNPase (Sigma).

4.3 RESULTS

4.3.1 Characteristics of CD146+ hESC

CD146+ expression is shown in hEB section or differentiating hESC colonies by immunofluorescent staining (Figure 4-1). CD146+ cells are located in the outer layer of cystic hEB and the outer edge of differentiating hESC colonies.

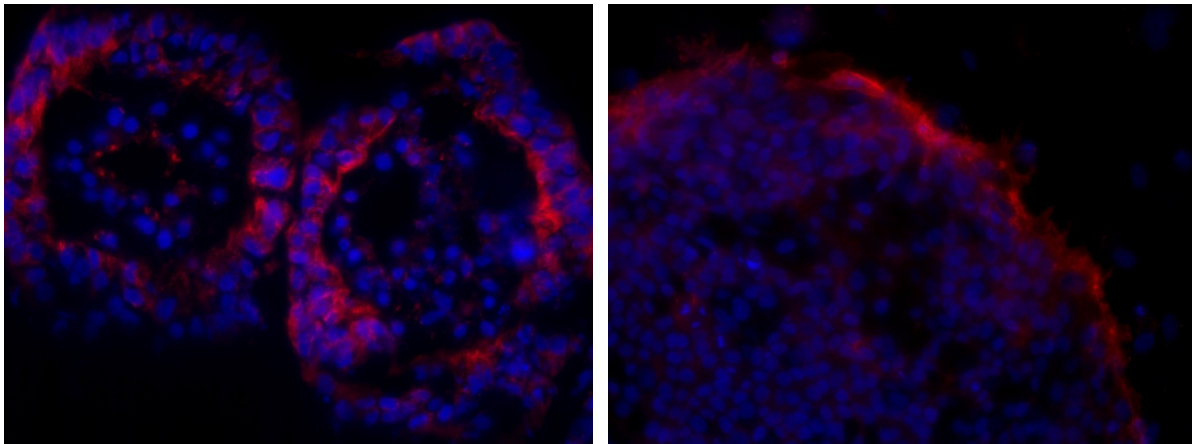


Figure 4-1. Immunofluorescent staining of CD146 (red) on day-8 hEB (left) and a medium differentiated day-2 hESC colony (right)

Different stages of hEB and medium differentiated hESC were collected to examine their marker expression by FACS analysis. CD146 and NG2 were used for the perivascular cells and CD34 was used to mark endothelial or hematopoietic progenitor cells. As soon as hEB differentiation starts, CD146 and NG2 expression was dramatically increased, peaking around day-8 (Figure 4-2). CD146 and NG2 expression showed similar kinetics of up- and down-regulation.

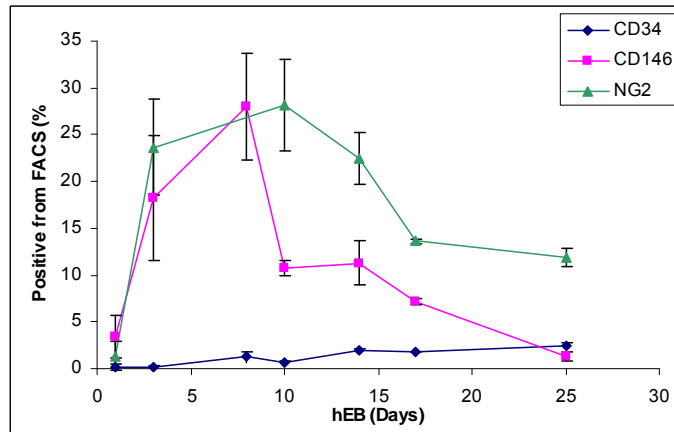


Figure 4-2. FACS analysis of different stages of hEB on expression of CD34, CD146, and NG2.

Medium-differentiated hESC were collected in different stages and analyzed by FACS. CD146 expression peaked at day-2 of differentiation, which is earlier than hEB differentiation. There was little or no expression of endothelial cell markers (CD34 and CD144) at day-2 differentiation.

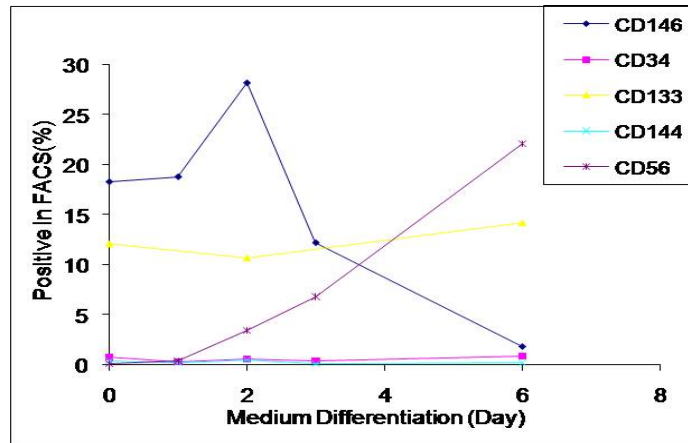


Figure 4-3. FACS analysis of different days of medium-differentiated hESC on expression of CD146, CD34, CD133, CD144, and CD56.

Frozen sections of day-6 hEB were stained with CD34, CD146, and NG2 (Figure 4-4). CD34-positive cells appear scattered in hEB while, CD146 and NG2 positive cells formed a circular shape in hEB.

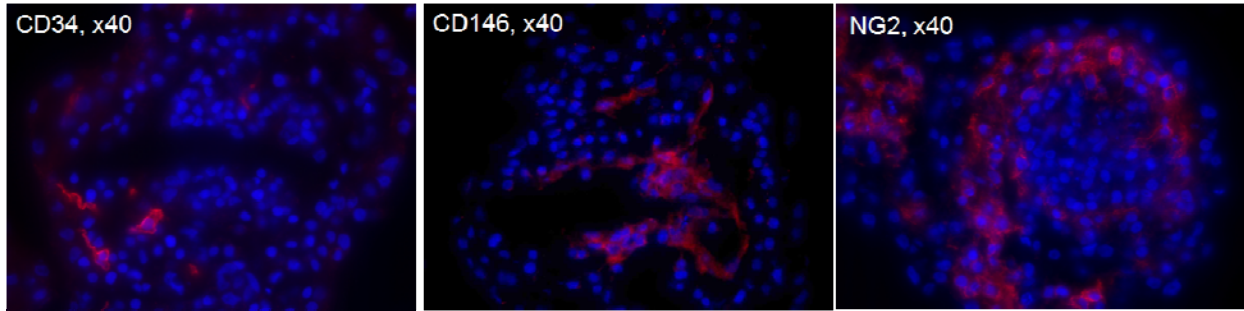


Figure 4-4. CD34, CD146, and NG2 staining of frozen sections of day-6 hEB.

FACS sorting charts are shown in Figure 4-5. Both day-8 hEB and day-2 medium-differentiated hESC showed abundant expression of CD146. CD34 expression differed between hEB, which co-expressed CD34 and CD146, and medium-differentiated hESC, which only expressed CD34. Both differentiation methods, however, allowed for sorting by CD146+ and CD146- population for further lineage differentiation.

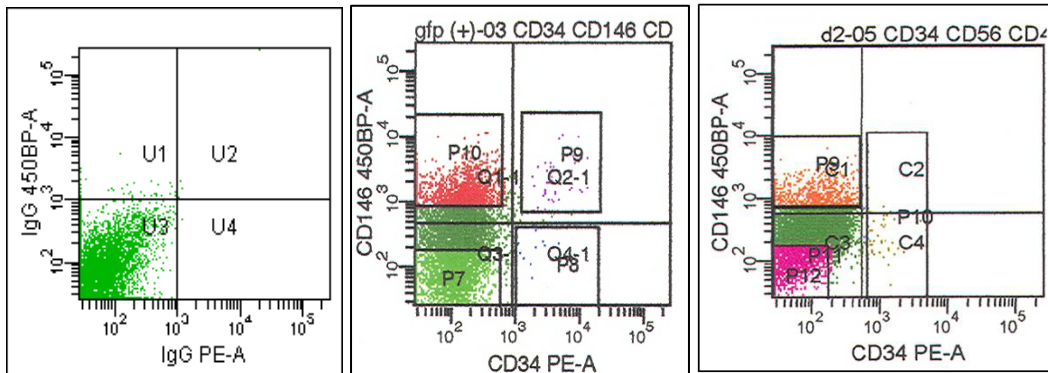


Figure 4-5. FACS analysis on expression of CD146 and CD34; isotype controls (left), day-8 hEB (middle), and day-2 medium differentiated hESC (right).

4.3.2 Myogenic potential

Both CD146+ and CD146- day-8 hEB cells expressed desmin and α -SMA after 10 days of *in vitro* myogenic differentiation. Desmin-positive cells did not form multi-nucleated myofibers, which are commonly observed in myotubes, but did generate circular shapes of cells. Myogenic differentiated CD146+ hEB cells exhibited co-expression of desmin and α -SMA but post-myogenic differentiated CD146- hEB cells included both co-expression of α -SMA and desmin as well as α -SMA single positive smooth muscle cells.

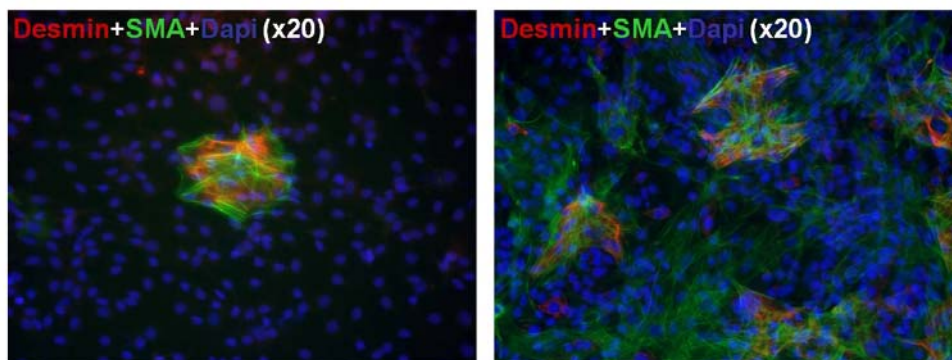


Figure 4-6. *In vitro* myogenic differentiation of CD146+ hEB (left) and CD146- hEB (right).

CD146+ day-8 hEB were injected into the gastrocnemius of cardiotoxin-conditioned SCID/NOD mice to examine their *in vivo* myogenic differentiation potential. Three weeks after transplantation, anti-human dystrophin positive myofibers were observed in the injected section of muscle (Figure 4-7). Most of the dystrophin-positive myofibers were small in size and the nuclei

were located in the center of the myofibers, which is a typical phenotype for newly generated myofibers.

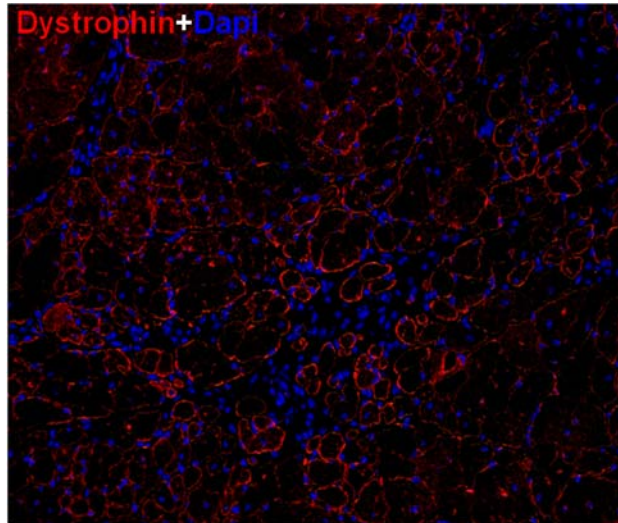


Figure 4-7. Dystrophin-positive muscle fibers derived from CD146 pericyte-like hESC.

CD146+ day-8 hEB cells were also injected with green fluorescence beads in another set of recipient mice to recognize the injection sites. We observed green fluorescence beads and desmin-positive, small sized myofibers in the same location.

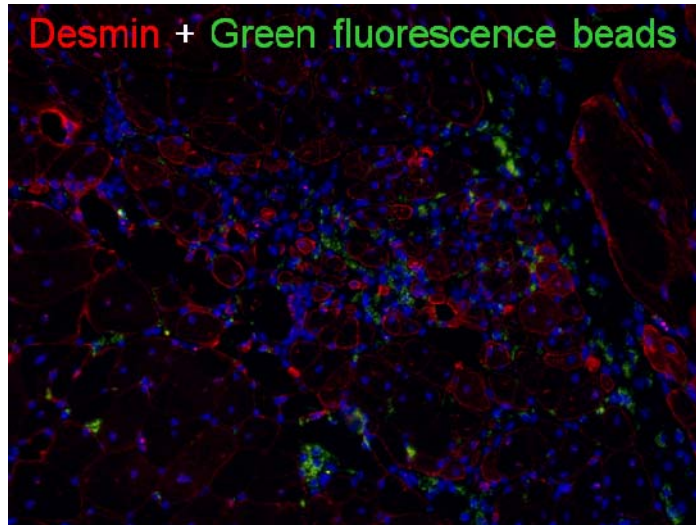


Figure 4-8. Desmin staining of SCID/NOD mice muscle that was injected with day-8 CD146+ hEB cells and green fluorescent beads (3 weeks post-transplantation).

The chimeric mice muscles that were injected with day-8 CD146+ hEB cells were stained with human nuclear antigen (HNA) and confirmed the presence of human cells.

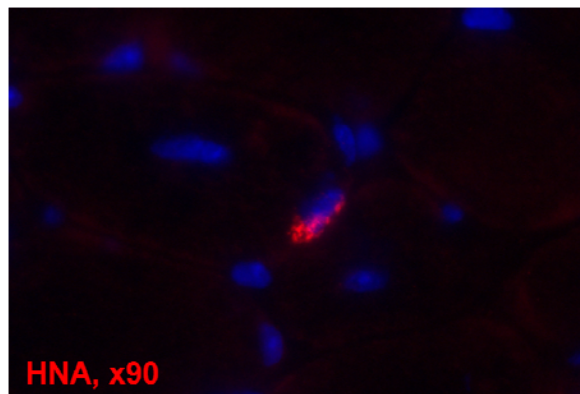


Figure 4-9. Human nuclear antigen (HNA)-positive human cells in the muscle of SCID/NOD mice that were injected with day-8 CD146+ hEB cells.

4.3.3 Hematopoiesis

CD146+ hESC were cultured under hematopoietic differentiation conditions (supported by coculture of MS5). Groups of cells formed cobblestone morphology, while others were characterized as floating cells with mature hematopoietic cell morphology (Figure 4-10).

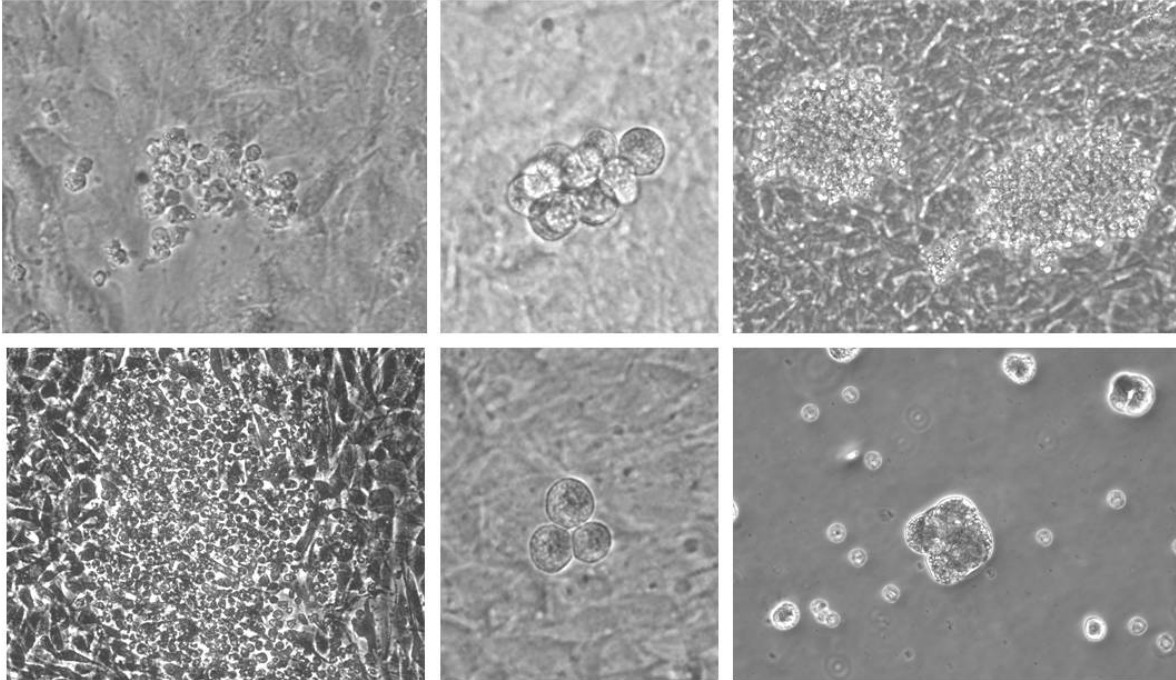


Figure 4-10. Hematopoietic differentiation of CD146+ hESC on MS5 stromal cells.

After co-culture with MS5 murine stromal cells for long term proliferating cell expansion, cells were collected by trypsinization and re-cultured in methycellulose hematopoietic colony assay medium. While CD146+ hESC did not express CD45 in the beginning of differentiation, after hematopoietic differentiation, approximately 20% did. The expression of CD146 decreased to about 5%, at which point CD34 and CD56 expression was also observed (Figure 4-11). However, these cells did not form the typical hematopoietic colonies, i.e., colony forming units-granulocytes/macrophage (CFU-GM) or erythroid colonies.

Instead, they formed hEB that included CD45+ hematopoietic cells (Figure 4-10, lower right). This is might be due to the fact that day-2 medium differentiated hESC still included undifferentiated stem cells, leading to the formation of hEB in semisolid medium. In order to observe the hematopoietic differentiation potential of CD146+ pericyte like-hESC, it is recommended to perform the experiment with day-8 CD146+ CD34- CD45- hEB cells.

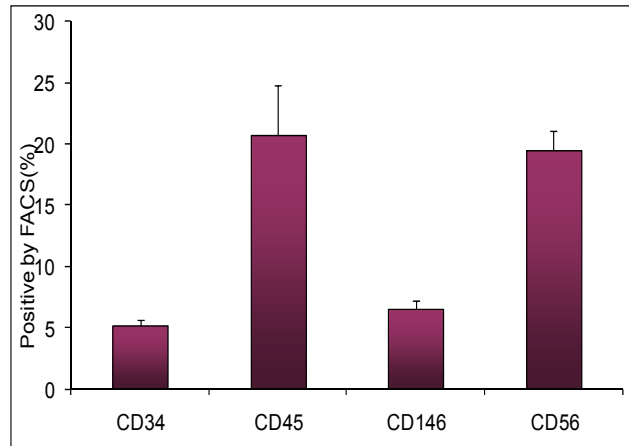


Figure 4-11. FACS analysis after hematopoietic differentiation of CD146+ hESC.

4.3.4 Neurogenesis

CD146+ hESC were stained with nestin and neurofilament (NF) before and after neural differentiation. CD146+ hESC did not express NF, but the majority of cells expressed nestin. A few NF expressing cells were observed as differentiation began, and all survived cells under 10 days of neural differentiation conditions expressed NF. These NF-positive cells did not express nestin suggesting that the cells went through the terminal differentiation.

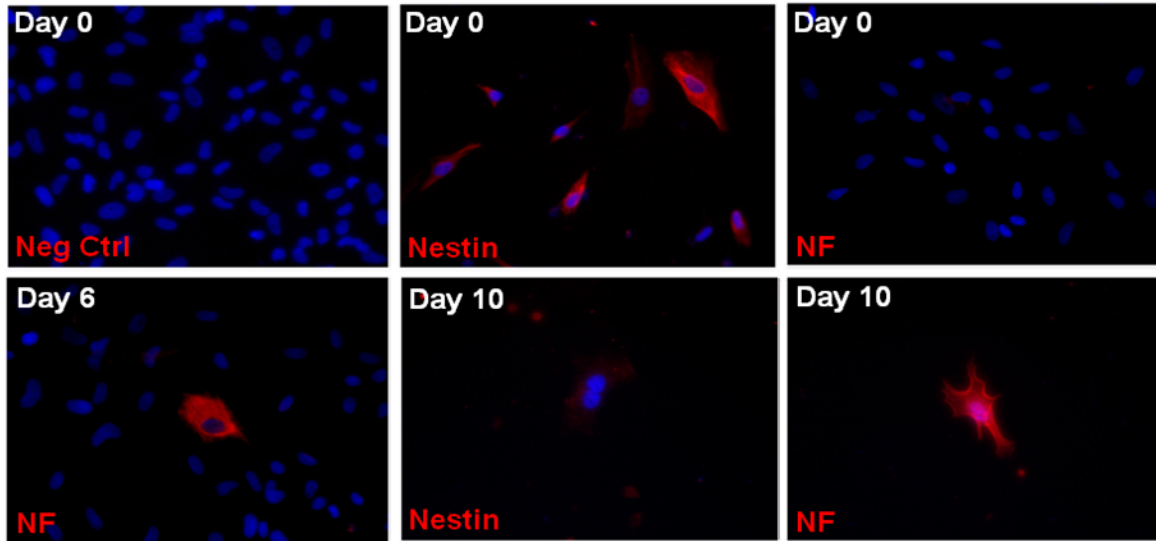


Figure 4-12. Nestin and neurofilament (NF) expression of CD146+ hESC before (Day 0) and after (Day 6 and Day 10) neural differentiation.

CD146+ day-2 medium-differentiated hESC were under neural differentiation for 10 days. Many of them did not survive the culture conditions. Cell culture was initiated with 1×10^4 cells/cm², but only a few cells were still attached post-differentiation. Cells still alive after the differentiation expressed NF but no other neuronal cell markers tested, including tyrosine hydroxylase (TH), which is involved in the conversion of phenylalanine to dopamine, and CNPase, which is a marker for oligodendrocytes (Figure 4-14). Interestingly, CD146- day-2 medium-differentiated hESC expressed these two functional neuronal markers after differentiation. More numbers of cells survived after 10 days of neuronal differentiation condition. Differentiated cells lost expression of nestin, but were highly positive for NF, TH, and CNPase (Figure 4-15).

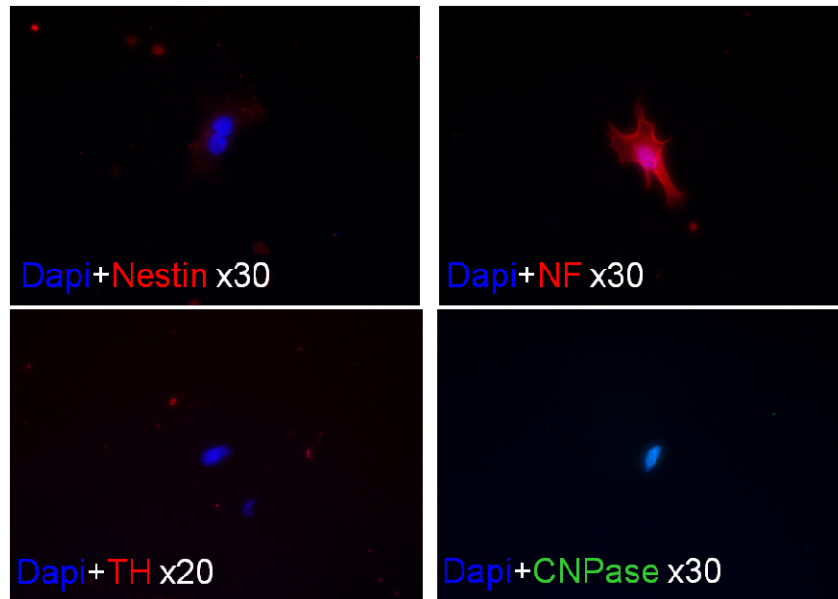


Figure 4-13. Neuronal marker expression of CD146+ hESC after 10 days of *in vitro* differentiation.

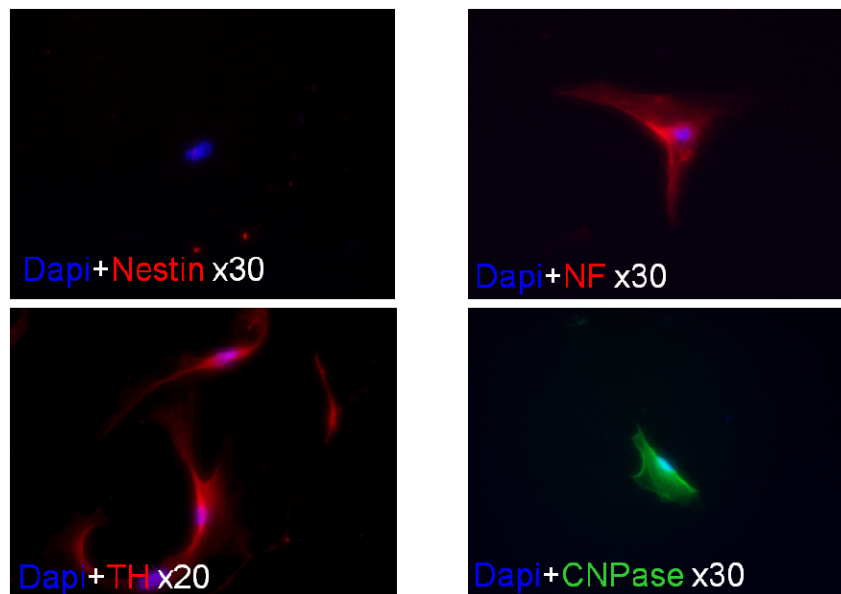


Figure 4-14. Neuronal marker expression of CD146- hESC after 10 days of *in vitro* differentiation.

4.4 DISCUSSION

Human embryonic stem cells (hESC) were differentiated by two methods (hEB and medium differentiation) that both used serum. The main difference between each of these methods is that hEB is a three-dimensional culture system that uses aggregates of hESC, while medium differentiation is a two-dimensional culture system where cells are grown in layer on a plate. In our experiments, the medium differentiation method induced faster emergence of CD146 expression (peaked at day 2) compared to the hEB system (peaked at day 8). We demonstrated that both methods allowed for the successful sorting of CD146⁺ pericyte-like hESC, which permitted us to perform further differentiation experiments. Pericyte-like hESC derived from both of the above methods could, for instance, undergo *in vivo* myogenic differentiation to produce myofibers when injected into cardiotoxin-injured muscle. Further, hematopoietic and neural differentiation were observed in experiments using CD146⁺ medium-differentiated hESC.

It is too early to, however, to make conclusive arguments regarding the hematopoietic differentiation potential of CD146⁺ hESC obtained from medium differentiation. It is assumed that the cell population derived from this method included some portion of undifferentiated cells, as we observed hEB formation instead of typical mature hematopoietic colony formation when these cells were grown in semi-solid hematopoietic methylcellulose medium. Also, we have not yet examined the hematopoietic potential of CD146⁺ CD34⁻ CD45⁻ hEB cells. We suggest the following two aspects are important to observe: (1) potential for differentiation into mature hematopoietic cells; and, (2) capacity to support other hematopoietic stem/progenitor cell expansion and self-renewal in a manner to stromal cells. It is known that bone marrow stromal cells support the low numbers of high hierarchical long-term proliferating hematopoietic stem cells [112-115]. One of the reasons for this may be the close anatomic location and interaction of

bone marrow stromal cells (or osteoblasts) and hematopoietic stem cells residing in bone marrow. Since perivascular cells have shown a high ability to differentiate into osteocytes [48, 81, 82, 90, 116], it would be interesting to observe whether this cell population has the ability to support hematopoiesis.

Data regarding neural differentiation demonstrated that CD146- hESC included higher numbers of ectodermal lineage cells. It was observed that CD146+ hESC did not remain healthy when placed under neurogenic differentiation conditions, with the majority of cells dying during the 10 days. Even though we could obtain neurofilament+ neural differentiated cells from CD146+ hESC, it was rare a population. We did, however, note that a greater number of CD146- hESC retained healthy morphology after 10 days in neurogenic differentiation conditions. In addition, functional neural markers, tyrosine hydroxylase (marker for dopaminergic neurons) and CNPase (marker for oligodendrocytes) were detected from differentiated CD146- hESC but not from CD146+ hESC.

To obtain more precise pericyte-like hESC, the use of additional pericyte markers (CD146, NG2, PDGFR- β , and/or alkaline phosphatase) has been suggested. It is true that more choices for directly conjugated monoclonal antibodies for pericytes are now commercially available; combination of such pericyte markers would enhance the ability to characterize and isolate the perivascular population from hEB. Furthermore, recent publications provide valuable information on identification and the developmental potential of perivascular cells [116-118] that would benefit future studies on perivascular cells derived from hESC.

In order to observe the CD146+ hESC/hEB cells as a potential mesenchymal stem cell population, it is important to observe more detailed mesenchymal lineages of differentiation including osteogenesis, adipogenesis, and chondrogenesis. Also, greater research into their

capacity for vasculogenesis/angiogenesis will promote the understanding of the, as yet, undefined developmental relationship between perivascular cells, endothelial cells, and smooth muscle cells.

4.5 CONCLUSION

In summary, we obtained CD146+ pericyte-like cells from differentiated hESC and hEB. They demonstrated high myogenic differentiation capacity, but examination of hematopoietic potential needs to be further explored with future experiments. CD146- differentiated hESC displayed a greater propensity to include ectodermal lineage cells compared to CD146+ cells as observed by the presence of dopaminergic neuron and oligodendrocyte marker-expressing cells. This study suggests that hESC represent a useful tool to investigate the developmental affiliation between perivascular cells, mesodermal precursors, and/or mesenchymal lineage cells.

5.0 HUMAN FETAL PLACENTA BLOOD VESSEL CELLS: MIGRATION AND MYOGENIC REGENERATION POTENTIAL

5.1 INTRODUCTION

Stem/progenitor cells are widely distributed in a variety of tissues throughout the fetal and adult human body (e.g., blood, bone marrow, liver, and muscle) [119-122]. Studies suggest that stem/progenitor cells may reside in the walls of blood vessels [118, 123-125], and, recently, we demonstrated that perivascular cells have the ability to regenerate skeletal muscle [48]. Therefore, we hypothesize that the vasculature within the human fetal placenta may serve as a source of stem/progenitor cells that could be useful in efforts to regenerate skeletal muscle fiber.

5.1.1 Human placental structure

The placenta is an extremely active organ that grows and develops throughout pregnancy. Human placenta is composed of 3 layers: amnion, chorion, and decidua (Figure 5-1) [126-129]. Among these three layers, the amnion and chorion are developed from the embryo, and the decidua is maternally derived. The amnion layer is composed of 2 cell types, which are epithelial and fibroblastic cells. The chorion part of placenta includes chorionic plate and chorionic villi (Figure 5-2) [130]. The chorionic villi provide an enormous surface area for the exchange of oxygen and nutrients from maternal to fetal blood. To give us an idea of the tremendous

vascularization within the chorionic villi, the length of the chorionic capillaries at term pregnancy are approximately 50 km. This large distribution of fetal blood vessels in the chorionic villous area explains why we elected to focus our study there.

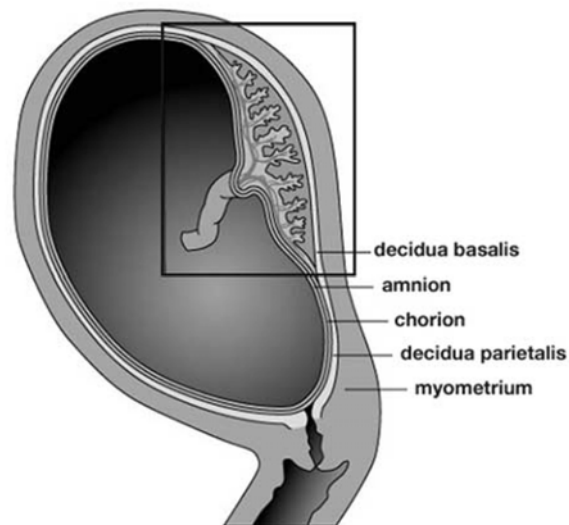


Figure 5-1. Structure of human placenta [128].

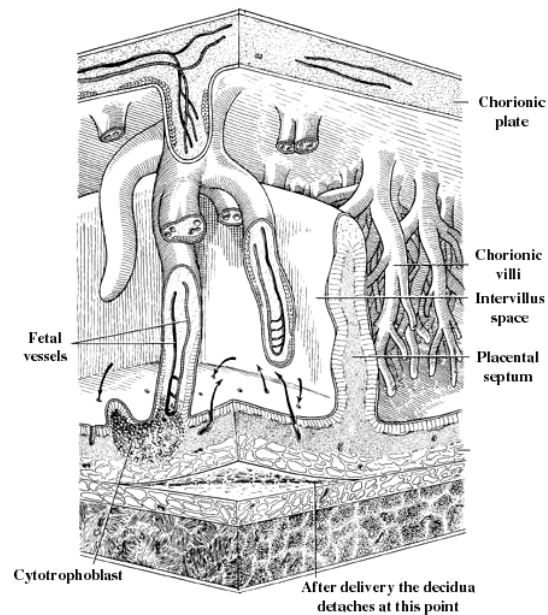


Figure 5-2. Scheme of human placenta chorionic plate and villi [130].

5.1.2 Stem cells derived from human placenta

The fetal tissues of the placenta can be a valuable source of stem/progenitor cells for regenerative medicine. Based on a number of articles, amniotic fluid and amniotic epithelial cells express stem cell markers (Oct-4, SSEA-3, SSEA-4, TRA-1-60, and/or TRA-1-81) and differentiate into various cell types including adipogenic, osteogenic, myogenic, endothelial, neuronal, and hepatic lineages. [129, 131-135]. In 1968, Pattillo, et al. identified and cultured trophoblastic stem cells from human villous placenta *in vitro* [136]. In addition, a few articles demonstrated that placenta villi stem cells exhibited chondrogenesis, osteogenesis, and adipogenesis [137, 138], suggesting the presence of mesenchymal progenitor cells. As cells in these studies were obtained from unsorted, out-grown implants of villi without detailed marker profile examination, it remains to be defined which cell population from the villous area is the stem/progenitor cell population.

5.1.3 CD146 in placenta

Angiogenesis, the growth of new blood vessel from pre-existing vessels, is a frequent event in fetal placenta; the main players in this process are trophoblasts, invasive endothelial cells, and pericytes [127, 136, 139]. Shih, et al. documented that CD146 (Mel-CAM) is expressed in the intermediate trophoblastic cell line, IST-1, which was established from a human placenta of 7 weeks gestation. This adhesion molecule, which expressed in the intermediate (extravillous) trophoblasts, is involved in migration and implantation. Shih, et al. also demonstrated that CD146 was not expressed in cytotrophoblasts and syncytiotrophoblasts [140]. In the mid-gestation of placenta (18 to 23 weeks of gestation), CD146 is not expressed in extravillous

trophoblasts but the perivascular cells of villi test positive for this marker based on our exclusive immuno-histological analysis. Taken together, this information would indicate that, CD146-expressing cells in fetal placenta are actively involved in migration, angiogenesis, the adhesion process, and the process of securing vascular walls as perivascular cells. Therefore, we aimed to examine whether CD146-expressing cells from the mid-gestation placenta exhibited these properties and provided myogenic potential.

5.2 METHODS

5.2.1 Isolation of vasculature from human fetal placenta

Blood vessels in the chorionic villi of fetal placenta were obtained from mid-gestation (18 to 23 weeks) of pregnancy (interruption with agreement in the form of a written consent). Whole fetal placenta was washed several times in phosphate buffered saline (PBS) until most red blood cells were removed. The villi area was separated from the chorionic plate and stretched out using 2 forceps to separate vessels from each other. Vessels were cut, under a dissecting microscope, with size of approximately 1mm³ for transplantation into mouse muscles (Figure 5-3), or 5 to 8 mm length for histological analysis.

Purified villi vasculature was cultured *in vitro* using different coating materials (0.2% gelatin, type-I collagen, fibronectin, or no-coating) and medium [proliferation medium (PM) or endothelial growth medium (EGM2, Lonza)]. Five to seven days later the first outgrowth of cells were observed, and cells could be seen actively growing out. When out-grown cells reached over 80% confluency, the vasculature pieces were moved into new coated or non-coated plates where

they were continued in culture. This procedure was performed every week up to the 10th out-growth. Monolayers of out-grown cells were further expanded in culture for another 1 to 2 passages in alpha-MEM (α -MEM, Invitrogen) supplemented with 20% FBS, and 1% PS, after which the cells were used for cell sorting.

5.2.2 Immunofluorescent staining

***In situ* staining of whole blood vessel vasculature:**

Pieces of purified vasculature from fetal placenta villi were placed either on a glass slide or in a 48-well culture plate, and stained with mouse anti-human CD34-pure (BD Pharmingen) followed by goat anti-mouse biotin (Dako) and streptavidin-Cy3 (Sigma). After that, CD146-FITC (Serotec) was co-stained for 2 hours at room temperature (RT). Stained vessels were mounted on a glass slide and observed under a microscope (Nikon Eclipse, TE2000-U).

Immunofluorescent staining on frozen sections of placenta villi:

Isolated vessels were embedded in tissue freezing medium (Triangle Biomedical Sciences), frozen in the vapor of liquid nitrogen, and cryosectioned in 6 to 7 μ m thick. Sections were stained for 2 hour at RT with mouse anti-human CD31 (Santa Cruz Biotechnology), CD34 (BD Pharmingen), CD56 (BD Pharmingen), CD144 (Santa Cruz Biotechnology), CD146 (BD Pharmingen), KDR (flk-1, Santa Cruz Biotechnology), alpha-smooth muscle actin (α SMA, Sigma, FITC conjugated), and rabbit anti-human vWF (US biological, FITC conjugated). Antibodies that are unconjugated for fluorochrom were stained with goat anti-mouse biotin (Dako) and streptavidin-Cy3 (Sigma) sequentially.

Immunocyto staining on culture cells:

Cells outgrown from vessels on gelatin coated plates in EGM2 (Lonza) were replated in 48-well plates for immunocyto staining. Cells were fixed in a mixture of cooled (-20°C) methanol and acetone (1:1) for 5 min and washed in PBS. Then, cells were incubated in purified rabbit anti-human PDGFR- β (Santa Cruz Biotechnology), mouse anti-human NG2 (BD Pharmingen), CD31 (Chemicon), CD44 (Invitrogen), CD90 (BD Pharmingen), CD144 (Bender MedSystems, Burlingame, CA), or CD146 (BD Pharmingen). Donkey anti-rabbit Alexa Fluor-488 (Molecular Probes) was incubated for visualization of PDGFR- β . For the other mouse anti-human unconjugated antibodies, biotinylated goat anti-mouse (Dako) and streptavidin-cy3 (Sigma) were incubated sequentially. Additionally, directly conjugated antibodies were co-stained using α -SMA-FITC (Dako), CD34-FITC (Miltenyi Biotec), CD146-FITC (Chemicon), or vWF-FITC (US Biological).

Cultured cells after *in vitro* myogenic differentiation were fixed in -20°C cooled methanol for 5 min prior to staining. Nonspecific binding of antibodies was blocked by incubation in 5% serum from animals in which secondary antibodies were raised. In order to use intracellular antibodies, cells were permeabilized with 0.3% triton in PBS. Mouse anti-human desmin (Sigma), myosin heavy chain-fast (MHC-f, Simga), and α -SMA-FITC (Sigma) were incubated with cells overnight at 4°C, and then goat anti-mouse biotin (Dako) and streptavidin-Cy3 (Sigma) were incubated sequentially the following day.

Immunofluorescent staining of frozen mouse muscle sections:

Harvested SCID/mdx mouse muscles were frozen in cooled methylbutane, at temperatures between -50 and -60°C, and sectioned to 6 to 10 μ m thickness. Sections were fixed in a 1:1

cooled methanol and acetone mixture at -20°C for 5 min prior to staining. Non-specific binding of antibodies was blocked by incubation with 5% serum (from animals in which secondary antibodies were raised) and 0.1% triton in PBS. Mouse anti-human dystrophin (hDys3, Novocastra, Newcastle upon Tyne, UK), spectrin (Novocastra), lamin A/C (Novocastra), human nuclear antigen (HNA, Chemicon), and rabbit anti-mouse dystrophin (mDys3, Abcam, Cambridge, MA) were incubated with samples overnight at 4°C, after which they were incubated with goat anti-mouse-biotin (Dako) and streptavidin-Cy3 (Sigma).

5.2.3 Flow cytometry analysis and cell sorting

Chorionic villi of placenta were dissociated by enzymatically in order to analyze by FACS analysis and cell sorting. Well washed and separated 4g of chorionic villi vasculature was minced and suspended in collagenase type I, II, and IV (all are 1 mg/mL, Sigma). After 30 min of incubation in a shaker with 120 rpm and 37°C, trypsin was added (final concentration 0.25%, Invitrogen) for another 10 min of incubation. Cells were filtered through 70 µm cell strainer and washed out remaining enzymes. Cell pellet was re-suspended in red cell lysis buffer and incubated for 15 min at RT. Followed by another centrifuge and wash, single cells were stained with mouse anti-human CD34-PE (DAKO), CD56-PE-Cy7 (BD Pharmingen), CD45-APC (BD Pharmingen), and CD146-FITC (Serotec).

5.2.4 *In vitro* myogenic differentiation

Cells obtained either from freshly dissociated placenta or from out-grown cells of villi vasculature were cultured under myogenic differentiation condition. Sorted and expanded cells were plated

in proliferation medium (PM; DMEM, 10% FBS, 10% horse serum, 1% chick embryo extract, 1% PS) at 2×10^4 cells/cm². When the cells reached approximately 70% confluency, half-diluted PM in DMEM was used in order to provide a lower concentration of serum. Gradient lowering of serum concentration proceeded until 2% serum concentration by dilution in DMEM was achieved. Medium was changed every other day, and cells were observed daily until multinucleated cells were observed.

5.2.5 *In vivo* myogenic differentiation

Four vessel pieces (1 mm³ each) were transplanted into the gastrocnemius muscle of SCID/mdx mice, which are genetically modified to not produce dystrophin protein and a model for Duchenne muscular dystrophy (DMD). Animals were sacrificed after 2 and 4 weeks of engraftment. Immunofluorescent staining was performed on cryosections to detect the expression of human specific antigen (HNA and lamin A/C), and myogenic markers [anti-human dystrophin (hDys3) and spectrin].

5.2.6 Adhesion assay

Out-grown cells from fetal placenta blood vessels were expanded for 1 to 2 passages and sorted on the expression of CD146. Then, cells were placed at concentration of 2×10^5 cells/well in 6-well plates which were either untreated, or pre-coated overnight with type-I collagen, 0.2% gelatin, 2 μ g/cm² fibronectin, or 1 mL/well FBS-saturation. One hour later, floating cells were removed and washed out in PBS. Cells attached in culture plates were fixed in 1% PFA for 15

min at RT, and stained with DAPI (Molecular Probes). Five images were randomly captured from each well to provide the average numbers of cells attached in each condition (n=3).

5.2.7 *In Vitro* Migration/ Wound Healing Assay

Sorted cells by their expression of CD146 or unsorted cells were plated in three wells of 12-well plates at a density of 5×10^5 cells/well in α -MEM supplemented with 20% FBS, and 1% PS, and cultured until confluent. A single wound was generated in the center of the cell monolayers by gentle elimination of the attached cells with a sterile plastic pipette tip [108]. Then, cells were washed in PBS twice and cultured in α -MEM supplemented with 2% FBS, and 1% PS. Three images were captured in each well (3 wells per each population), and 4 distances were measured from each picture to obtain averaged distance between the cells at day-0 (D_0 : distance at day-0). Twenty-four hours later, 3 images were taken in each well, and at least 10 distances were measured from each picture to obtain average distance between the cells at day-1 (D_1 : distance at day-1). Migration rate was calculated by following equation.

$$\text{Migration rate (\%)} = ((D_0 - D_1) / D_0) * 100$$

5.3 RESULTS

5.3.1 Isolation and characterization of placenta villi

Bundles of placenta villi were easily distinguishable by the large size of villous connection to the chorionic plate (Figure 5-3, top left, scheme of placenta structure). Purified villi were obtained by washing in PBS and removal of decidual area under dissecting microscope (Figure 5-3)

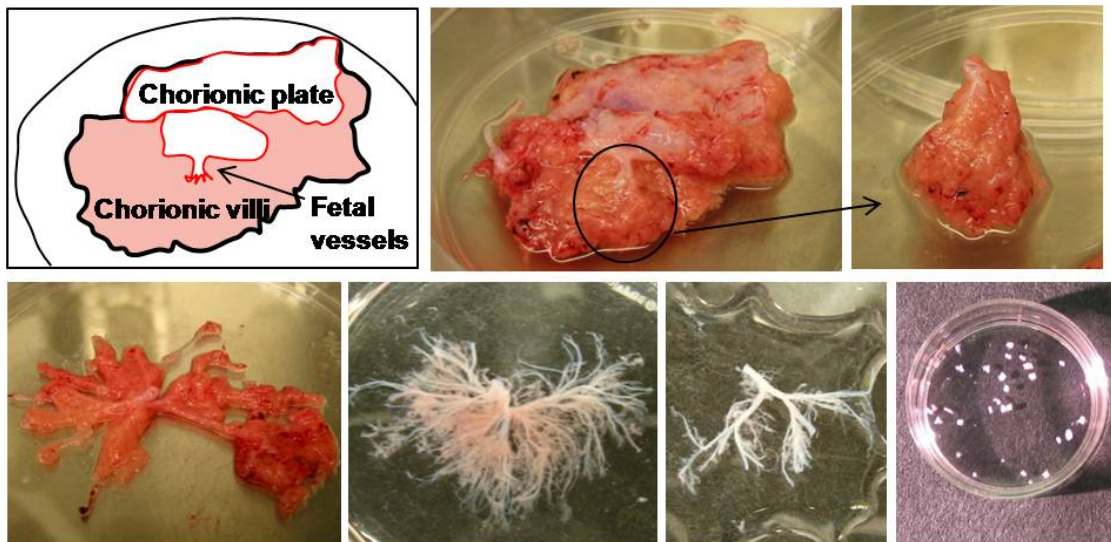


Figure 5-3. Isolation of placenta villi vasculature

Fetal blood vessels were spread on the surface or inside of the villi that are detected by staining of CD34 (Figure 5-4, top left, red) and CD146 (Figure 5-4, top middle, green), which corresponded to endothelial cells and pericytes, respectively (Figure 5-4, top right). CD34 expression is observed in the lumen of blood vessels, while CD146 expression was detected outside of the blood vessels. Cross sections of villi also showed fetal blood vessels composed of CD34⁺ or CD144⁺ endothelial cells and CD146⁺ pericytes/perivascular cells (Figures 5-4 and 5-

6). The outer membrane of the villi is composed of two layers of cells, supposedly, syncytial trophoblast and cytotrophoblasts. Immunofluorescent staining of cross-sections of chorionic villi confirmed the expression of CD133 for the cells located in the outer layer of villi (Figure 5-5). The inner part of chorionic villi included fetal blood vessels which stained positively for the expression of CD31, CD34, CD144, and CD146, and non-vascular cells or fibroblastic cells that were positive for α -SMA, CD56, and KDR (flk-1) (Figure 5-5).

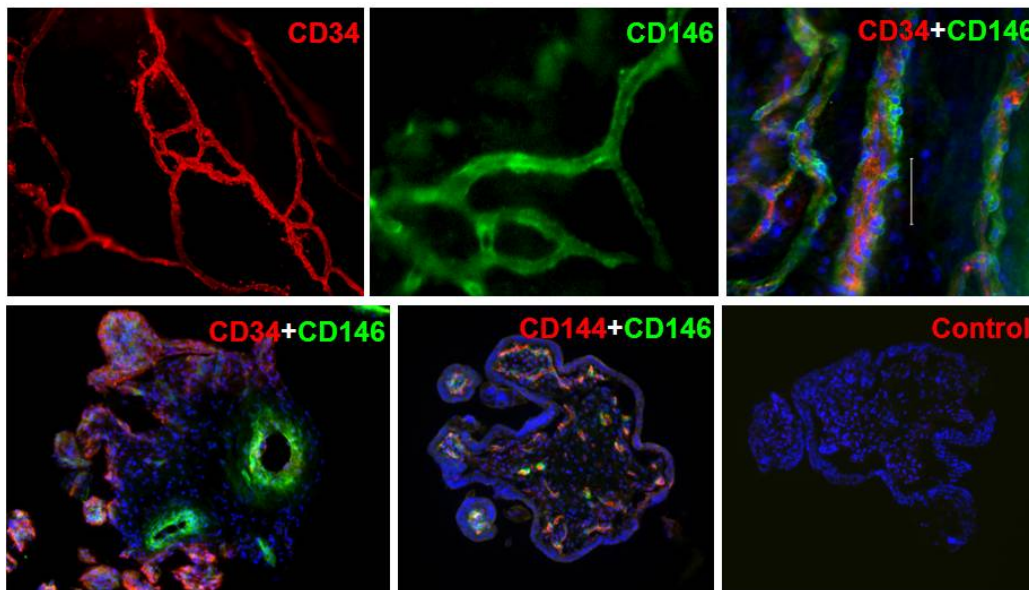


Figure 5-4. Immunofluorescent staining of villi vasculature.

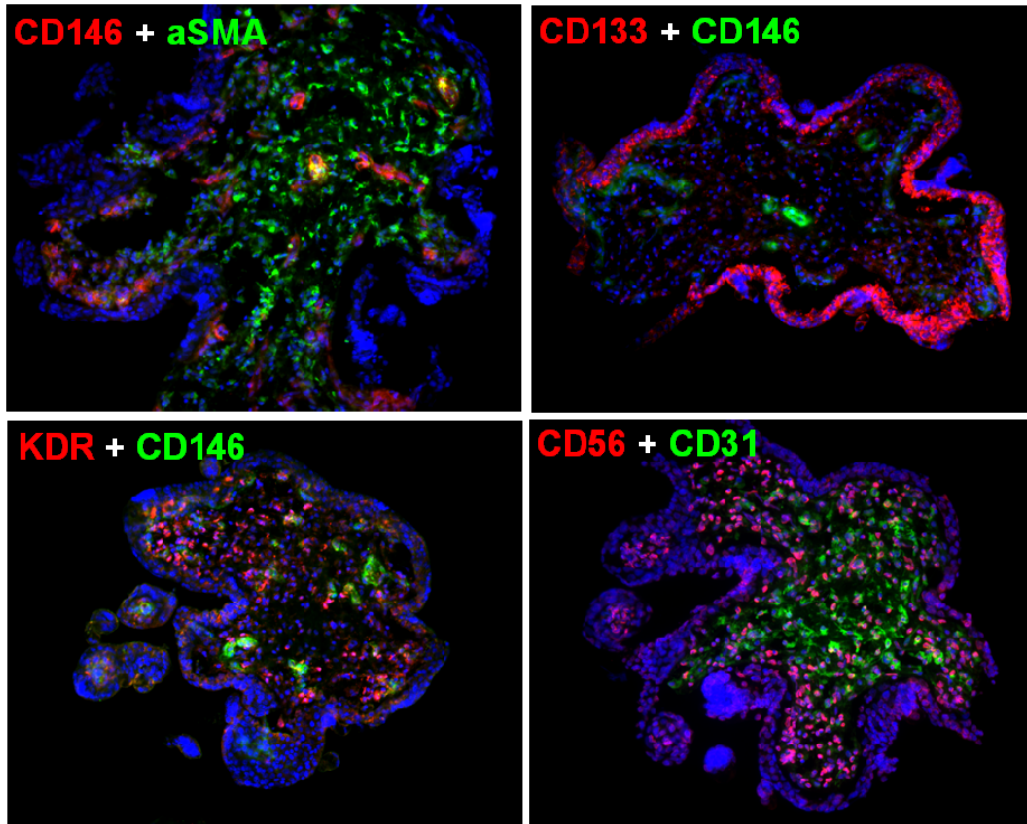


Figure 5-5. Immunofluorescent staining of cross sections of placenta villi

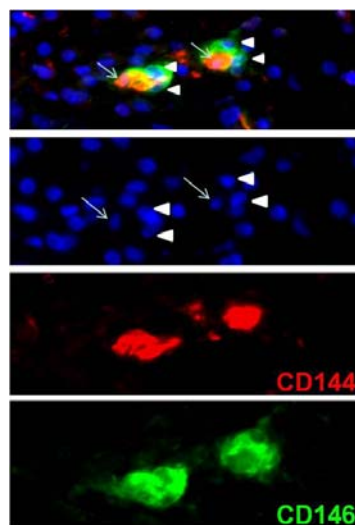


Figure 5-6. Immunofluorescent staining of villi micro-vasculature with CD144 and CD146

Enzymatically digested cell suspension of placenta villi included large numbers of CD45-positive cells ($31 \pm 11.7\%$, $n=3$). After gate of CD45+ and CD56+ cells, we could distinguish CD34+ endothelial cells ($3.5 \pm 2.6\%$, $n=8$) and CD146+ perivascular cells ($1.68 \pm 0.78\%$, $n=8$). Small percentages of CD34 and CD146 double-positive cells were also present (Figure 5-7).

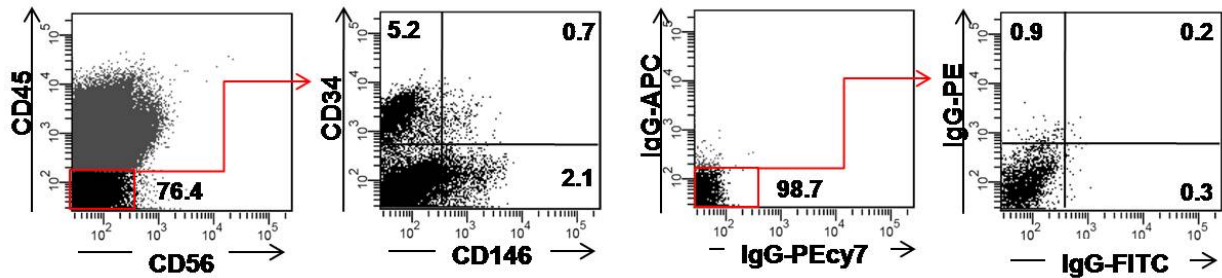


Figure 5-7. FACS analysis and sorting gates of enzymatically digested villi vasculature.

5.3.2 Characterization of vessel outgrown cells and enzymatically digested cells

Small pieces of purified placenta villi (2 to 3 mm length) were placed in collagen-coated, gelatin-coated, or non-coated plates with EGM2 or PM in order to induce cell out-growth. Polygonal and round shaped cells were observed from EGM2 out-grown cells, whereas fibroblastic morphology was seen from PM out-grown cells (Figure 5-8).

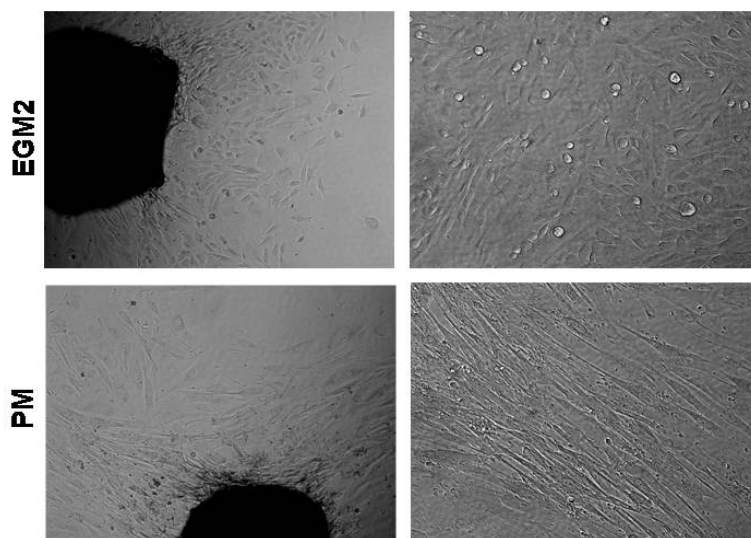


Figure 5-8. Phase contrast pictures of out-grown cells in EGM2 or PM.

The growth/proliferation rate was measured using a real-time image system that captured images of cell growth every 12 hours for 6 days. The results demonstrated that EGM2 significantly enhanced the growth rate compared to PM (Figure 5-9). There were no major differences in growth rate between cells cultured in coated or non-coated plates.

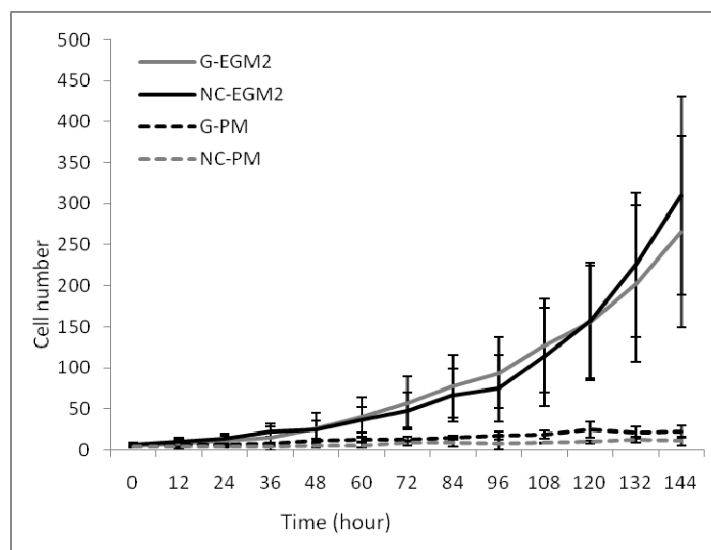


Figure 5-9. Proliferation rates of out-grown cells in different culture conditions

Despite the fact that no differences in proliferation rate were observed between cells grown on culture plates coated with different materials, we found that these extracellular matrix substances induced the out-growth of different cell populations. When villi vasculatures were placed in collage- or gelatin-coated plates in EGM2 medium, we observed the presence of CD146 and NG2 double-positive cells in gelatin coated plate but did not see such cells in collagen-coated plates (Figure 5-10). Since NG2 is another perivascular cell marker, we extended further experiments with cells out-grown on gelatin coated-plates using EGM2. Later on, out-grown cells were expanded 1 to 2 passages for sorting on expression of CD146.

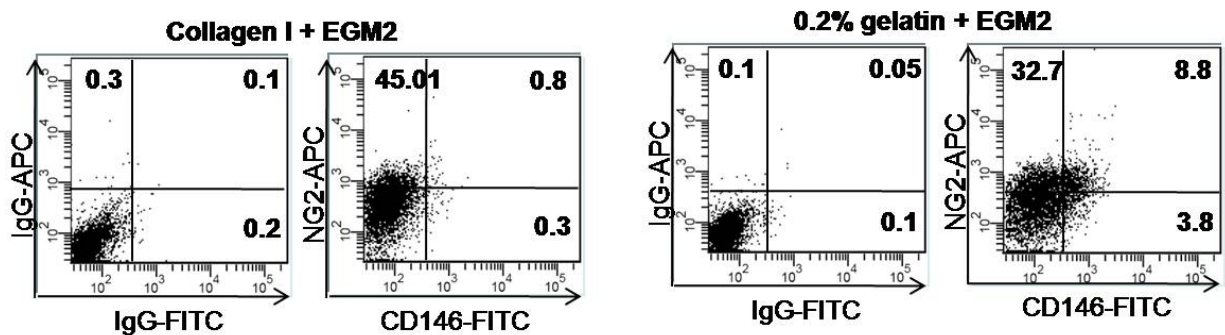


Figure 5-10. FACS analysis of out-grown cells from villi vasculature

Out-grown cells from gelatin-coated plates with EGM2 were replated into 48-well culture plates for immunocyto staining. Most of the cells expressing CD146 were also positive for PDGFR- β and NG2, suggesting that they were perivascular cells [48, 84, 93, 96, 116]. Few of the CD146-positive cells expressed α -SMA. Endothelial cell markers were rarely expressed in the out-grown cells from the villi, while the majority of out-grown cells expressed mesenchymal stem cells marker detected by CD44 and CD90 (Figure 5-11).

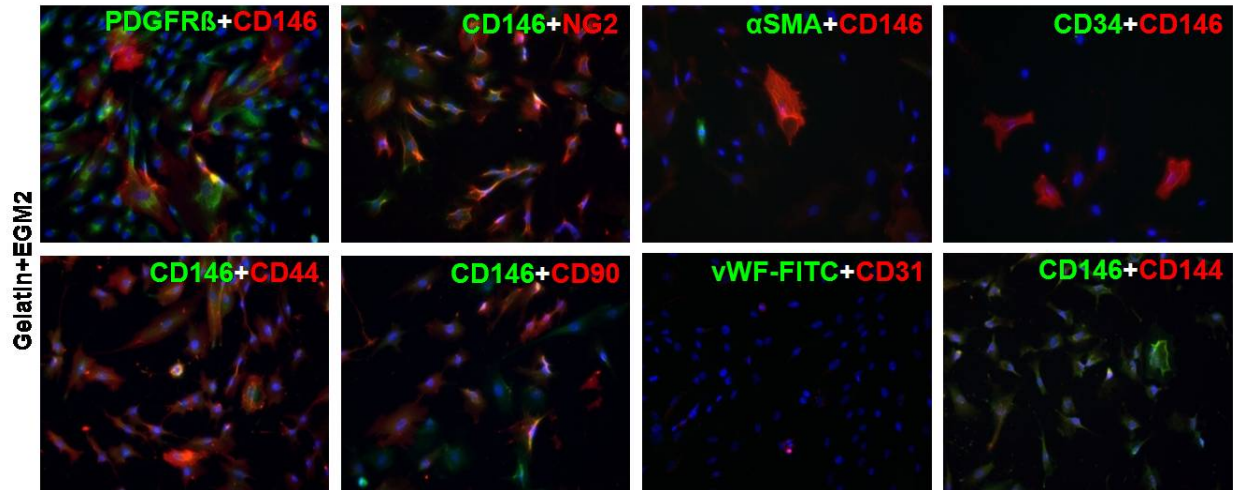


Figure 5-11. Immunocyto staining of out-grown cells

5.3.3 *In vivo* migration and myofiber formation from total vessel transplants

To demonstrate the myogenic potential of placental blood vessels, we transplanted purified villi vasculatures *in toto* into the gastrocnemius muscles of SCID/mdx mice. Human cells were detected in engrafted mouse muscles 2 and 4 weeks post-transplantation. Cross-sections of mouse muscles indicated that human placenta implants retained their vasculature structure (Figure 5-12, A with arrow and D). Human cells were detected inside of the implants (Figure 5-12, E and F) or outside (data not shown) by detection of hNA and Lamin A/C. We also observed participation of blood vessel-derived cells in muscle regeneration. Human dystrophin+ (hDys3+) myofibers were detected close to the engrafted area (Figure 5-12, dashed circle), and in more remote areas characterized by less hDys3+ fibers, suggesting the migration of the implanted human cells (Figure 5-12, square in B and higher magnification in C).

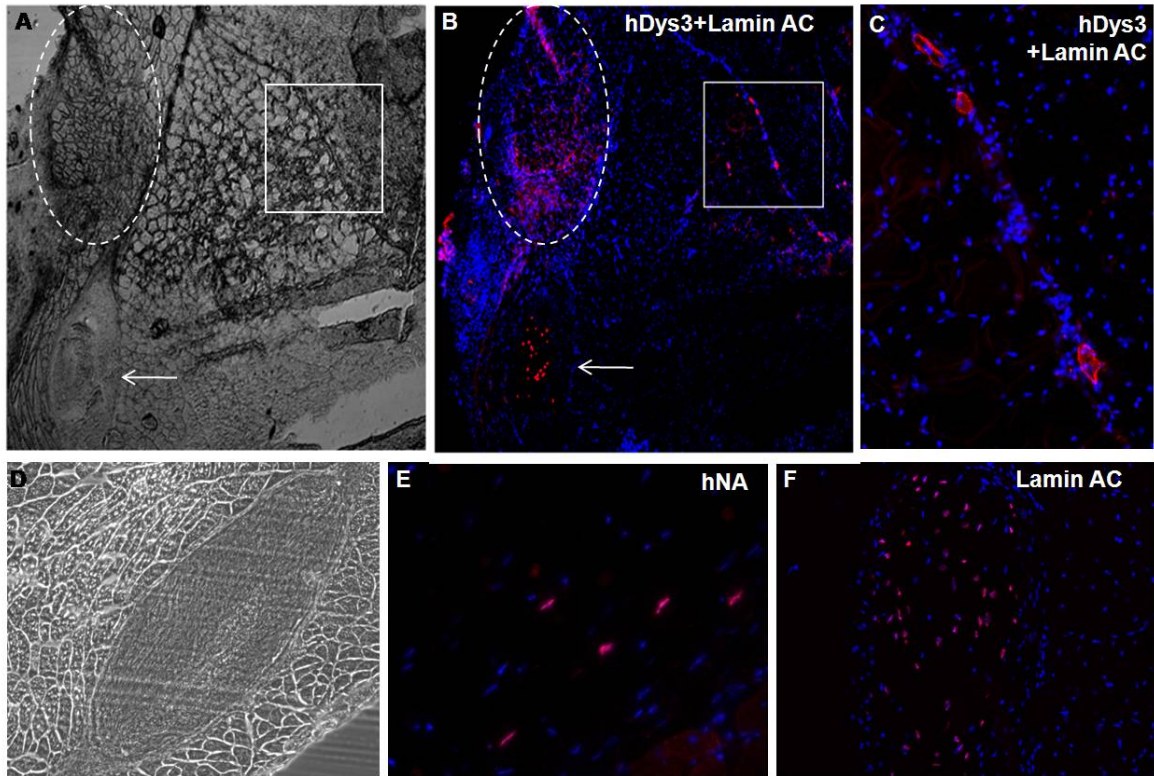


Figure 5-12. In vivo transplant of villi vasculature and human cell migration

Human myofibers were mostly small in size, with single, centered nuclei, and were typically clustered in a group formation (Figure 5-13). We could successfully detect hDys3+ myofibers in dystrophin-deficient mouse muscle (Figure 5-13, upper, right). When chimeric mouse muscles were stained with both spectrin and lamin A/C, we could observe lamin A/C in nuclei and spectrin in the membrane of fibers (Figure 5-13, lower right). These two mouse anti-human monoclonal antibodies were effectively used to evaluate human-originated myofibers by the specific location they were expressed. Spectrin is clearly positive only in the membrane of myofibers, while lamin A/C is particularly positive only in nuclei. The staining results of spectrin only (Figure 5-13, upper, middle) and spectrin combined with lamin A/C (Figure 5-13, lower, right) visibly demonstrate the difference. In addition to the human-originated myofibers, we

could also detect lamin A/C+ nuclei outside of muscle fibers which suggest that there are more than two types of human cells. SCID/mdx mouse, which underwent sham surgery without receiving human cells were used as a negative control, and did not show any cross-reaction with hDys3 antibody (Figure 5-13, lower, left). However, as part of the fibers stained positive for human spectrin in revertant fibers (Figure 5-13, lower, middle), we could use the combination of spectrin and lamin A/C to verify the origin of spectrin+ myofibers in chimeric mouse muscles.

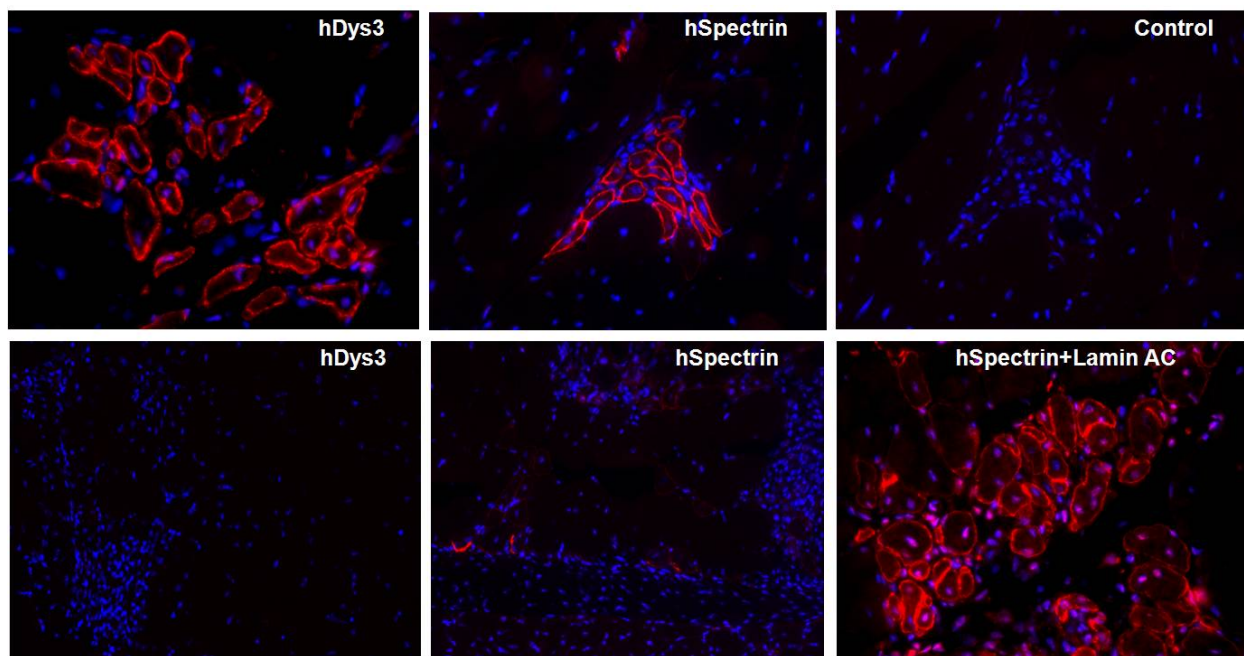


Figure 5-13. *In vivo* myofiber formation of human placenta villi vasculature.

5.3.4 *In vitro* myogenesis of sorted populations from placenta villi

Placenta villi were enzymatically digested and sorted to obtain perivascular cells (CD146+ CD34- CD45- CD56-, described as CD146+ cells), endothelial cells (CD34+ CD146- CD45-

CD56-, described as CD34- cells), non-vascular cells (CD34- CD45- CD56- CD146-, described as CD34- CD146- cells), and unsorted cells. Sorted cell populations were expanded in culture using α -MEM supplemented with serum for up to 5 passages. Perivascular cells showed elongated cytoplasmic arms, while CD34+ endothelial cells showed polygonal morphology (Figure 5-14).

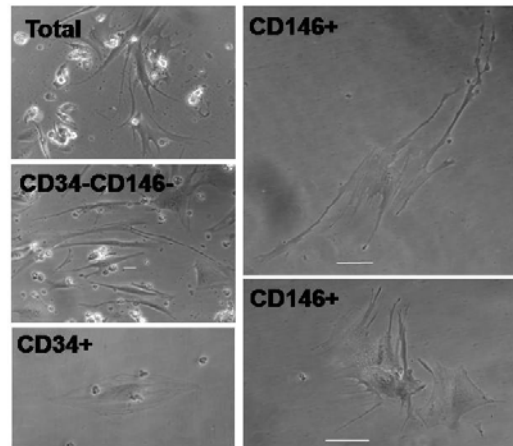


Figure 5-14. Phase contrast images of sorted vascular and non-vascular populations from human placenta villi.

Culture-expanded cells were apportioned at density of 2×10^4 cells/cm² and cultured in myogenic differentiation conditions. Fifteen days after differentiation, the CD34+ and CD146+ vascular populations included significantly higher numbers of desmin+ cells in quantitative comparisons (Figure 5-15, right). However, the morphology of desmin+ cells in these two populations varied. CD146+ cells formed elongated, occasionally multi-nucleated myofibers, while CD34+ cells generated single nuclei with scattered desmin+ cells (Figure 5-15, left).

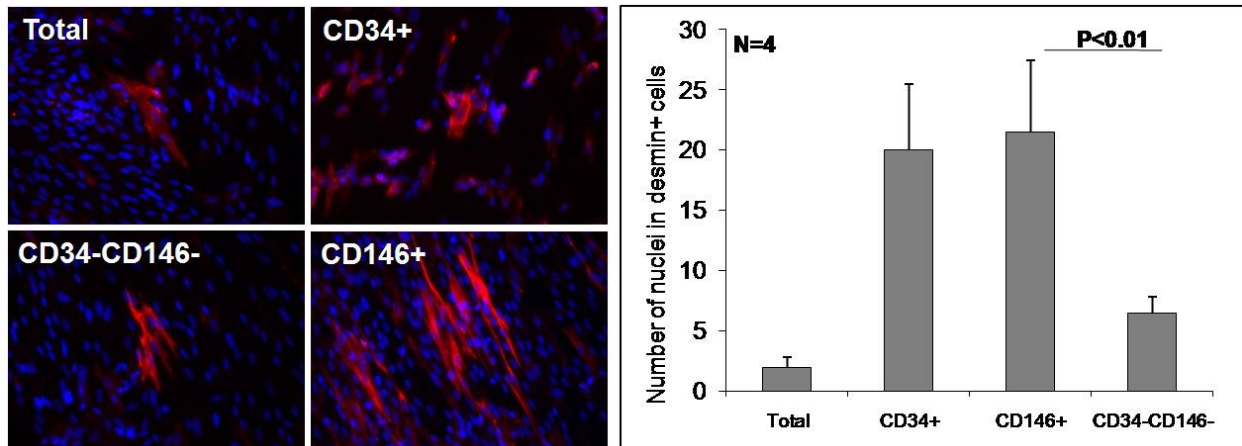


Figure 5-15. *In vitro* myogenic differentiation for 15 days stained with Desmin (red, left) and quantification of the four populations (right).

We examined gene expression of CD56 (NCAM) in the vascular populations (CD34+ and CD146+), non-vascular cells (CD34- CD146-), unsorted and culture-expanded cells (total), and unsorted, freshly isolated cells (case 1 and case 2, representing two individual donors). CD56 is a commonly used myogenic marker that is expressed in myoblasts [125, 141-143]. The mRNA expression of CD56 was up-regulated after myogenic differentiation (Post-diff) in all populations compared to pre-differentiation (Pre-diff). In a manner corresponding to the *in vitro* myogenic results shown in Figure 5-15, the CD146+ population showed the highest amount of CD56 expression after differentiation. Interestingly, the CD56 expression of the CD146+ population post-differentiation was substantially higher than human fetal muscle, which was used as a positive control (Figure 5-16, far right).

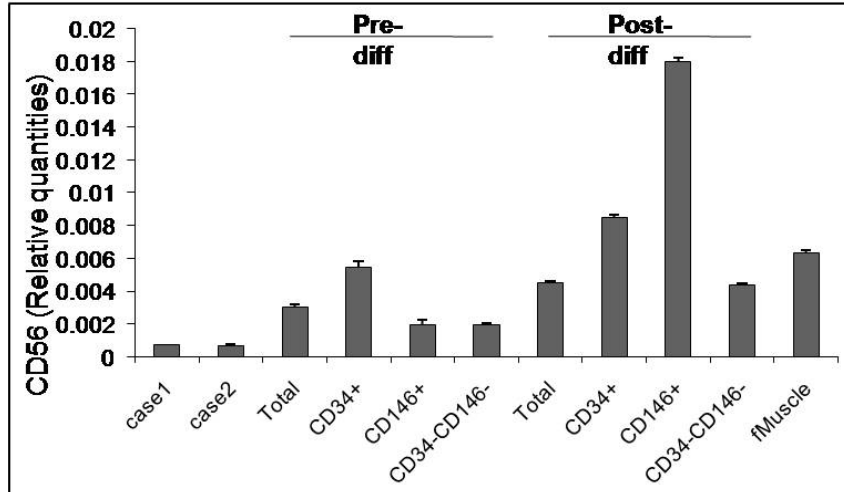


Figure 5-16. Quantitative RT-PCR for mRNA expression of CD56 on pre- and post-differentiated cells.

Out-grown cells from villi vasculatures were also cultured in myogenic differentiation conditions. When the cells were induced to out-grow from villi vasculature in different culture medium (PM and EGM2), we could observe that the numbers of desmin+ cells varied even before the differentiation began (Figure 5-17, left). After 18 days of differentiation, higher numbers of desmin+ myofibers (defined by more than 3 nuclei per myofiber; Figure 5-17, right middle and right low) were detected from PM-derived cells than EGM2-derived cells. Since the number of desmin+ cells was significantly higher before differentiation in EGM2-derived cells, it is assumed that the desmin+ cells merged to form myofibers without generating more desmin+ cells. In PM case, the numbers of desmin+ cells were lower before differentiation, but higher numbers of myofibers were produced compared to cells derived in EGM2. It is likely, then, that PM-derived cells were more committed to myogenic lineages and were more efficient at producing higher numbers of myofibers than EGM2-derived cells.

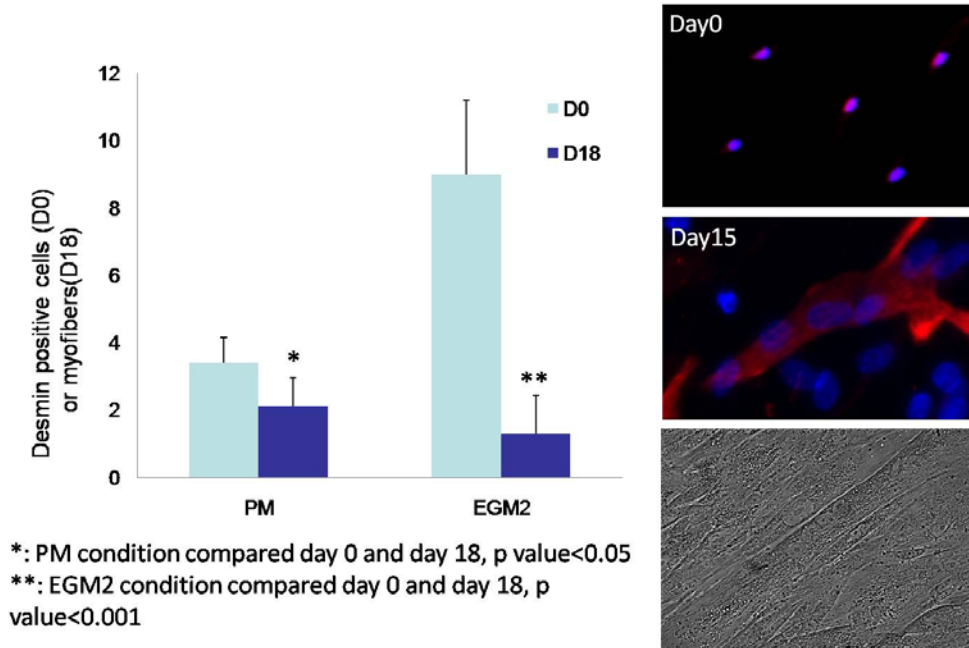


Figure 5-17. *In vitro* myogenic differentiation of out-grown cells from different culture conditions.

5.3.5 Angiogenic effect of human cells on host environment

It has been reported that regeneration capacity is highly related to the angiogenesis/ neo-vascularization of injured host tissue [92, 108, 125, 144-146]. This is not only to supply nutrients and oxygen to this damaged area, but also to facilitate the migration of progenitor cells from bone marrow or the adjacent stem cell niche. Therefore, we examined the angiogenic effects of injected different types of human cells into host tissue, i.e., the gastrocnemius SCID/mdx mice. We injected identical numbers (1×10^4 cells per muscle) of vascular (CD34+ and CD146+), non-vascular (CD34- CD146-), and unsorted (Total) populations that were freshly isolated from placenta villi and injected them without performing culture expansion. Two weeks post-injection, the muscles were harvested, frozen, cryosectioned, and stained for vWF to quantify the

blood vessels concentration. Mid-gestation human fetal muscle (fMuscle) was cryosectioned and stained in the same manner for comparison (Figure 5-18, B, right). As a negative control, we used PBS-injected SCID/mdx mouse muscle (Neg Ctrl, Figure 5-18, B, left). All human cell-injected muscles were found to contain higher numbers of blood vessels than the PBS-injected SCID/mdx mouse muscles. However, the numbers of vWF+ blood vessels in these populations varied. CD146+ cell-injected muscles included significantly higher numbers of blood vessels than CD34+ cell- or non-vascular cell-injected muscles. It is difficult to say if the human cells participated in the actual generation of blood vessels, because vWF antibody also stained for mouse blood vessels. In order to determine whether human cells contributed to angiogenesis, staining with human specific antibody for endothelial cell detection has to be performed. Our comparisons on total numbers of blood vessels after injection of different human cells recognize that receiving human perivascular cells clearly induced a positive angiogenic effect that could significantly enhance muscle regeneration.

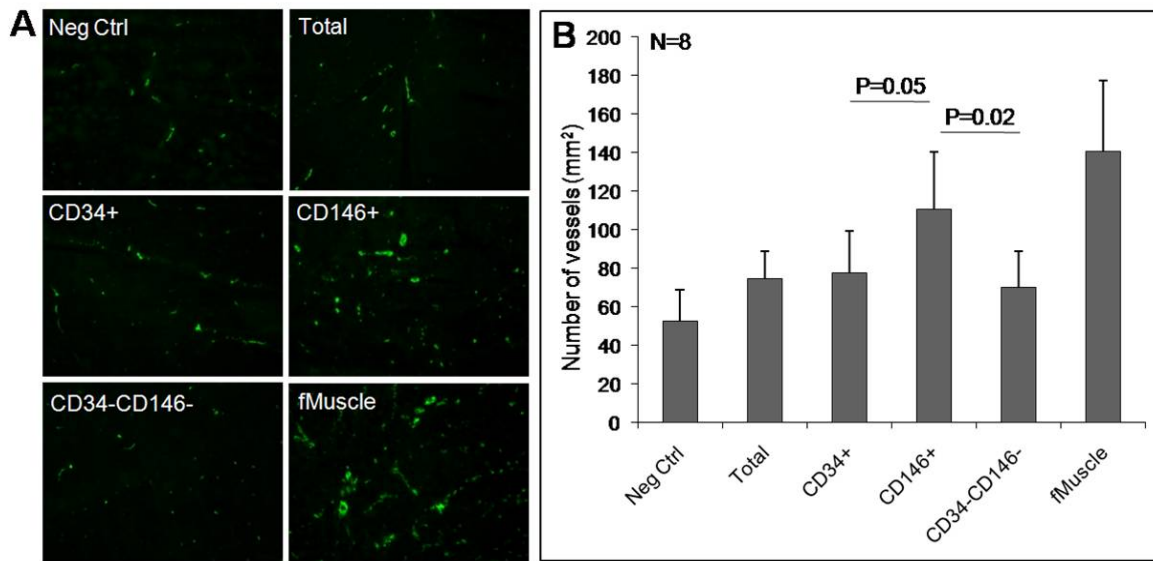


Figure 5-18. Angiogenic effect on SCID/mdx mouse muscle after injection of human cells.

5.3.6 Adhesion and migration assays on CD146+ and CD146- cells

In order to distinguish whether CD146+ out-grown cells have a greater ability to respond to extracellular matrix by migrating efficiently, out-grown cells from villi vasculature were sorted on expression of CD146 for further evaluation. CD146+, CD146-, and unsorted out-grown cells were plated and grown to over 90% confluency, then, a single wound was generated in the center of the cell monolayer in order to observe subsequent space filling cell migration (Figure 5-19, Day 0). After the empty space was created, cell debris were removed and medium was exchanged for medium with a low concentration of serum (2%) to prevent proliferation during the migration/wound healing assay. After 24 hours, CD146+ cells demonstrated much faster movement compared to that of the CD146- population (Figure 5-19, Day 1, and Figure 5-20).

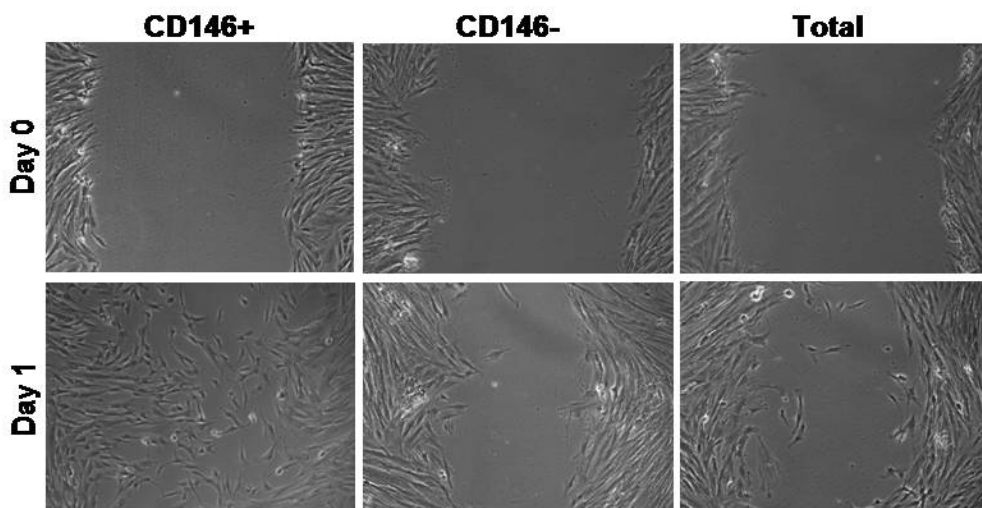


Figure 5-19. Migration assay of CD146+ or CD146- cells sorted from out grown cells.

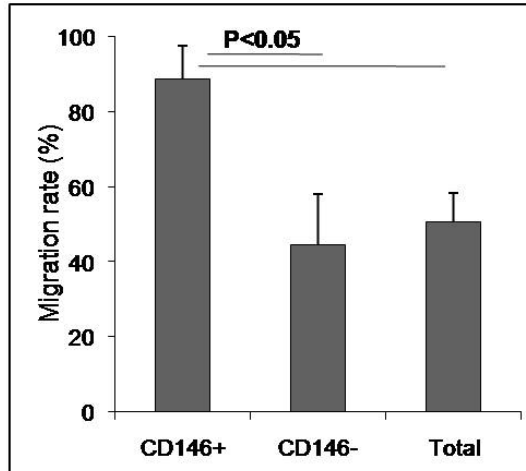


Figure 5-20. Quantification of migration assay.

The adhesion process is related to cell migration, remodeling, and signaling pathways for survival and growth that are mediated through the different adhesion molecules and ligands [106, 108, 147-149]. To observe the differences in adhesion capacity between CD146+ and CD146- cells on different extracellular substrates, these two populations were inoculated, in equal concentration, onto uncoated plates and plates coated with collagen, gelatin, fibronectin, or FBS. One hour later, unattached cells were removed and adherent cells were counted. CD146+ cells displayed faster attachment to three of the tested extracellular coating substances: collagen, gelatin, and fibronectin. CD146- cells adhered faster on non-coated plated and on the surface saturated with FBS (Figure 5-21).

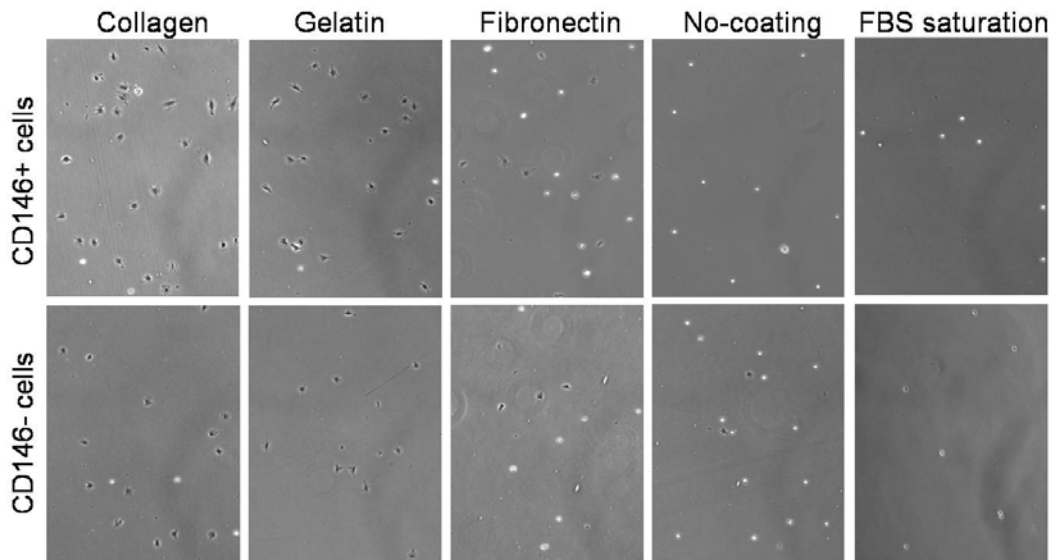
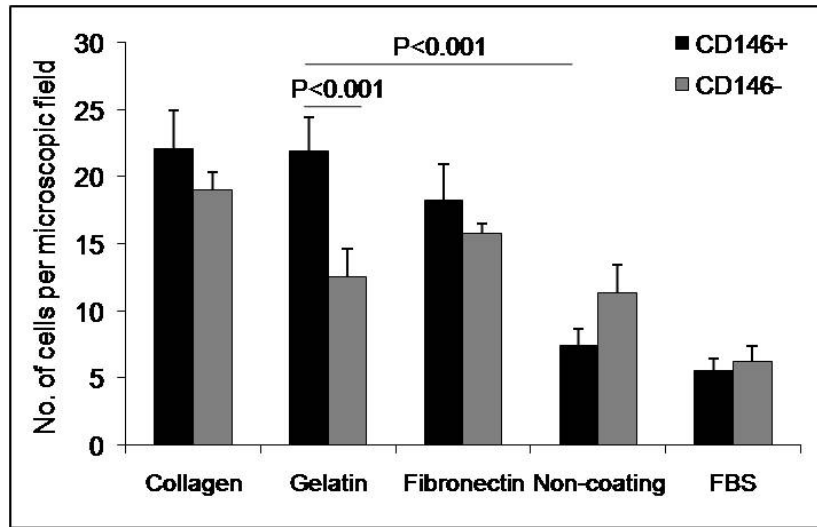


Figure 5-21. Adhesion assay of CD146+ or CD146- sorted out-grown cells on different extracellular substrates.

5.3.7 Mesenchymal stem cell marker expression of cells outgrown from placenta villi

Out-grown cells from placenta villi vasculature were analyzed for their mesenchymal stem cell marker expression by flow cytometry. CD146+ and CD146- cells were sorted from out-grown cells (with gelatin and EGM2) and expanded in culture for 1 to 2 passages. Both populations expressed all 4 mesenchymal stem cell markers (CD105, CD90, CD73, and CD44) with variances in percentages. The most significant difference was the expression of CD90. Over 60% of the CD146+ cells tested positive for the expression of CD90, but lower than 5% in CD146- cells did (Table 5-1). The histograms of FACS analysis are shown in Figure 5-22. These two cell populations were also examined for their mRNA expression of Brachyury which is an early mesodermal stem cell marker. Both populations displayed positive mRNA expression of Brachyury (Figure 5-23, line 2 and 3), but the expression in CD146+ cells was more pronounced than the expression in CD146- cells. Both cell populations included similar levels of the housekeeping gene, GAPDH (Figure 5-23, line 4 and 5). Human fetal muscle was used as a positive control for Brachyury expressing cells (Figure 5-23, line 1).

Table 5-1. Mesenchymal stem cell marker expression of CD146+ and CD146- sorted cells from placenta villi vasculature out-grown cells.

FACS (%)	CD146	CD105	CD90	CD73	CD44
CD146+ cells	91.3	98.7	60.3	57.2	94.6
CD146- cells	13.8	99.5	4.3	77.4	95.7

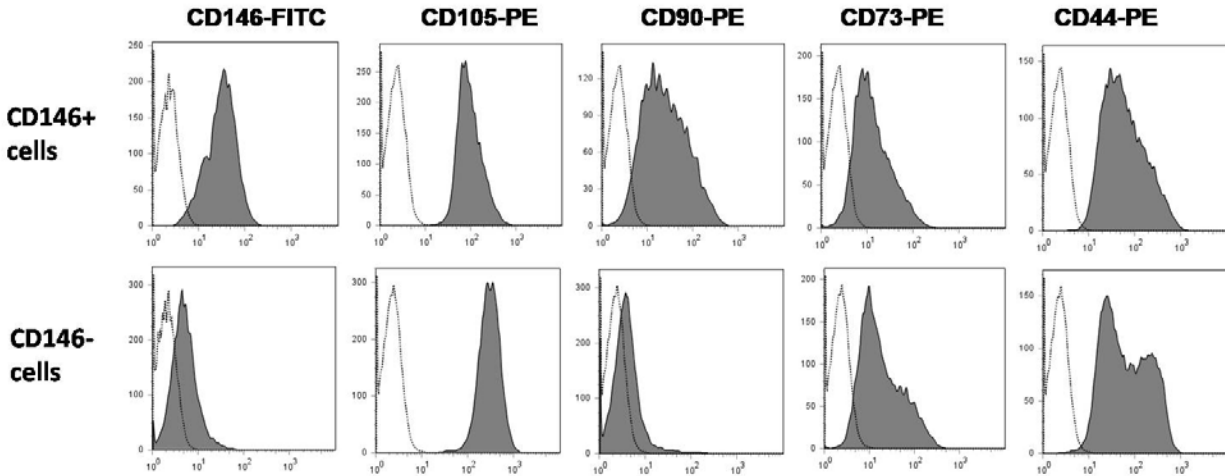


Figure 5-22. FACS analysis of MSC markers on CD146+ and CD146- sorted out grown cells.

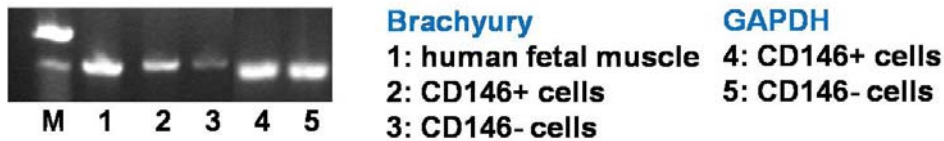


Figure 5-23. mRNA expression (RT-PCR) of Brachyury on CD146+ and CD146- out-grown cells from placenta villi vasculature (M: size marker).

5.4 DISCUSSION

The results of this study suggest that human fetal placental blood vessels contain progenitor cells with myogenic potential that are able to migrate into dystrophic muscle and participate in muscle regeneration. In order to identify this population, freshly isolated vascular, non-vascular, and total populations were compared quantitatively for their *in vitro* myogenic differentiation and *in*

vivo angiogenic effect within host tissue. In addition to these measures, we performed an *in vitro* migration assay, adhesion assay, and an examination of mesenchymal stem cell marker expression. Our results indicate that the CD146⁺ perivascular cell population exhibits a greater capacity for myogenic differentiation, recruitment of host angiogenesis, migration, and interaction with extracellular matrices. Importantly, CD146⁺ perivascular cells were found to have higher mRNA expression of Brachyury, suggesting that this cell population might locate in a higher hierarchy of mesenchymal cell lineage.

Cells out-grown in different media and on different substrates were characterized by cell populations that expressed different antigens. In the case of cells grown on collagen- and gelatin-coated plates with EGM2, we found cells that were CD146⁺ NG2⁺ in the gelatin-coated plate but CD146⁻ NG2⁺ cells from collagen-coated plate. This demonstrates that culture conditions can control the migration of certain populations from the villi vasculature. It may not be a coincidence to observe that CD146⁺ cells selectively migrated out from the vasculature on gelatin-coated plates and actively interacted with the extracellular matrix, as matrix metalloproteinase 2 (MMP2, gelatinase A) and MMP9 (gelatinase B) are involved in the breakdown of extracellular matrix in normal physiological processes, including embryonic development, reproduction, and tissue remodeling. CD146⁺ cells included much higher numbers (> 60%) of CD90 (Thy-1)⁺ cells, while CD146⁻ cells did less (< 5%). It has been suggested in the literature that CD90 is involved in cell-cell and cell-matrix interactions, with implications on neurite outgrowth, nerve regeneration, apoptosis, metastasis, inflammation, and fibrosis [150-153]. Therefore, our culture conditions for out-grown cells from placenta villi were optimal to select high myogenic, migrating, mesenchymal stem cell-like CD146⁺ perivascular cells.

The fact that placenta is a naturally discarded human organ provides an incentive to investigate it as a stem cell source. Our data on the myogenic potential of placental vascular stem cells suggests a potential for regenerative therapy for muscular dystrophic disease. The placenta villi vascular cells demonstrated high migration into skeletal muscle, and generated hDys3+ myofibers following transplantation into SCID/mdx mice gastrocnemius muscle. This leads us to hypothesize that placenta can be utilized for patients who have DMD. For instance, placental cells could be banked and the major histocompatibility complex (MHC) matched allogenic placental cells could provide as a material for cell-based therapeutic or curative resource. This hypothesis may be studied in depth in the near future, as the dystrophic dog is a readily available large animal model for the study of therapeutic approaches for DMD. Placenta from normal dogs can be used and examined for muscle regenerative potential in dystrophic dogs. Certainly, many of issues remain to be determined before translation can occur for clinical approaches, including safeness/stability of placenta-derived cells *in vivo*, and any possible immunologic reaction resulting from transplantation.

5.5 CONCLUSION

We observed that human fetal placental villi vasculature included a stem cell population residing in blood vessel walls that had the capacity to produce myofibers when transplanted in the skeletal muscle of dystrophic mice. Detailed profiles including surface marker expression, migration, interaction with extracellular matrix, and mesenchymal properties were examined in sub-populations of villi vasculatures, leading us to conclude that CD146+ perivascular cells have

a robust ability to provide myogenic repair of skeletal muscle, and impart a positive angiogenic effect within the host tissue. We posit then, that the placenta may represent a potentially invaluable and readily available source of cells for stem cell-based therapy to treat neuromuscular diseases.

5.6 ACKNOWLEDGMENT

This project could be done with great help of Drs. Baohong Cao, Manuela Gavina, Chien-Wen Chen, Bin Sun, and Bridget Deasy. We also thank to Drs. Louis Casteilla and Toshio Miki for providing their expertise.

6.0 DISCUSSION

In this study, four objectives were achieved to establish approaches to understand the development of hematopoietic, endothelial, and perivascular cells. Firstly, we established optimal conditions to promote differentiation of hESC toward hematopoietic and endothelial progenitor cells using the hEB system. The hESC and hEB system were confirmed as a valuable tool to derive early stem cells which are not otherwise accessible due to their early emergence in human embryos. Secondly, the chick embryo was developed as an *in vivo* surrogate model to study proliferation, migration, and differentiation of a hemangioblastic cell population. Our chick embryo model provided proof-of-principle that human angio-hematopoietic progenitor cells could develop into mature erythroid, myeloid, and endothelial cells in a single model. Thirdly, CD146⁺ differentiated hESC and hEB cells were studied as pericyte-like hESC. Sorted CD146⁺ cells from medium-differentiated hESC and/or hEB exhibited a high potential for myogenic differentiation, and a somewhat lesser potential for neural differentiation. Finally, perivascular cells from mid-gestation of human placenta were evaluated as a possible stem cell source for myogenic regeneration. Purified placenta villi vasculature cells that were transplanted into the skeletal muscle of SCID/mdx mice were found to migrate and produce human dystrophin positive myofibers. CD146⁺ perivascular cells of placental villi displayed great potential to differentiate into myogenic lineage, to migrate, to interact with extracellular matrix, and to express mesenchymal stem cell markers.

Even though many of the mechanisms, differentiation pathways, and cell-cell interactions in ontogeny of blood and vascular system are known, some of them are still remained to be clear. The existence of hemangioblasts is close to be accepted as a truth from hypothesis, since a fair amount of evidence has previously documented its existence [8, 154-165]. The hESC and hEB differentiation system provides an excellent alternative to the use of early embryos for the identification of the hemangioblast. Figure 6-1 provides the scheme of developmental hierarchy from hESC to lineage differentiated cells. hESC expressing Oct-4 and other pluripotent markers spontaneously differentiate into mesodermal precursors expressing Brachyury via hEB and the proper medium. Thereafter, BMP4, VEGF, and bFGF are involved in the process of guiding these mesodermal precursors into hemangioblast and/or meso-angioblast that further propagate into hematopoietic, endothelial, and perivascular cells. Recently, it has been found that pericytes and myogenic endothelial cells can produce skeletal muscle cells [48, 93, 96, 118, 125]. The relationship between meso-angioblasts and hemangioblasts, the possible progenitor cells for perivascular cells, and the differentiation potential of perivascular cells to produce endothelial or smooth muscle cells are still undefined. Our studies provide approaches and some overall understanding of these matters, specifically via the use of hESC and hEB. We also utilized fetal placenta perivascular cells to investigate their stem cell potential to produce myogenic cells; this confirmed the myogenic capacity of perivascular cells derived from other organs (muscle, pancreas and fat). The identification of mesenchymal stem cell properties for fetal placenta pericytes illuminated another possible differentiative route, and provided greater understanding of the potential relationship among the cells located in this developmental hierarchy.

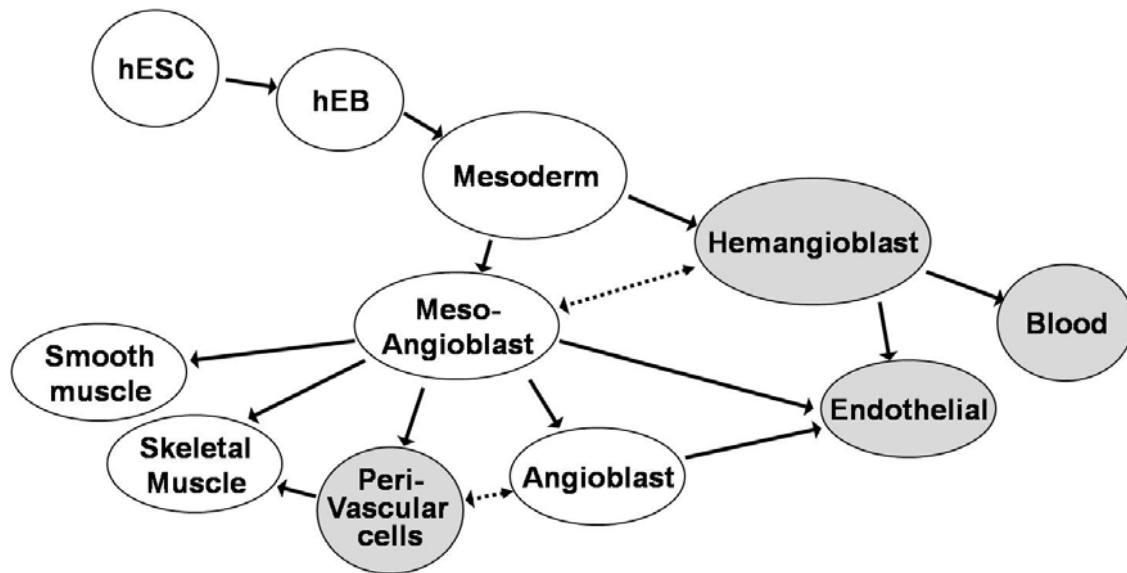


Figure 6-1. Scheme of the developmental interactions from hESC to lineage differentiated cells.

In summary, this study demonstrated approaches to study early events of hematopoietic and endothelial cell formation using hESC and hEB. We also showed that perivascular cells had high myogenic potential and mesenchymal progenitor cell properties. Examination of additional molecular determinants of the hemangioblast will be helpful for further defining the molecular and cellular pathways leading from mesoderm to hemangioblast, as well as the development of endothelial, and primitive and definitive hematopoietic cells. Characterization of the developmental potential of mesodermal precursor cells, hemangioblasts, and perivascular cells *in vitro* and *in vivo* will ultimately provide a route for their practical usage in clinical applications.

APPENDIX A

ACRONYM, ABBREVIATION, AND SYMBOL DEFINITIONS

2-ME	2-mercaptoethanol
7-AAD	7-amino-actinomycin
α -FP	alpha-fetoprotein
α -MEM	alpha-modified Dulbecco's medium
α -SMA	alpha-smooth muscle actin
ACE	Angiotensin converting enzyme, CD143
AGM	Aorta-gonad-mesonephros
AGTR-1	Angiotensin II type-1 receptor
AGTR-2	Angiotensin II type-2 receptor
ANOVA	Analysis of variance
Angio	Angiotensinogen
APC	Allophycocyanin
BF	Bursa of Fabricius
bFGF	Basic fibroblast growth factor
BHA	Buthylated hydroxyanisole
BMP4	Bone morphogenetic protein-4

CD	Cluster differentiation
CFU-GM	Colony forming units-granulocyte/macrophage
DMD	Duchenne muscular dystrophy
DMEM	Dulbecco's modified Eagle's medium
E2	Embryonic day 2
EDTA	Ethylenediaminetetraacetic acid
EGF-2	Endothelial growth medium-2
EPC	Endothelial progenitor cells
EPO	Erythropoietin
ESCRO	Embryonic stem cell research oversight
FACS	Fluorescence activated cell sorting
FBS	Fetal bovine serum
FCS	Fetal calf serum
FITC	Fluorescence isothiocyanate
GAPDH	Glyceraldehyde 3-phosphate dehydrogenase
G-CSF	Granulocyte-colony stimulating factor
hDys3	Human dystrophin
hESC	Human embryonic stem cells
hEB	Human embryoid bodies
HH stage	Hamburger and Hamilton (HH) stage
HNA	Human nuclear antigen
HSC	Hematopoietic stem cells
HUVEC	Human umbilical vein endothelial cells

IMDM	Iscove's modified Dulbecco's medium
KOSR	Knockout serum replacement
mESC	Mouse embryonic stem cells
mEB	Mouse embryoid bodies
MEM-NEAA	MEM non-essential amino acid
MHC-f	Myosin heavy chain-fast
MMP2	Matrix metalloproteinase 2
mRNA	Messenger ribonucleic acid
NCAM	Neural cell adhesion molecule, CD56
NF	Neurofilament
NG-2	Neuroglial antigen 2
Oct-4	Octamer-4
PBS	Phosphate buffered saline
PBSC	Peripheral blood stem/progenitor cells
PDGFR- β	Platelet-derived growth factor receptor-beta
PE	Phycoerythrin
PFA	Paraformaldehyde
PM	Proliferation medium
PMEF	Primary mouse embryonic fibroblast
PS	Penicillin/streptomycin
q-RT-PCR	Quantitative-reverse transcriptase-polymerase chain reaction
RAS	Renin-angiotensin system
RT	Room temperature

SCID/NOD	Severe combined immunodeficiency/nonobese diabetic
SCID/mdx	Severe combined immunodeficiency/X-linked muscular dystrophy
SCL	Stem cell leukaemia
SFEM	Serum free expansion medium
SSEA-1	Stage specific embryonic antigen-1
TH	Tyrosine hydroxylase
UEA-1	Ulex europaeus agglutinin-1
VEGFR-2	Vascular endothelial growth factor receptor-2, KDR, Flk-1
vWF	von Willebrand factor

APPENDIX B

THE $2^{-\Delta\Delta C_T}$ METHOD [56]

Comparative quantification (fold change expression) of each target gene was performed based on cycle threshold (C_T) normalized to actin using the $2^{-\Delta\Delta C_T}$ method [44, 56, 57]. The relative expression of each normalized target gene (i.e., Angiotensinogen, AGTR-1, and AGTR-2) was compared with the actin-normalized expression of the target gene (ΔC_T) in highly purified day-9 BB9+ hEB cells or blast colonies.

$$(\Delta C_T \text{ day-9 BB9+ hEB cells}) = (C_{T, \text{Target gene}} - C_{T, \text{Actin}})$$

$$(\Delta C_T \text{ blast colonies}) = (C_{T, \text{Target gene}} - C_{T, \text{Actin}})$$

Fold change expression of blast colonies from day-9 BB9+ hEB cells was calculated as $2^{-\Delta\Delta C_T}$, where

$$\Delta\Delta C_T = (\Delta C_T \text{ blast colonies}) - (\Delta C_T \text{ day-9 BB9+ hEB cells}).$$

APPENDIX C

ANTIGEN EXPRESSIONS FOR DETECTION OF FOLLOWING CELL TYPES

Note: only the cell types that are related for this dissertation are mentioned.

Antigen	Cells include positive antigen expression
CD3	T cells
CD4	T cells
CD8	T cells
CD11b	Monocytes
CD13	Monocytes, granulocytes
CD14	Monocytes
CD15	Monocytes, granulocytes
CD19	B cells
CD31	Endothelial cells
CD34	Hematopoietic progenitor cells, endothelial cells
CD38	T cells, plasma cells, multi-lineage committed progenitors
CD41	Platelets, megakaryocytes
CD43	T cells, granulocytes, monocytes

CD44	Leukocytes, erythrocytes
CD45	Hematopoietic cells
CD56	Myoblasts, natural killer (NK) cells with CD45 expression
CD71	Erythroid cells
CD73	Endothelial cells, mesenchymal stem cells
CD90	Mesenchymal stem cells, hematopoietic stem cells, fibroblasts
CD105	Endothelial cells, mesenchymal stem cells
CD117	Hematopoietic stem cells
CD133	Endothelial progenitor cells, hematopoietic stem cells
CD143	Endothelial cells, hemangioblast
CD144	Endothelial cells
CD146	Endothelial cells, perivascular cells
CD164	Stromal cells, hematopoietic progenitor cells with CD34 expression
CD235a	Red blood cells

BIBLIOGRAPHY

1. Kaufman, D.S., et al., *Hematopoietic colony-forming cells derived from human embryonic stem cells*. Proc Natl Acad Sci U S A, 2001. **98**(19): p. 10716-21.
2. Wang, L., et al., *Endothelial and hematopoietic cell fate of human embryonic stem cells originates from primitive endothelium with hemangioblastic properties*. Immunity, 2004. **21**(1): p. 31-41.
3. Ng, E.S., et al., *Forced aggregation of defined numbers of human embryonic stem cells into embryoid bodies fosters robust, reproducible hematopoietic differentiation*. Blood, 2005. **106**(5): p. 1601-3.
4. Zambidis, E.T., et al., *Hematopoietic differentiation of human embryonic stem cells progresses through sequential hematoendothelial, primitive, and definitive stages resembling human yolk sac development*. Blood, 2005. **106**(3): p. 860-70.
5. Chang, K.H., et al., *Definitive-like erythroid cells derived from human embryonic stem cells coexpress high levels of embryonic and fetal globins with little or no adult globin*. Blood, 2006. **108**(5): p. 1515-23.
6. Vodyanik, M.A., J.A. Thomson, and Slukvin, II, *Leukosialin (CD43) defines hematopoietic progenitors in human embryonic stem cell differentiation cultures*. Blood, 2006. **108**(6): p. 2095-105.
7. Lu, S.J., et al., *Generation of functional hemangioblasts from human embryonic stem cells*. Nat Methods, 2007. **4**(6): p. 501-9.
8. Kennedy, M., et al., *Development of the hemangioblast defines the onset of hematopoiesis in human ES cell differentiation cultures*. Blood, 2007. **109**(7): p. 2679-87.
9. Thomson, J.A., et al., *Embryonic stem cell lines derived from human blastocysts*. Science, 1998. **282**(5391): p. 1145-7.
10. Evans, M.J. and M.H. Kaufman, *Establishment in culture of pluripotential cells from mouse embryos*. Nature, 1981. **292**(5819): p. 154-6.
11. Thomson, J.A. and V.S. Marshall, *Primate embryonic stem cells*. Curr Top Dev Biol, 1998. **38**: p. 133-65.

12. Draper, J.S., et al., *Surface antigens of human embryonic stem cells: changes upon differentiation in culture*. J Anat, 2002. **200**(Pt 3): p. 249-58.
13. Murry, C.E. and G. Keller, *Differentiation of embryonic stem cells to clinically relevant populations: lessons from embryonic development*. Cell, 2008. **132**(4): p. 661-80.
14. Vodyanik, M.A., et al., *Human embryonic stem cell-derived CD34+ cells: efficient production in the coculture with OP9 stromal cells and analysis of lymphohematopoietic potential*. Blood, 2005. **105**(2): p. 617-26.
15. Jezierski, A., A. Swedani, and L. Wang, *Development of hematopoietic and endothelial cells from human embryonic stem cells: lessons from the studies using mouse as a model*. ScientificWorldJournal, 2007. **7**: p. 1950-64.
16. Weisel, K.C., et al., *Extended In-vitro Expansion of Adult, Mobilized CD34+ Cells without Significant Cell Senescence using a Stromal Cell Co-culture System with Single Cytokine Support*. Stem Cells Dev, 2008.
17. Martin, G.R. and M.J. Evans, *Differentiation of clonal lines of teratocarcinoma cells: formation of embryoid bodies in vitro*. Proc Natl Acad Sci U S A, 1975. **72**(4): p. 1441-5.
18. Keller, G., et al., *Hematopoietic commitment during embryonic stem cell differentiation in culture*. Mol Cell Biol, 1993. **13**(1): p. 473-86.
19. Keller, G.M., *In vitro differentiation of embryonic stem cells*. Curr Opin Cell Biol, 1995. **7**(6): p. 862-9.
20. Rohwedel, J., et al., *Muscle cell differentiation of embryonic stem cells reflects myogenesis in vivo: developmentally regulated expression of myogenic determination genes and functional expression of ionic currents*. Dev Biol, 1994. **164**(1): p. 87-101.
21. Doetschman, T.C., et al., *The in vitro development of blastocyst-derived embryonic stem cell lines: formation of visceral yolk sac, blood islands and myocardium*. J Embryol Exp Morphol, 1985. **87**: p. 27-45.
22. Lindenbaum, M.H. and F. Grosveld, *An in vitro globin gene switching model based on differentiated embryonic stem cells*. Genes Dev, 1990. **4**(12A): p. 2075-85.
23. Wiles, M.V. and G. Keller, *Multiple hematopoietic lineages develop from embryonic stem (ES) cells in culture*. Development, 1991. **111**(2): p. 259-67.
24. Burkert, U., T. von Ruden, and E.F. Wagner, *Early fetal hematopoietic development from in vitro differentiated embryonic stem cells*. New Biol, 1991. **3**(7): p. 698-708.
25. Schmitt, R.M., E. Bruyns, and H.R. Snodgrass, *Hematopoietic development of embryonic stem cells in vitro: cytokine and receptor gene expression*. Genes Dev, 1991. **5**(5): p. 728-40.

26. Chen, U., M. Kosco, and U. Staerz, *Establishment and characterization of lymphoid and myeloid mixed-cell populations from mouse late embryoid bodies, "embryonic-stem-cell fetuses"*. Proc Natl Acad Sci U S A, 1992. **89**(7): p. 2541-5.
27. Chen, U., *Differentiation of mouse embryonic stem cells to lympho-hematopoietic lineages in vitro*. Dev Immunol, 1992. **2**(1): p. 29-50.
28. Gutierrez-Ramos, J.C. and R. Palacios, *In vitro differentiation of embryonic stem cells into lymphocyte precursors able to generate T and B lymphocytes in vivo*. Proc Natl Acad Sci U S A, 1992. **89**(19): p. 9171-5.
29. Muller, A.M. and E.A. Dzierzak, *ES cells have only a limited lymphopoietic potential after adoptive transfer into mouse recipients*. Development, 1993. **118**(4): p. 1343-51.
30. Nakano, T., H. Kodama, and T. Honjo, *Generation of lymphohematopoietic cells from embryonic stem cells in culture*. Science, 1994. **265**(5175): p. 1098-101.
31. Chadwick, K., et al., *Cytokines and BMP-4 promote hematopoietic differentiation of human embryonic stem cells*. Blood, 2003. **102**(3): p. 906-15.
32. Zambidis, E.T., et al., *Emergence of human angiohematopoietic cells in normal development and from cultured embryonic stem cells*. Ann N Y Acad Sci, 2007. **1106**: p. 223-32.
33. Itskovitz-Eldor, J., et al., *Differentiation of human embryonic stem cells into embryoid bodies compromising the three embryonic germ layers*. Mol Med, 2000. **6**(2): p. 88-95.
34. Conley, B.J., et al., *Derivation, propagation and differentiation of human embryonic stem cells*. Int J Biochem Cell Biol, 2004. **36**(4): p. 555-67.
35. Kaufman, D.S. and J.A. Thomson, *Human ES cells--haematopoiesis and transplantation strategies*. J Anat, 2002. **200**(Pt 3): p. 243-8.
36. Narayan, A.D., et al., *Human embryonic stem cell-derived hematopoietic cells are capable of engrafting primary as well as secondary fetal sheep recipients*. Blood, 2006. **107**(5): p. 2180-3.
37. Tavian, M., et al., *The human embryo, but not its yolk sac, generates lympho-myeloid stem cells: mapping multipotent hematopoietic cell fate in intraembryonic mesoderm*. Immunity, 2001. **15**(3): p. 487-95.
38. Tavian, M. and B. Peault, *The changing cellular environments of hematopoiesis in human development in utero*. Exp Hematol, 2005. **33**(9): p. 1062-9.
39. Bollerot, K., C. Pouget, and T. Jaffredo, *The embryonic origins of hematopoietic stem cells: a tale of hemangioblast and hemogenic endothelium*. APMIS, 2005. **113**(11-12): p. 790-803.

40. Tavian, M., M.F. Hallais, and B. Peault, *Emergence of intraembryonic hematopoietic precursors in the pre-liver human embryo*. *Development*, 1999. **126**(4): p. 793-803.
41. Tavian, M., et al., *Aorta-associated CD34+ hematopoietic cells in the early human embryo*. *Blood*, 1996. **87**(1): p. 67-72.
42. Tavian, M. and B. Peault, *Embryonic development of the human hematopoietic system*. *Int J Dev Biol*, 2005. **49**(2-3): p. 243-50.
43. Jaffredo, T., et al., *From hemangioblast to hematopoietic stem cell: an endothelial connection?* *Exp Hematol*, 2005. **33**(9): p. 1029-40.
44. Zambidis, E.T., et al., *Expression of ACE (CD143) identifies and regulates primitive hemangioblasts derived from human pluripotent stem cells*. *Blood*, 2008.
45. Ramshaw, H.S., et al., *Monoclonal antibody BB9 raised against bone marrow stromal cells identifies a cell-surface glycoprotein expressed by primitive human hemopoietic progenitors*. *Exp Hematol*, 2001. **29**(8): p. 981-92.
46. Jokubaitis, V.J., et al., *Angiotensin-converting enzyme (CD143) marks hematopoietic stem cells in human embryonic, fetal, and adult hematopoietic tissues*. *Blood*, 2008. **111**(8): p. 4055-63.
47. Dieterlen-Lievre, F. and N.M. Le Douarin, *From the hemangioblast to self-tolerance: a series of innovations gained from studies on the avian embryo*. *Mech Dev*, 2004. **121**(9): p. 1117-28.
48. Crisan, M., *A perivascular origin for mesenchymal stem cells in multiple human organs*. *Cell Stem Cell*, 2008.
49. Oberlin, E., et al., *Blood-forming potential of vascular endothelium in the human embryo*. *Development*, 2002. **129**(17): p. 4147-57.
50. Choi, K., et al., *A common precursor for hematopoietic and endothelial cells*. *Development*, 1998. **125**(4): p. 725-32.
51. Heffelfinger, S.C., *The renin angiotensin system in the regulation of angiogenesis*. *Curr Pharm Des*, 2007. **13**(12): p. 1215-29.
52. Deshayes, F. and C. Nahmias, *Angiotensin receptors: a new role in cancer?* *Trends Endocrinol Metab*, 2005. **16**(7): p. 293-9.
53. Savary, K., et al., *Role of the renin-angiotensin system in primitive erythropoiesis in the chick embryo*. *Blood*, 2005. **105**(1): p. 103-10.
54. Schutz, S., et al., *Early expression of all the components of the renin-angiotensin-system in human development*. *Am J Pathol*, 1996. **149**(6): p. 2067-79.

55. Hubert, C., et al., *The hematopoietic system: a new niche for the renin-angiotensin system*. Nat Clin Pract Cardiovasc Med, 2006. **3**(2): p. 80-5.
56. Livak, K.J. and T.D. Schmittgen, *Analysis of relative gene expression data using real-time quantitative PCR and the 2(-Delta Delta C(T)) Method*. Methods, 2001. **25**(4): p. 402-8.
57. Zhang, H., et al., *Circulating endothelial progenitor cells in multiple myeloma: implications and significance*. Blood, 2005. **105**(8): p. 3286-94.
58. Grady, E.F., et al., *Expression of AT2 receptors in the developing rat fetus*. J Clin Invest, 1991. **88**(3): p. 921-33.
59. Akishita, M., et al., *Expression of the AT2 receptor developmentally programs extracellular signal-regulated kinase activity and influences fetal vascular growth*. J Clin Invest, 1999. **103**(1): p. 63-71.
60. McKinney-Freeman, S.L. and G.Q. Daley, *Towards hematopoietic reconstitution from embryonic stem cells: a sanguine future*. Curr Opin Hematol, 2007. **14**(4): p. 343-7.
61. Zanjani, E.D., et al., *Transplantation of hematopoietic stem cells in utero*. Stem Cells, 1997. **15 Suppl 1**: p. 79-92; discussion 93.
62. Almeida-Porada, G., C. Porada, and E.D. Zanjani, *Plasticity of human stem cells in the fetal sheep model of human stem cell transplantation*. Int J Hematol, 2004. **79**(1): p. 1-6.
63. Almeida-Porada, G., et al., *The human-sheep chimeras as a model for human stem cell mobilization and evaluation of hematopoietic grafts' potential*. Exp Hematol, 2007. **35**(10): p. 1594-600.
64. Sabin, F., *Studies on the origin of the blood-vessels and of red-blood corpuscles as seen in the living blastoderm of chicks during the second day of incubation*. Contributions to Embryology, 1920. **9**: p. 214-262.
65. Murray, P., *The development in vitro of the blood of the early chick embryo*. Proc. R. Soc. Lond., 1932. **111**: p. 497-521.
66. Moore, M.A. and J.J. Owen, *Chromosome marker studies on the development of the haemopoietic system in the chick embryo*. Nature, 1965. **208**(5014): p. 956 passim.
67. LeDouarin, N.M. and F.V. Jotereau, *Origin and renewal of lymphocytes in avian embryo thymuses studied in interspecific combinations*. Nat New Biol, 1973. **246**(149): p. 25-7.
68. Le Douarin, N.M., et al., *Origin of hemopoietic stem cells in embryonic bursa of Fabricius and bone marrow studied through interspecific chimeras*. Proc Natl Acad Sci U S A, 1975. **72**(7): p. 2701-5.

69. Dieterlen-Lievre, F., et al., *Early haemopoietic stem cells in the avian embryo*. J Cell Sci Suppl, 1988. **10**: p. 29-44.
70. Le Douarin, N.M., et al., *Ontogeny of the avian thymus and bursa of Fabricius studied in interspecific chimeras*. Ann Immunol (Paris), 1976. **127**(6): p. 849-56.
71. Le Douarin, N. and F. Jotereau, *[Embryologic origin of thymus lymphocytes in bird embryos]*. C R Acad Sci Hebd Seances Acad Sci D, 1973. **276**(4): p. 629-32.
72. Goldstein, R.S., et al., *Integration and differentiation of human embryonic stem cells transplanted to the chick embryo*. Dev Dyn, 2002. **225**(1): p. 80-6.
73. Goldstein, R.S., *Transplantation of human embryonic stem cells to the chick embryo*. Methods Mol Biol, 2006. **331**: p. 137-51.
74. Coles, B.L., et al., *Facile isolation and the characterization of human retinal stem cells*. Proc Natl Acad Sci U S A, 2004. **101**(44): p. 15772-7.
75. Sigurjonsson, O.E., et al., *Adult human hematopoietic stem cells produce neurons efficiently in the regenerating chicken embryo spinal cord*. Proc Natl Acad Sci U S A, 2005. **102**(14): p. 5227-32.
76. Wang, L., et al., *Generation of hematopoietic repopulating cells from human embryonic stem cells independent of ectopic HOXB4 expression*. J Exp Med, 2005. **201**(10): p. 1603-14.
77. Blazsek, I., J. Chagraoui, and B. Peault, *Ontogenic emergence of the hematoma, a morphogenetic stromal unit that supports multipotential hematopoietic progenitors in mouse bone marrow*. Blood, 2000. **96**(12): p. 3763-71.
78. Zambidis, E.T., et al., *Blood-forming endothelium in human ontogeny: lessons from in utero development and embryonic stem cell culture*. Trends Cardiovasc Med, 2006. **16**(3): p. 95-101.
79. Ferreira, L.S., et al., *Vascular progenitor cells isolated from human embryonic stem cells give rise to endothelial and smooth muscle like cells and form vascular networks in vivo*. Circ Res, 2007. **101**(3): p. 286-94.
80. Andreeva, E.R., et al., *Continuous subendothelial network formed by pericyte-like cells in human vascular bed*. Tissue Cell, 1998. **30**(1): p. 127-35.
81. Schor, A.M., et al., *Pericyte differentiation*. Clin Orthop Relat Res, 1995(313): p. 81-91.
82. Doherty, M.J. and A.E. Canfield, *Gene expression during vascular pericyte differentiation*. Crit Rev Eukaryot Gene Expr, 1999. **9**(1): p. 1-17.
83. Darland, D.C., et al., *Pericyte production of cell-associated VEGF is differentiation-dependent and is associated with endothelial survival*. Dev Biol, 2003. **264**(1): p. 275-88.

84. Hughes, S. and T. Chan-Ling, *Characterization of smooth muscle cell and pericyte differentiation in the rat retina in vivo*. Invest Ophthalmol Vis Sci, 2004. **45**(8): p. 2795-806.
85. Alliot, F., et al., *Pericytes and periendothelial cells of brain parenchyma vessels co-express aminopeptidase N, aminopeptidase A, and nestin*. J Neurosci Res, 1999. **58**(3): p. 367-78.
86. Dore-Duffy, P., et al., *Pericyte migration from the vascular wall in response to traumatic brain injury*. Microvasc Res, 2000. **60**(1): p. 55-69.
87. Lugassy, C., et al., *Pericyte-like location of GFP-tagged melanoma cells: ex vivo and in vivo studies of extravascular migratory metastasis*. Am J Pathol, 2004. **164**(4): p. 1191-8.
88. Yonenaga, Y., et al., *Absence of smooth muscle actin-positive pericyte coverage of tumor vessels correlates with hematogenous metastasis and prognosis of colorectal cancer patients*. Oncology, 2005. **69**(2): p. 159-66.
89. Pfister, F., et al., *Pericyte migration: A novel mechanism of pericyte loss in experimental diabetic retinopathy*. Diabetes, 2008.
90. Farrington-Rock, C., et al., *Chondrogenic and adipogenic potential of microvascular pericytes*. Circulation, 2004. **110**(15): p. 2226-32.
91. Alliot-Licht, B., et al., *Dexamethasone stimulates differentiation of odontoblast-like cells in human dental pulp cultures*. Cell Tissue Res, 2005. **321**(3): p. 391-400.
92. Collett, G.D. and A.E. Canfield, *Angiogenesis and pericytes in the initiation of ectopic calcification*. Circ Res, 2005. **96**(9): p. 930-8.
93. Dellavalle, A., et al., *Pericytes of human skeletal muscle are myogenic precursors distinct from satellite cells*. Nat Cell Biol, 2007. **9**(3): p. 255-67.
94. De Angelis, L., et al., *Skeletal myogenic progenitors originating from embryonic dorsal aorta coexpress endothelial and myogenic markers and contribute to postnatal muscle growth and regeneration*. J Cell Biol, 1999. **147**(4): p. 869-78.
95. Qu-Petersen, Z., et al., *Identification of a novel population of muscle stem cells in mice: potential for muscle regeneration*. J Cell Biol, 2002. **157**(5): p. 851-64.
96. Peault, B., et al., *Stem and progenitor cells in skeletal muscle development, maintenance, and therapy*. Mol Ther, 2007. **15**(5): p. 867-77.
97. Pickl, W.F., et al., *MUC18/MCAM (CD146), an activation antigen of human T lymphocytes*. J Immunol, 1997. **158**(5): p. 2107-15.

98. Elshal, M.F., et al., *CD146 (Mel-CAM), an adhesion marker of endothelial cells, is a novel marker of lymphocyte subset activation in normal peripheral blood*. *Blood*, 2005. **106**(8): p. 2923-4.
99. Vainio, O., et al., *HEMCAM, an adhesion molecule expressed by c-kit⁺ hemopoietic progenitors*. *J Cell Biol*, 1996. **135**(6 Pt 1): p. 1655-68.
100. Chan, B., et al., *Critical roles of CD146 in zebrafish vascular development*. *Dev Dyn*, 2005. **232**(1): p. 232-44.
101. Holzmann, B., et al., *Tumor progression in human malignant melanoma: five stages defined by their antigenic phenotypes*. *Int J Cancer*, 1987. **39**(4): p. 466-71.
102. Shih, I.M., et al., *Isolation and functional characterization of the A32 melanoma-associated antigen*. *Cancer Res*, 1994. **54**(9): p. 2514-20.
103. Xie, S., et al., *Expression of MCAM/MUC18 by human melanoma cells leads to increased tumor growth and metastasis*. *Cancer Res*, 1997. **57**(11): p. 2295-303.
104. Wu, G.J., et al., *Increased expression of MUC18 correlates with the metastatic progression of mouse prostate adenocarcinoma in the TRAMP model*. *J Urol*, 2005. **173**(5): p. 1778-83.
105. Solovey, A.N., et al., *Identification and functional assessment of endothelial PIH12*. *J Lab Clin Med*, 2001. **138**(5): p. 322-31.
106. Shih, I.M., *The role of CD146 (Mel-CAM) in biology and pathology*. *J Pathol*, 1999. **189**(1): p. 4-11.
107. Tsukamoto, Y., et al., *The role of gicerin, a novel cell adhesion molecule, in development, regeneration and neoplasia*. *Histol Histopathol*, 2001. **16**(2): p. 563-71.
108. Kang, Y., et al., *Knockdown of CD146 reduces the migration and proliferation of human endothelial cells*. *Cell Res*, 2006. **16**(3): p. 313-8.
109. Sone, M., et al., *Different differentiation kinetics of vascular progenitor cells in primate and mouse embryonic stem cells*. *Circulation*, 2003. **107**(16): p. 2085-8.
110. Boyd, N.L., et al., *BMP4 promotes formation of primitive vascular networks in human embryonic stem cell-derived embryoid bodies*. *Exp Biol Med (Maywood)*, 2007. **232**(6): p. 833-43.
111. Yamahara, K., et al., *Augmentation of neovascularization in hindlimb ischemia by combined transplantation of human embryonic stem cells-derived endothelial and mural cells*. *PLoS ONE*, 2008. **3**(2): p. e1666.
112. Weiss, L. and U. Geduldig, *Barrier cells: stromal regulation of hematopoiesis and blood cell release in normal and stressed murine bone marrow*. *Blood*, 1991. **78**(4): p. 975-90.

113. Paul, S.R., et al., *Stromal cell-associated hematopoiesis: immortalization and characterization of a primate bone marrow-derived stromal cell line*. Blood, 1991. **77**(8): p. 1723-33.
114. Toksoz, D., et al., *Support of human hematopoiesis in long-term bone marrow cultures by murine stromal cells selectively expressing the membrane-bound and secreted forms of the human homolog of the steel gene product, stem cell factor*. Proc Natl Acad Sci U S A, 1992. **89**(16): p. 7350-4.
115. Liu, J., et al., *[Influence of chemotherapy on hematopoietic microenvironment and effect of autologous bone marrow stromal cell infusion on the recovery of hematopoiesis after chemotherapy]*. Zhonghua Xue Ye Xue Za Zhi, 2001. **22**(7): p. 341-3.
116. Covas, D.T., et al., *Multipotent mesenchymal stromal cells obtained from diverse human tissues share functional properties and gene-expression profile with CD146+ perivascular cells and fibroblasts*. Exp Hematol, 2008. **36**(5): p. 642-54.
117. Sorrentino, A., et al., *Isolation and characterization of CD146(+) multipotent mesenchymal stromal cells*. Exp Hematol, 2008.
118. Cossu, G. and P. Bianco, *Mesoangioblasts--vascular progenitors for extravascular mesodermal tissues*. Curr Opin Genet Dev, 2003. **13**(5): p. 537-42.
119. Caplan, A.I., *Mesenchymal stem cells*. J Orthop Res, 1991. **9**(5): p. 641-50.
120. Mackenzie, T.C. and A.W. Flake, *Multilineage differentiation of human MSC after in utero transplantation*. Cytotherapy, 2001. **3**(5): p. 403-5.
121. Lennon, D.P. and A.I. Caplan, *Isolation of human marrow-derived mesenchymal stem cells*. Exp Hematol, 2006. **34**(11): p. 1604-5.
122. Battula, V.L., et al., *Human placenta and bone marrow derived MSC cultured in serum-free, b-FGF-containing medium express cell surface frizzled-9 and SSEA-4 and give rise to multilineage differentiation*. Differentiation, 2007. **75**(4): p. 279-91.
123. Cortes, F., et al., *Differential expression of KDR/VEGFR-2 and CD34 during mesoderm development of the early human embryo*. Mech Dev, 1999. **83**(1-2): p. 161-4.
124. Tavian, M., et al., *The vascular wall as a source of stem cells*. Ann N Y Acad Sci, 2005. **1044**: p. 41-50.
125. Zheng, B., et al., *Prospective identification of myogenic endothelial cells in human skeletal muscle*. Nat Biotechnol, 2007. **25**(9): p. 1025-34.
126. Turner, *Observations on the Structure of the Human Placenta*. J Anat Physiol, 1872. **7**(Pt 1): p. 120-380 9.

127. Strauss, F., [*Structure and Function of the Human Placenta.*]. *Bibl Gynaecol*, 1964. **28**: p. 3-29.
128. In 't Anker, P.S., et al., *Isolation of mesenchymal stem cells of fetal or maternal origin from human placenta*. *Stem Cells*, 2004. **22**(7): p. 1338-45.
129. Miki, T., et al., *Stem cell characteristics of amniotic epithelial cells*. *Stem Cells*, 2005. **23**(10): p. 1549-59.
130. Junqueira, L.C., Carneiro J, Kelley, R.O., *Basic Histology*. 1989: Appleton and Lange.
131. Prusa, A.R. and M. Hengstschlager, *Amniotic fluid cells and human stem cell research: a new connection*. *Med Sci Monit*, 2002. **8**(11): p. RA253-7.
132. Prusa, A.R., et al., *Oct-4-expressing cells in human amniotic fluid: a new source for stem cell research?* *Hum Reprod*, 2003. **18**(7): p. 1489-93.
133. Miki, T. and S.C. Strom, *Amnion-derived pluripotent/multipotent stem cells*. *Stem Cell Rev*, 2006. **2**(2): p. 133-42.
134. De Coppi, P., et al., *Isolation of amniotic stem cell lines with potential for therapy*. *Nat Biotechnol*, 2007. **25**(1): p. 100-6.
135. Miki, T., et al., *Identification of stem cell marker-positive cells by immunofluorescence in term human amnion*. *J Reprod Immunol*, 2007. **75**(2): p. 91-6.
136. Pattillo, R.A., et al., *In vitro identification of the trophoblastic stem cell of the human villous placenta*. *Am J Obstet Gynecol*, 1968. **100**(4): p. 582-8.
137. Igura, K., et al., *Isolation and characterization of mesenchymal progenitor cells from chorionic villi of human placenta*. *Cytotherapy*, 2004. **6**(6): p. 543-53.
138. Zhang, X., et al., *Mesenchymal progenitor cells derived from chorionic villi of human placenta for cartilage tissue engineering*. *Biochem Biophys Res Commun*, 2006. **340**(3): p. 944-52.
139. Kaufmann, P., J. Stark, and H.E. Stegner, *The villous stroma of the human placenta. I. The ultrastructure of fixed connective tissue cells*. *Cell Tissue Res*, 1977. **177**(1): p. 105-21.
140. Shih, I., et al., *Expression of Mel-CAM in implantation site intermediate trophoblastic cell line, IST-1, limits its migration on uterine smooth muscle cells*. *J Cell Sci*, 1998. **111** (Pt 17): p. 2655-64.
141. Knudsen, K.A., S.A. McElwee, and L. Myers, *A role for the neural cell adhesion molecule, NCAM, in myoblast interaction during myogenesis*. *Dev Biol*, 1990. **138**(1): p. 159-68.

142. Belles-Isles, M., et al., *Rapid selection of donor myoblast clones for muscular dystrophy therapy using cell surface expression of NCAM*. Eur J Histochem, 1993. **37**(4): p. 375-80.
143. Stewart, J.D., et al., *Characterization of proliferating human skeletal muscle-derived cells in vitro: differential modulation of myoblast markers by TGF-beta2*. J Cell Physiol, 2003. **196**(1): p. 70-8.
144. Deasy, B.M., R.J. Jankowski, and J. Huard, *Muscle-derived stem cells: characterization and potential for cell-mediated therapy*. Blood Cells Mol Dis, 2001. **27**(5): p. 924-33.
145. Cao, B., et al., *Cell therapy for muscle regeneration and repair*. Phys Med Rehabil Clin N Am, 2005. **16**(4): p. 889-907, viii.
146. Invernici, G., et al., *Human Fetal Aorta Contains Vascular Progenitor Cells Capable of Inducing Vasculogenesis, Angiogenesis, and Myogenesis in Vitro and in a Murine Model of Peripheral Ischemia*. Am J Pathol, 2007.
147. Angers-Loustau, A., J.F. Cote, and M.L. Tremblay, *Roles of protein tyrosine phosphatases in cell migration and adhesion*. Biochem Cell Biol, 1999. **77**(6): p. 493-505.
148. Caceres, M., et al., *Effect of platelet-rich plasma on cell adhesion, cell migration, and myofibroblastic differentiation in human gingival fibroblasts*. J Periodontol, 2008. **79**(4): p. 714-20.
149. Mousa, S.A., *Cell adhesion molecules: potential therapeutic & diagnostic implications*. Mol Biotechnol, 2008. **38**(1): p. 33-40.
150. Wetzel, A., et al., *Increased neutrophil adherence in psoriasis: role of the human endothelial cell receptor Thy-1 (CD90)*. J Invest Dermatol, 2006. **126**(2): p. 441-52.
151. Wiesmann, A., et al., *Decreased CD90 expression in human mesenchymal stem cells by applying mechanical stimulation*. Head Face Med, 2006. **2**: p. 8.
152. Campioni, D., et al., *Loss of Thy-1 (CD90) antigen expression on mesenchymal stromal cells from hematologic malignancies is induced by in vitro angiogenic stimuli and is associated with peculiar functional and phenotypic characteristics*. Cytotherapy, 2008. **10**(1): p. 69-82.
153. Fiegel, H.C., et al., *Lack of Thy1 (CD90) expression in neuroblastomas is correlated with impaired survival*. Pediatr Surg Int, 2008. **24**(1): p. 101-5.
154. Choi, K., *Hemangioblast development and regulation*. Biochem Cell Biol, 1998. **76**(6): p. 947-56.
155. Lacaud, G., et al., *Regulation of hemangioblast development*. Ann N Y Acad Sci, 2001. **938**: p. 96-107; discussion 108.

156. Choi, K., *The hemangioblast: a common progenitor of hematopoietic and endothelial cells*. J Hematother Stem Cell Res, 2002. **11**(1): p. 91-101.
157. Mikkola, H.K. and S.H. Orkin, *The search for the hemangioblast*. J Hematother Stem Cell Res, 2002. **11**(1): p. 9-17.
158. Pelosi, E., et al., *Identification of the hemangioblast in postnatal life*. Blood, 2002. **100**(9): p. 3203-8.
159. Lacaud, G., G. Keller, and V. Kouskoff, *Tracking mesoderm formation and specification to the hemangioblast in vitro*. Trends Cardiovasc Med, 2004. **14**(8): p. 314-7.
160. Loges, S., et al., *Identification of the adult human hemangioblast*. Stem Cells Dev, 2004. **13**(3): p. 229-42.
161. Park, C., Y.D. Ma, and K. Choi, *Evidence for the hemangioblast*. Exp Hematol, 2005. **33**(9): p. 965-70.
162. Wang, Y.S. and H. Xu, [*Hemangioblast in hematopoietic development of embryo*]. Sheng Li Ke Xue Jin Zhan, 2007. **38**(2): p. 139-42.
163. Yao, H.Y., B. Liu, and N. Mao, [*Relationship between hematopoietic development and endothelial cells (hemangioblast or hemogenic endothelium)--review*]. Zhongguo Shi Yan Xue Ye Xue Za Zhi, 2007. **15**(1): p. 198-201.
164. Ribatti, D., *Hemangioblast does exist*. Leuk Res, 2008. **32**(6): p. 850-4.
165. Xiong, J.W., *Molecular and developmental biology of the hemangioblast*. Dev Dyn, 2008. **237**(5): p. 1218-31.